

# Performance and Emissions Analysis of Pre-mixed and Partially Pre-mixed Charge Compression Ignition Combustion.

By

Charu Vikram Chandrashekhar Srivatsa

Submitted to the graduate degree program in The Department of Mechanical Engineering and  
the Graduate Faculty of the University of Kansas in partial fulfillment of the requirements  
for the degree of Master of Science.

---

Chair: Dr. Christopher Depcik

---

Dr. Huazhen Fang

---

Dr. Gibum Kwon

Date Defended: 17 January 2017

The thesis committee for Charu Vikram Chandrashekhar Srivatsa  
certifies that this is the approved version of the following thesis:

Performance and Emissions Analysis of Pre-mixed and Partially  
Pre-mixed Charge Compression Ignition Combustion.

---

Chair: Dr. Christopher Depcik

Date Approved: 2017

## **Abstract**

Due to raising concerns of depleting petroleum reserves coupled with global warming, the interest in Compression Ignition (CI) engines is more than ever primarily due to the comparatively superior efficiency of CI engines over Spark Ignition (SI) engines. However, nitrogen oxides ( $\text{NO}_x$ ) and Particulate Matter (PM) emissions, and the nature of their trade-off is a major hurdle for CI engines to meet the future emissions regulations. In the last two decades, Low Temperature Combustion (LTC), a method stated to be effective in reducing both  $\text{NO}_x$  and PM emissions simultaneously, has received justifiable attention. In this thesis, the importance of mitigating various emissions from CI engines and the relevant challenges is presented in Chapter 1. Subsequently, brief literature reviews of the various types of LTC; namely, Homogeneous Charge Compression Ignition (HCCI), Pre-mixed Charge Compression Ignition (PCI), and Multi-point Fuel Injection (MPFI) are included in Chapter 2.

Details of the single cylinder CI engine lab facility at the University of Kansas (KU) are given in Chapter 3. Additionally, performance and emissions results of a PCI combustion trial are presented. Here, the fuel injection timing was modified at various stages to shift from conventional to PCI combustion regime. Based on the results obtained, a follow up experimental study similar to the previous one was conducted to explore the advantages and restrictions of Partially Pre-mixed Compression Ignition (PPCI) combustion (Chapter 4). Furthermore, an in house built zero-dimensional heat release model was utilized to analyze the in-cylinder pressure data of both the tests conducted. In general, the performance, emissions, and heat release model results indicated good agreement with the trends published in the literature.

## **Acknowledgements**

First and above all, I thank the Department of Mechanical Engineering at KU for providing me an opportunity to pursue Master of Science. This work was made possible by the guidance of Dr. Christopher Depcik of the Department of Mechanical Engineering. The door to Dr. D's office was always open whenever I ran into a trouble spot or had a question about my research or writing. My lab mates Shah Saud Alam, Khalaf Alzeebi, Jonathan Mattson, Brian Gessler, Matthew Cole, Ronald Booth, and Bailey Spickler by their support and humor substantially helped in making this thesis work fun and enjoyable. Particularly, Jonathan Mattson's assistance during engine testing and reviewing the chapters helped immensely in completing the work on time. Finally, I would like to thank my father Chandrashekhar, mother Annapoorna, my brother Amit Srivatsa, and my girlfriend Jyoti for their constant encouragement and motivation.

## Table of Contents

Nomenclature.....	x
1.1 Introduction.....	1
1.2 Compression Ignition Combustion.....	1
1.3 Compression Ignition Engine Emissions Formation.....	5
<b>Chapter II: Literature Review.....</b>	<b>20</b>
2.1 Introduction.....	20
2.2 Homogeneous Charge Compression Ignition Combustion Brief Literature Review.....	23
2.3 Pre-mixed Charge Compression Ignition Combustion Brief Literature Review.....	25
2.4 Multi-point Fuel Injection Combustion Brief Literature Review.....	31
<b>Chapter III: Pre-mixed Charge Compression Ignition Combustion in a High Compression Ratio Engine.....</b>	<b>46</b>
3.1 Abstract.....	46
3.2 Introduction.....	46
3.3 Experimental Setup.....	49
3.4 Fuel Injection Timing Sweep.....	53
3.5 60° and 100° BTDC Injection Timing Fuel Sweep.....	64
3.6 Conclusion.....	69
<b>Chapter IV: Performance and Emissions Analysis of Partially Pre-mixed Charge Compression Ignition Combustion.....</b>	<b>70</b>
4.1 Abstract.....	70
4.2 Introduction.....	70
4.3 Experimental Results.....	73
4.4 Conclusion.....	91

## List of Figures

Figure 1: The four strokes of compression ignition engine operation [2].....	2
Figure 2: The in-cylinder fuel dispersion and instantaneous combustion simulation visuals [3]. ....	2
Figure 3: Total national emissions of the criteria air pollutants in 2011 [7].....	5
Figure 4: Air fuel mixture characteristics in the combustion chamber [1] .....	6
Figure 5: Hydrocarbon emissions characteristics with changing engine load [2].....	7
Figure 6: Dependency between NO formed and combustion temperature and air-fuel ratio [2].....	10
Figure 7: Block diagram of an electronic fuel injection system [12].....	13
Figure 8: Single hole fuel injector nozzle [13].....	14
Figure 9: Multi hole injector nozzle [14] .....	15
Figure 10: Pintle fuel injector nozzle [15] .....	15
Figure 11: Pintaux fuel injector nozzle [14] .....	16
Figure 12: Impinged spray injection nozzle [2] .....	17
Figure 13: Impinged spray injection setup [16] .....	17
Figure 14: Illustration of the NO <sub>x</sub> - PM tradeoff that occurs when employing EGR [17] .....	21
Figure 15: Screenshot of fuel injection timing ECU map.....	52
Figure 16: In-cylinder pressure vs. crank angle for 21.0 mg/stroke fuel injection quantity for fuel injection timing (a) 12.5 to 30° BTDC, and (b) 35 to 80° BTDC.....	55
Figure 17: Rate of heat release vs. crank angle for 21.0 mg/stroke fuel injection quantity for fuel injection timing (a) 12.5 to 30° BTDC, and (b) 35 to 80° BTDC.....	56
Figure 18: In-cylinder temperature vs. crank angle for selected injection events from injection timing sweep trial.....	56
Figure 19: Fuel injection quantity and equivalence ratio vs. fuel injection timing for fuel injection timing sweep trial.....	59
Figure 20: Nitrogen oxides and FSN emissions results at various fuel injection timings.....	59

Figure 21: Image of the filter papers from the AVL Smoke Meter during emissions measurement for 35° to 80° BTDC injection events (left to right).....	60
Figure 22: THC and CO emissions results at various fuel injection timings. ....	61
Figure 23: Formaldehyde and acetaldehyde emissions results at various fuel injection timings.....	62
Figure 24: In-cylinder pressure vs. crank angle for 60°BTDC fuel injection timing for fuel injection quantity (a) 37.0 to 13.4 mg/stroke, and (b) 11.8 to 3.6 mg/stroke.....	65
Figure 25: In-cylinder temperature vs. crank angle for selected injection events at 60 BTDC from injection quantity sweep trial. ....	65
Figure 26: Second derivative of pressure vs. crank angle for 60° BTDC fuel injection timing for fuel injection quantities 37, 22.4, and 11.8 mg/stroke. ....	66
Figure 27: Fuel injection timing for 11.8 mg/stroke injection quantity vs. FSN and fuel injection quantity for 60° BTDC injection timing vs FSN. ....	67
Figure 28: (a) In-cylinder pressure vs. crank angle and (b) second derivative of pressure vs. crank angle for 100° BTDC fuel injection timing for fuel injection quantity 30.0 to 11.8 mg/stroke. ....	68
Figure 29: (a) In-cylinder pressure and (b) rate of heat release vs. crank angle at 0.5 N-m engine torque for fuel injection timing from 12.5° to 35.0° BTDC. ....	76
Figure 30: (a) Second derivative of pressure and (b) in-cylinder temperature vs. crank angle at 0.5 N-m engine torque for fuel injection timing from 12.5° to 35.0° BTDC.....	77
Figure 31: (a) Average temperature slope and (b) actual torque vs. fuel injection timing for 0.5 N-m engine load conditions. ....	77
Figure 32: (a) In-cylinder pressure and (b) rate of heat release vs. crank angle at 1.0 N-m engine torque for fuel injection timing from 12.5° to 35.0° BTDC. ....	79
Figure 33: (a) Second derivative of pressure and (b) in-cylinder temperature vs. crank angle at 1.0 N-m engine torque for fuel injection timing from 12.5° to 35.0° BTDC.....	79
Figure 34: (a) Average temperature slope and (b) actual torque vs. fuel injection timing for 1.0 N-m engine load conditions. ....	80

Figure 35: (a) Rate of heat release and (b) in-cylinder pressure vs. crank angle at 1.5 N-m engine torque for fuel injection timing from 12.5° to 35.0° BTDC. ....	81
Figure 36: (a) Second derivative of pressure and (b) in-cylinder temperature vs. crank angle at 1.5 N-m engine torque for fuel injection timing from 12.5° to 35.0° BTDC. ....	81
Figure 37: (a) Average temperature slope and (b) actual torque vs. fuel injection timing for 1.5 N-m engine load conditions. ....	82
Figure 38: In-cylinder pressure vs. crank angle at 0.5, 1.0, and 1.5 N-m load conditions for (a) 25.0° BTDC and (b) 30.0° BTDC fuel injection timing. ....	83
Figure 39: Fuel injection quantity and equivalence ratio vs. fuel injection timing for fuel injection timing sweep. ....	84
Figure 40: (a) Nitrogen oxides, FSN, and particulate matter, and (b) carbon monoxide and hydrocarbon emissions at 0.5 N-m load for various fuel injection timings. ....	85
Figure 41: Carbon monoxide and formaldehyde emissions at 0.5 N-m load for various fuel injection timings. ....	87
Figure 42: (a) Nitrogen oxides and particulate matter, and (b) carbon monoxide and hydrocarbon emissions at 1.0 N-m load for various fuel injection timings. ....	88
Figure 43: (a) Nitrogen oxides and particulate matter, and (b) carbon monoxide and hydrocarbon emissions at 1.5 N-m load for various fuel injection timings. ....	88
Figure 44: (a) Nitrogen oxides, (b) carbon monoxide, (c) hydrocarbon emissions, and (d) FSN for PCI and PPCI trials at various fuel injection timings. ....	91



## List of Tables

Table 1. Yanmar single cylinder engine specifications .....	50
Table 2. Default ECU fuel parameters [64]. .....	51
Table 3. Properties of tested fuel. ....	53

## **Nomenclature**

ATDC	After top dead center
A/F	Air to fuel ratio
BDC	Bottom dead center
BMEP	Brake mean effective pressure
CI	Compression ignition
CN	Cetane number
CO	Carbon monoxide
CO <sub>2</sub>	Carbon dioxide
CR	Compression ratio
DI	Direct injection
ECU	Engine control unit
EFIS	Electronic fuel injection system
EPA	Environmental protection agency
FSN	Filter smoke number
FTIR	Fourier transform infrared
FVMF	Fuel vapor mass fraction
HC	Hydrocarbon
HCCI	Homogeneous charge compression ignition
HI	Homogeneity index
HO <sub>2</sub>	Hydroperoxyl
ICE	Internal Combustion Engines
IMEP	Indicated mean effective pressure

KU	University of Kansas
LTC	Low temperature combustion
MK	Modulated kinetics
MPFI	Multi-point fuel injection
NA	Naturally aspirated
NO <sub>2</sub>	Nitrogen dioxide
NO <sub>x</sub>	Nitrogen oxides
NTC	Negative temperature co-efficient
OH	Hydroxide
O <sub>2</sub>	Oxygen
PCI	Pre-mixed charge compression ignition
PM	Particulate matter
PPCI	Partially pre-mixed charge compression ignition
ROHR	Rate of heat release
SFC	Specific fuel consumption
SI	Spark ignition
SOC	Start of combustion
SOI	Start of injection
TDC	Top dead center
ULSD	Ultra-low sulphur diesel

## **1.1 Introduction**

Automobiles provide the backbone of society and the economy while facilitating industrial progress. Decades of research and innovations have led to the development of robust and relatively noiseless Internal Combustion Engines (ICE). During this time, the global increase in the number of vehicles and concerns about the combustion of fossil fuels has led to the development of alternative fuels. However, irrespective of the fuel used to power an ICE, undesirable emissions will be generated. The Environmental Protection Agency (EPA) classifies unburnt hydrocarbons (HC), carbon dioxide (CO<sub>2</sub>), carbon monoxide (CO), nitrogen monoxide, nitrogen dioxide (NO<sub>2</sub>), sulphur oxides, and PM as the exhaust emission species that pose the greatest risk to the environment and humans. The major effects of these emissions include global warming, acid rain, smog, respiratory and health hazards. In order to understand the formation of these species and what can be accomplished to mitigate their existence, it is important to review the combustion process.

## **1.2 Compression Ignition Combustion**

CI engines are known for their relatively low fuel consumption, good durability, and high thermal efficiency as compared to SI engines [1]. In Figure 1, a schematic representation of a four-stroke CI combustion cycle is presented. During the intake stroke, the piston moves from its position at top-dead-center (TDC) towards bottom-dead-center (BDC) in order to induct air into the cylinder. In the second stroke, the piston moving back to TDC from BDC compresses the added air while the intake valve is closed. This compression of air in the cylinder results in an air temperature usually above the auto-ignition temperature of the fuel, which is injected into the cylinder near TDC. In the third stroke, the fuel that is injected in one pulse or at several time intervals is then burnt converting the chemical energy of the fuel into heat energy. This energy release raises the cylinder pressure that creates a force on the piston driving it back towards BDC. During the final stroke, the expanded gases are expelled from the cylinder through the exhaust valve with the help of the piston moving back to TDC from BDC.

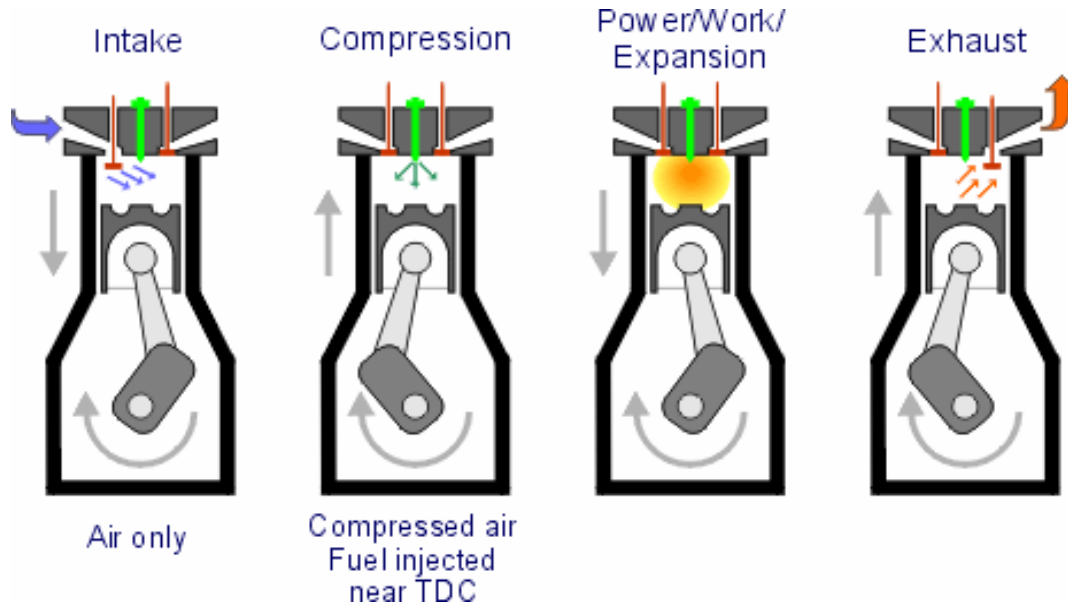


**Figure 1: The four strokes of compression ignition engine operation [2].**

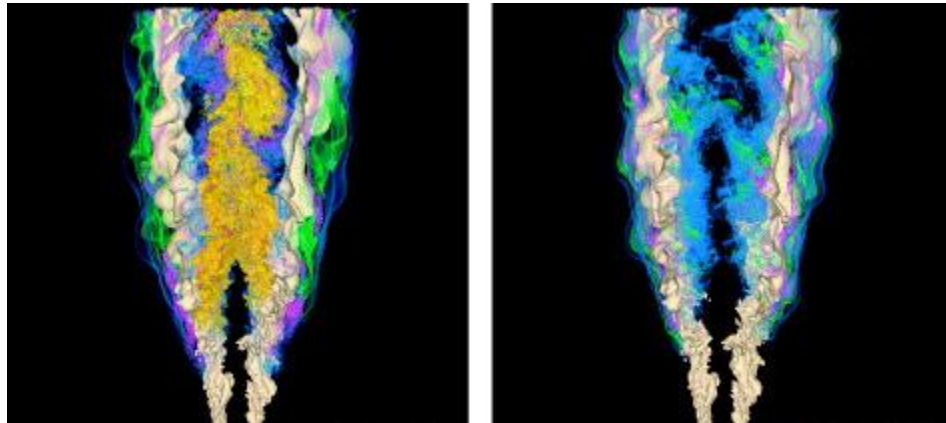


**Figure 2: The in-cylinder fuel dispersion and instantaneous combustion simulation visuals [3].**

During this four-stroke process, fuel is often injected at high pressures into the combustion chamber a few degrees before top dead center (BTDC) towards the end of the compression stroke. This injected fuel mixes with the compressed air to form pockets of fuel rich, stoichiometric, and fuel deficient regions. In the entire volume of the combustion chamber, the fuel is spread such that the equivalence ratios range from zero to infinity with near stoichiometric fuel-air regions typically starting the burning process [4]. To illustrate, the right image of Figure 2 shows this fuel dispersion process due to its interaction with pressurized air towards

the end of the compression process. On the left of this image, the regions with near stoichiometric air to fuel ratios (A/F) self-ignite with a propagating flame front. The various colors represent the concentration of fuel in that region of the chamber at the instant when fuel is injected. As one can imagine, the incomplete mixing of fuel and air can lead to a wide variety of emission species.

As a result, the most important aspect of the CI combustion process is the mixing of fuel and air, often referred to as mixture preparation. A short time after injection, the instantaneous ignition of a relatively lesser amount of premixed fuel and air occurs. This instantaneous ignition, or premixed burn, is considered the Start of Combustion (SOC) and can be marked by a sharp in-cylinder pressure increase. Generally, the time difference between the Start of Injection (SOI) and SOC is called the ignition delay. The combustion chamber pressure, temperature, Compression Ratio (CR), fuel injection time, fuel spray pattern, geometry of the chamber, and swirl pattern of intake air all influence this ignition delay time. After this delay, atomization, vaporization, and combustion continue until all the injected fuel has burned.

To understand how the fuel breaks down and its eventual combustion, the ignition delay period can be discretized further into both physical and chemical delays. The physical delay is the period taken by the liquid fuel to atomize, vaporize, and mix with the compressed and relatively high-density air. Atomization depends on the fuel injection pressure, spray pattern, fuel injector hole diameter, and viscosity of fuel. The vaporization process depends on the size of the droplets, fuel distribution, velocity of injected fuel, pressure and temperature of the combustion chamber, and volatility of the fuel. Moreover, the fuel-air mixing process also depends on the design of the injector nozzle and combustion chamber. Following the physical delay, chemical delay is the period for the fuel-air mixture to reach its auto-ignition temperature. This delay depends on the homogeneity of the mixture, cylinder temperature, and Cetane Number (CN) of the fuel.

The ignition delay period also depends on the load of the engine, analyzed here as a function of the same intake pressure and temperature. At low loads, the cylinder walls are relatively cold and the intake air is not heated significantly; hence, the ignition delay is higher (i.e., lower vaporization and heating). Moreover,

less fuel is injected resulting in less areas of ready pockets of fuel-air for combustion. At high load conditions with the cylinder walls being significantly hotter and more fuel being injected, the ignition delay is relatively short. Unlike low load conditions, the flame now propagates and engulfs the entire combustion chamber volume.

Overall, there are three stages of CI combustion:

1. Pre-mix burn: Fuel accumulated due to ignition delay burns instantaneously during this stage. This is the primary source of noise during CI combustion.
2. Diffusion burn: The pre-mix burn flame vaporizes and burns the fuel injected later into the combustion chamber. Based on the fuel distribution and quality of the fuel-air mixture, the combustion chamber will form relatively hot and cold regions. This uneven distribution of heat flux, temperature, and fuel-air ratios are the main reasons for emissions formation in CI engines (discussed in more depth later).
3. Late combustion phase: During this phase, PM particles oxidize in the presence of oxygen ( $O_2$ ) at high temperatures as the flame extinguishes. A part of the unburned fuel that may escape into the crevice volume is burnt in this stage as it reenters the main chamber. However, given that the fuel is direct injected, typically the crevice volume fraction is low.

The duration of each stage of combustion depends on the ignition delay period and the quality of mixture formation. The combustion temperature, pressure, and Rate of Heat Release (ROHR) also depend on these factors. Furthermore, different species of emissions in varying concentrations are formed during the pre-mix and diffusion burn phases. These species may or may not get reduced when combustion concludes as this depends on the combustion temperature and  $O_2$  available [1, 5, 6]. Ideally, the target of an engine designer is to provide an environment to form a homogeneous air fuel mixture in order to ensure complete combustion with minimal emissions. However, CI engines fail to provide this type of environment because of their heterogeneous and wide varying fuel-air combustion processes.

### 1.3 Compression Ignition Engine Emissions Formation

In theory, because CI engines operate globally lean (excess O<sub>2</sub>) they should be able to complete combustion with only CO<sub>2</sub>, water, and nitrogen as products in the exhaust. Clearly, this is an ideal situation and difficult to achieve in practical engines given the nature of heterogeneous combustion, dissociation, and chemical kinetics. As a result, ICEs are one of the major contributors of air pollutants as shown in Figure 3 [7]. Therefore, it is important to understand the formation of these emission species to comprehend the possible methods of mitigating them. For purposes of brevity, only those formation processes pertinent to the engine employed in this effort (discussed in a later chapter) will be reviewed. This includes fuel-air mixing effects, the influence of engine load, and the characteristics of the injection event including injector pressure and timing.

Sector	CO	NO <sub>x</sub>	VOC	PM-10	PM-2.5	SO <sub>2</sub>
<b>Highway vehicles</b>	<b>33.09</b>	<b>3.76</b>	<b>2.94</b>	<b>0.09</b>	<b>0.08</b>	<b>0.03</b>
	53.0%	31.3%	24.3%	1.2%	0.1%	0.4%
<b>Other off-highway</b>	<b>5.47</b>	<b>2.35</b>	<b>0.67</b>	<b>0.12</b>	<b>0.11</b>	<b>0.14</b>
	8.8%	19.6%	5.5%	1.5%	1.4%	1.7%
<b>Transportation total</b>	<b>38.56</b>	<b>6.11</b>	<b>3.61</b>	<b>0.21</b>	<b>0.19</b>	<b>0.17</b>
	61.8%	50.9%	29.8%	2.7%	4.2%	2.1%
<b>Stationary source fuel combustion</b>	<b>4.77</b>	<b>4.39</b>	<b>0.29</b>	<b>1.02</b>	<b>0.98</b>	<b>7.01</b>
	7.6%	36.6%	2.4%	13.0%	21.3%	87.0%
<b>Industrial processes</b>	<b>1.93</b>	<b>1.02</b>	<b>4.37</b>	<b>0.54</b>	<b>0.48</b>	<b>0.77</b>
	3.1%	8.5%	36.0%	6.9%	10.3%	9.5%
<b>Waste disposal and recycling total</b>	<b>1.56</b>	<b>0.13</b>	<b>0.17</b>	<b>0.28</b>	<b>0.27</b>	<b>0.03</b>
	2.5%	1.1%	1.4%	3.5%	5.9%	0.3%
<b>Miscellaneous</b>	<b>15.60</b>	<b>0.35</b>	<b>3.69</b>	<b>5.78</b>	<b>2.70</b>	<b>0.08</b>
	25.0%	2.9%	30.4%	73.8%	58.4%	1.0%
<b>Total of all sources</b>	<b>62.42</b>	<b>12.01</b>	<b>12.13</b>	<b>7.84</b>	<b>4.63</b>	<b>8.06</b>
	100.0%	100.0%	100.0%	100.0%	100.0%	100.0%

**Figure 3: Total national emissions of the criteria air pollutants in 2011 [7].**

#### 1.3.1 Hydrocarbon Emissions

Unburned HCs are typically formed due to incomplete combustion, partial oxidation, or post-flame oxidation [5]. The HCs in the exhaust typically consist of original fuel molecules, decomposed fuel molecules, and/or recombined intermediate compounds [8]. Partial combustion of lubricating oil is



also a potential source of HC emissions. The root cause for HC emissions in CI engines can be narrowed down largely to locally “over lean” and “over rich” mixtures [1].

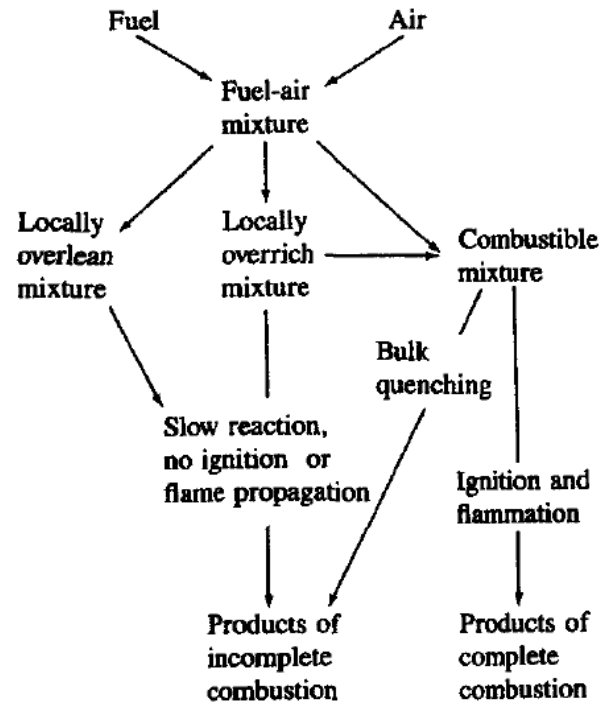


**Figure 4: Air fuel mixture characteristics in the combustion chamber [1]**

In specific, fuel and air mixing in the combustion chamber forms a range of air fuel mixtures as represented by Figure 4. Regions with a stoichiometric air-to-fuel ratio ignite instantaneously on reaching a favorable ignition temperature. The flame that results subsequently propagates throughout the combustion chamber, and the flame quenches when it encounters the wall. This flame quench reduces the temperature drastically leaving a part of the fuel unburned, resulting in HC emissions. Moreover, the propagating flame can reach regions that may have locally over lean and over rich mixtures. In cases where  $O_2$  is abundant and temperature is relatively high, the propagating flame helps to achieve complete combustion of the fuel, provided the mixture is within the fuel-air flammability limit. However, when air availability is limited, the fuel can undergo either a slow reaction or no ignition resulting in reduced flame propagation. This again contributes to HC emissions. In cases where the combustion temperature is insufficient to assist in mixing, vaporizing,

and burning, there is a slow decomposition of fuel molecules with potentially no ignition or flame propagation. This is another avenue related to exhaust HC emissions.

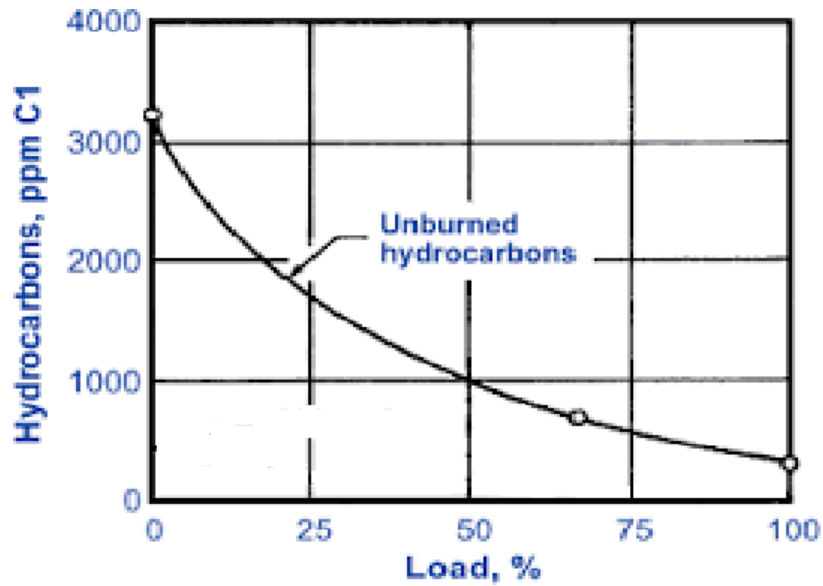


**Figure 5: Hydrocarbon emissions characteristics with changing engine load [2].**

At lower engine loads, the amount of fuel injected into the combustion chamber is low. Since the engine operates globally lean, the majority of this fuel injected will burn before reaching the cylinder walls; hence, reducing the amount of HC emissions due to wall wetting. However, situations of “over leaning” can be achieved under low loads when the fuel-air mixture falls outside the flammability limits. At high load conditions, the amount of fuel injected into the combustion chamber is comparatively high growing the possibility of fuel reaching the walls before burning and subsequently increasing the amount of wall wetting. However, again due to availability of  $O_2$  and less “over leaning” potential, the combustion temperature is comparatively high under high load scenarios. This assists in burning most of the unburned HC molecules including those sticking to the cylinder wall. These trends with load are illustrated in Figure 5. Typically, HC emissions are greater at low load conditions as compared to high load operating conditions.

With respect to injector characteristics, increasing the nozzle opening pressure boosts the velocity at which the fuel enters the combustion chamber. When fuel at high velocities is injected into high-density air, the injected fuel disperses better and mixing is improved. This amplifies combustion efficiency and reduces the HC emissions. However, injecting high velocity fuel into air that is at a comparatively lower pressure and density can result in significant fuel penetration. This could potentially increase the amount of fuel wall wetting and grow HC emissions. Hence, it is pertinent to monitor fuel injection pressure as a function of engine speed and load. While considering the time of fuel injection, advancing the timing enables an extension in the ignition delay, assisting in the formation of a homogeneous mixture. However, since the air density and pressure is comparatively low, fuel penetration is high resulting in increased wall wetting and potentially increased HC emissions. Injecting late after TDC (i.e., delayed) results in a more heterogeneous combustion event and a greater amount of diffusion burn due to late combustion. This can result in more “over rich” mixtures and greater HC emissions. Therefore, at each load and speed, there is an optimum injection timing that promotes the lowest HC emissions.

### 1.3.2 Particulate Matter Emissions

PM emissions are created due to the incomplete combustion of fuel and are predominantly formed during the diffusion burn stage. The combustion of “over-rich” mixtures results in the formation of carbon particles [9]. At temperatures greater than 500°C, the PM molecules are mostly clusters of several agglomerated small carbon spheres. At temperatures lower than 500°C, the particle size is relatively large and they tend to adsorb unburned HCs and metals along with lubricant and polynuclear aromatic HCs. Oxidation of these carbon clusters is possible when they come in contact with lean mixture combustion flame. However, when the carbon clusters encounter a rich mixture combustion flame, they act as a thermal sink reducing the combustion efficiency. This results in an increase of PM emissions.

Advancing the fuel injection timing creates an extended time for air and fuel mixture preparation. This assists in the formation of a nearly homogeneous mixture reducing the possibility of “over rich” conditions. Moreover, close to constant volume combustion may be achieved in such a scenario resulting in a quick increase of the in-cylinder pressure and temperature. This ensures that all the carbon particles formed due to pyrolysis of fuel are burned reducing the PM emissions.

Injecting fine fuel droplets facilitates an even distribution and easier dispersion of fuel in the combustion chamber. Additionally, as discussed earlier, injecting the fuel at high velocities helps in better mixing and vaporization of fuel. Both these scenarios help in improving the combustion efficiency by increasing the combustion temperature, subsequently assisting in the reduction of PM emissions. However, using nozzles with comparatively bigger holes reduces the fuel dispersion rate affecting the overall mixture formation. This reduces the combustion temperature due to lower combustion efficiency and PM emissions will increase.

### 1.3.3 Nitrogen Oxides Emissions

$\text{NO}_x$  emissions are predominantly formed due to the dissociation of  $\text{N}_2$  present in the air at high temperatures. It is observed that temperatures higher than 2000 K are necessary to break the  $\text{N}_2$  triple bond activation energy. The N radicals that result subsequently oxidize with the available  $\text{O}_2$  to form NO. Furthermore, the rapid conversion of NO to  $\text{NO}_2$  also occurs at high temperatures in the presence of  $\text{O}_2$ . While the reverse conversion of NO to  $\text{N}_2$  is also possible, this is a slow process and the time available during the expansion process is insufficient for this reaction to proceed. Moreover,  $\text{NO}_2$  can convert back to NO at high temperatures; however, the temperature drop during the expansion process reduces the rate of this reaction. Newhall and Shahed found that  $\text{NO}_x$  formation during combustion of rich mixtures are at higher rates when compared to combustion of stoichiometric or lean mixtures [10]. While the  $\text{NO}_x$  formation rate of lean mixture combustion is comparatively low, the end concentration is higher due to the rapid dissociation at high

temperatures and availability of excess  $O_2$ . Hence, NO emissions are higher for lean mixtures than rich mixtures as represented in Figure 6. Conversely, a further increase in the air-to-fuel ratio leads to reduced lean flame regions in the combustion chamber. This results in a lower combustion temperature decreasing dissociation and the associated NO formation.

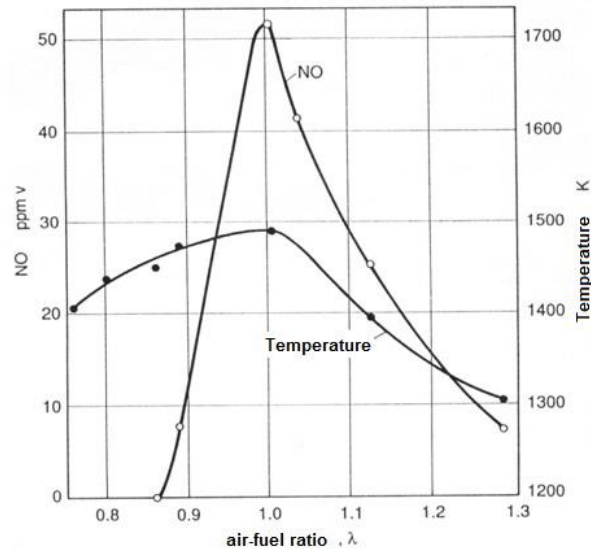


**Figure 6: Dependency between NO formed and combustion temperature and air-fuel ratio [2]**

Advancing the fuel injection timing, as explained before, results in a higher combustion temperature; hence, this will increase NO emissions. However, delaying the fuel injection timing does not provide sufficient time for the physical preparation process. This yields a heterogeneous air-fuel mixture followed by relatively poor combustion efficiencies and lower combustion temperatures. Since dissociation requires high temperatures, NO emissions produced in such scenarios are comparatively lower.

#### 1.3.4 Carbon Monoxide Emissions

CO emissions are typically formed due to incomplete CI combustion. In specific, during the combustion of over rich mixtures, the CO formed as the fuel breaks down is not converted completely to  $CO_2$ . This is due to the deficiency of  $O_2$  available and relatively low combustion

temperatures. Hence, a linear increase in equivalence ratio ( $\Phi$ ) results in a nearly linear increase in CO emissions. Combustion of lean mixtures also produces CO; however, at high temperatures CO converts to CO<sub>2</sub>, due to the availability of O<sub>2</sub>. At relatively higher temperatures, CO<sub>2</sub> can dissociate back into CO similar to the formation process of NO. As expansion progresses, there is a reduction in the amount of CO converting into CO<sub>2</sub> and the amount of reverse dissociation due to the drop in the temperature of the combustion chamber.

The combustion regime for ICEs has shifted towards a leaner burn scenario, due to several advantages over rich mixture combustion, such as the potential for better combustion and thermal efficiencies along with (generally) lower HC, PM (when air is sufficiently mixed with fuel), and CO emissions. However, NO<sub>x</sub> emissions from lean burn combustion are higher. It is important to mitigate NO<sub>x</sub> emissions because of their harmful effects on the environment and human health. Lessening NO<sub>x</sub> through engine design modifications has improved over the years with good progress. However, stringent EPA regulations have forced automotive designers to give equal, if not more, importance to aftertreatment devices. For the same reason, utilizing catalytic converters in vehicles is a necessity and has been mandated on all American cars since 1975 [11]. However, since these aftertreatment devices and their associated systems can be somewhat expensive, it would be ideal to prevent these hazardous emissions from forming in the first place.

In particular, LTC is a promising method to reduce NO<sub>x</sub> and PM emissions simultaneously without a major fuel penalty. This methodology is described in detail in the following section. Due to the potential of LTC and advancements yet to be made, it is worthwhile for universities to devote resources to this field. For the department of mechanical engineering at KU, this study could be performed in the single cylinder research facility setup by previous graduate students Eric Cecrle, Michael Mangus, Chenaniah Langness, and Jonathan Mattson. Due to several limitations of the engine, apparatus, and resources, fuel injection parameters (i.e., fuel injection timing, fuel quantity, and injection pressure) are the only variables changed during the experiments conducted in the subsequent chapters.

## **1.4 Electronic Fuel Injection System**

Before understanding the apparatus used in KU's single cylinder engine laboratory, it is important to comprehend the working principle of an Electronic Fuel Injection System (EFIS) typically used in modern vehicles. This system, as shown in Figure 7, consists of a fuel tank, supply pump or feed pump, fuel filter, fuel injector, fuel rail, fuel pressure regulator, throttle valve switch, airflow sensor, Engine Control Unit (ECU), lambda sensor, engine temperature sensor, battery, and ignition start switch. The fuel accumulated in the fuel rail is at a constant high pressure, sufficient for uninterrupted fuel injection. This eliminates the common problem of mechanical fuel pumps where the fuel injection can be jerky with sudden pressure spikes. Additionally, mechanical injection systems have a comparatively higher fuel injection delay. Since the EFIS maintains a constant fuel pressure in the rail, the fuel injection process does not incur a sudden pressure rise offering the advantage of quieter operation. Furthermore, this system can regulate the injection timing and volume with comparatively less delay. This assists in efficient engine operation, improved engine control, and lower emissions.

The ECU is the brain of the EFIS and gathers information from various sensors to generate fuel injection control signals. The electric signals are sent to various actuators that help in the effective control of fuel injection timing, duration, quantity, and pressure. The sensors used for the control of signal generation are: intake air temperature thermocouple, air mass flow meter, throttle pedal angle position sensor, rail fuel pressure sensor, angle encoder for crank angle position, lambda meter for O<sub>2</sub> measurement, engine temperature sensor, and battery potential difference information. The various actuators employed are the throttle valve switch, suction control valve, and fuel pressure regulator. While the ECU is “thinking”, fuel is drawn up from the fuel tank by the fuel pump and sent through a filter. The fuel is then pressurized to the injection pressure in the supply pump and fed to the fuel rail where it accumulates. In multi-cylinder engines, fuel lines connect individual injectors to the fuel rail. In this case, the fuel rail is popularly known as the common rail. The fuel in the injector is eventually sprayed into the combustion chamber based on the ECU control signal.

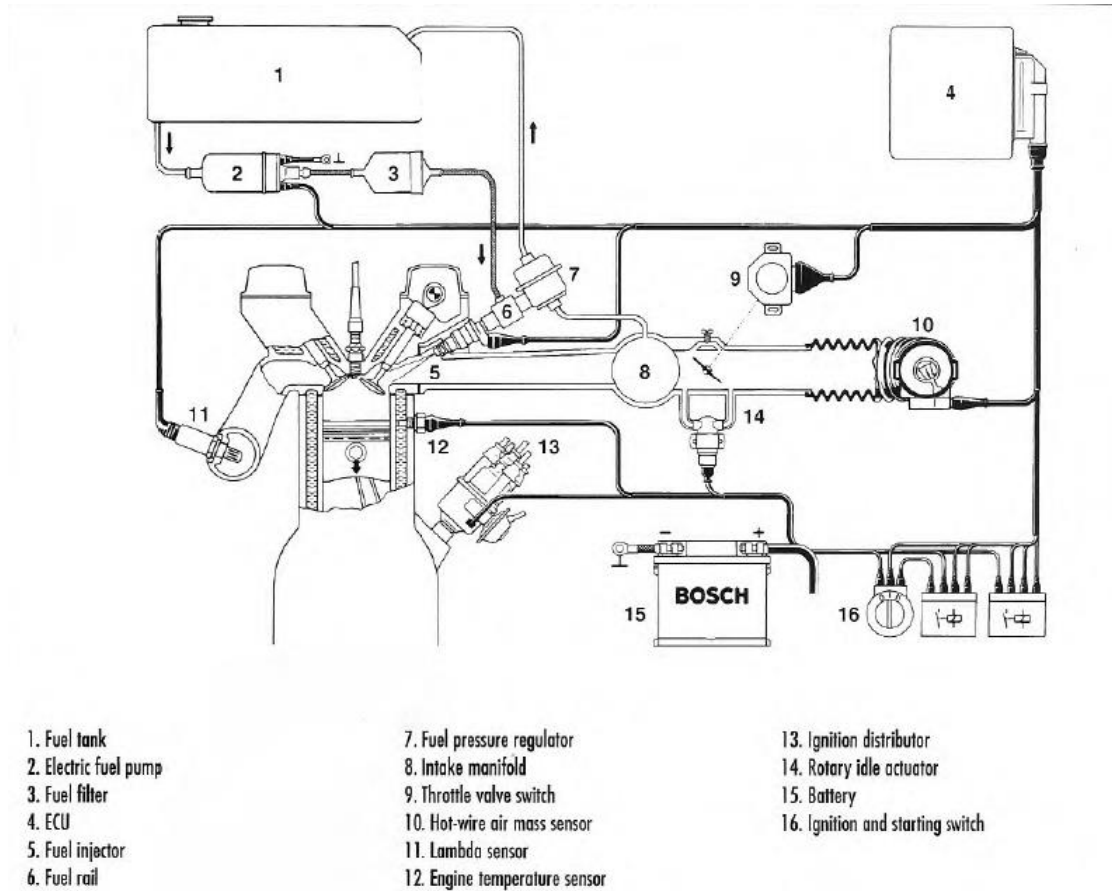


**Figure 7: Block diagram of an electronic fuel injection system [12]**

The injected fuel spray pattern depends on the geometry of the injector and the injector nozzle. The quality of fuel-air mixture is predominantly determined by the design of the fuel injector. Specifically, in engines that do not utilize any external or internal methods of creating turbulence in the combustion chamber, the type of injector used determines the quality of atomization. Maximum utilization of the combustion chamber volume by the fuel is vital. Concentrating all the fuel into a certain part of the chamber reduces the interaction between air and fuel. Increasing the number of injector holes improves atomization, as the injected fuel area is higher. This is the reason to employ multi-hole injectors. Additionally, it is easier for fine fuel droplets to disperse into the compressed air as compared to larger fuel droplets. This can be achieved by reducing the size of the injector holes. The most critical component of the injector that has a significant impact on the characteristics of the fuel injected is the injector nozzle.



The nozzle is designed to effectively break down the fuel into fine droplets. Even though turbulence and pressure in the combustion chamber influence the atomization process, the impact of the nozzle design is more significant. The type of combustion chamber used and the application of the engine determines the selection of a particular nozzle design. The most common types of nozzle designs are: single-hole, multi-hole, pintle, pintaux, and impinged spray injection.

As the name suggests, for the single-hole nozzle a single hole is provided in the center of the nozzle body as shown in Figure 8, and all the fuel is forced through this single orifice. The major disadvantage of this nozzle design is that the fuel tends to dribble towards the end of each fuel injection event. Additionally, the spray angle is too narrow to facilitate good mixing.

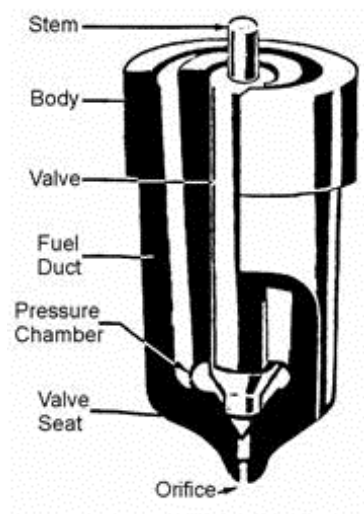


**Figure 8: Single hole fuel injector nozzle [13]**

The design of the multi-hole nozzle, as shown in Figure 9, is similar to the single hole nozzle with the obvious difference being the number of orifice holes (from 2 to 18) bored into the tip of the nozzle. Typically, the holes are radially distributed around the nozzle tip to increase the area where the fuel can be distributed. The advantage of this system is better distribution of fuel spatially; hence, improving the quality of mixture formation. This type of injector nozzle is used in majority of automobiles today.

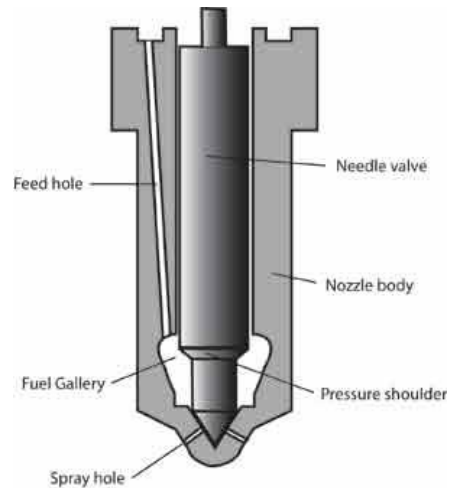


**Figure 9: Multi hole injector nozzle [14]**

Pintle-type injectors are typically used in aircraft engines. The injector valve has an extension that extrudes into the mouth of the nozzle, as depicted in Figure 10. As the fuel pressure forces the injector needle to lift, the fuel flows into the combustion chamber with a hollow cone shape. The nozzle extension and the injector body form an included angle of about  $60^\circ$  that forces the fuel to take the hollow cone shape. The circular motion of fuel droplets help with atomization and reduce the fuel penetration in the combustion chamber. The added advantages of such an injector are the comparatively low fuel dribbling along with reductions in carbon deposits on the nozzle.

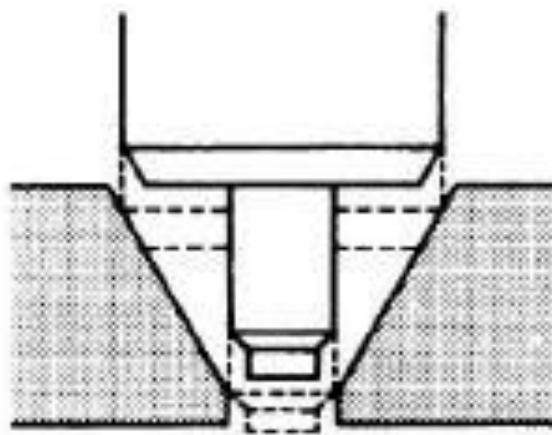


**Figure 10: Pintle fuel injector nozzle [15]**

The pintaux nozzle is a type of pintle nozzle with an extended hole drilled in the nozzle body, as shown in Figure 11. A small amount of fuel is injected through the auxiliary hole before the main hole opens. This is similar to a pilot injection before a main injection (similar to MPFI, discussed later). The duration between the pilot and the main injection depends on the fuel pressure. However, the difference between the timing of the pilot and main injection is small. At low speeds, the pressure is not sufficient for the main hole to open and all the fuel is injected through the auxiliary hole. This gives the advantage of better mixing of fuel during cold start. Nevertheless, the injection characteristics of a multi-hole injector nozzle is comparatively better than a pintaux nozzle.

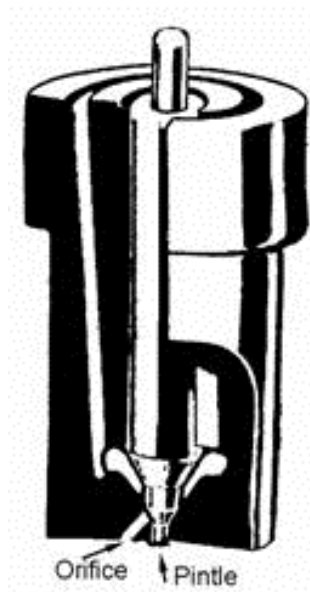


**Figure 11: Pintaux fuel injector nozzle [14]**

Impinged spray injection nozzles have holes designed such that the fuel jets coming out of the injector (at wide angles) encounter each other in pairs before entering the cylinder, as shown in Figure 12. This breaks down the fuel resulting in finer fuel droplets and reduces penetration. However, fuel injected at wide angles and high velocities problematically encourages fuel wall wetting. On the other hand, impinged spray systems offer the advantage of low fuel wall wetting at high injection pressures.

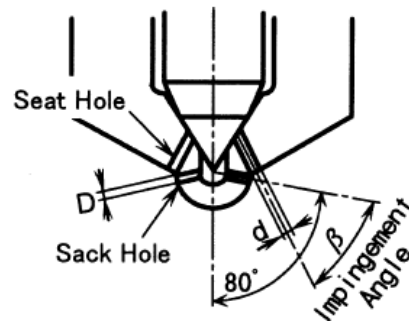


**Figure 12: Impinged spray injection nozzle [2]**

Similar impinged injector results can be achieved by utilizing a combination of two or more of the previous injectors strategically placed such that the fuel sprayed impinge with each other in the combustion chamber as shown in Figure 13. The injectors used for this are typically single, multi-hole, or pintle types. However, the common disadvantage of using this impingement strategy restricts the operating range of the engine to low and partial load conditions. Clearly, the purpose of utilizing the described injectors are unique. However, the advantages and restrictions of the injector used needs to be verified through practical engine testing, especially when it is obvious that fuel injection system affects both performance and emissions in CI combustion.

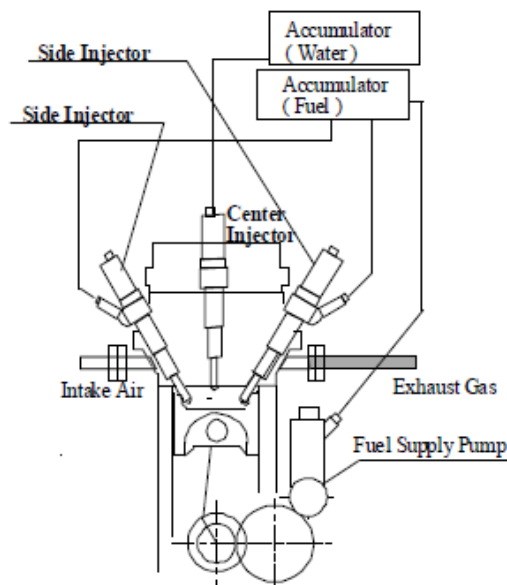


**Figure 13: Impinged spray injection setup [16]**

## 1.5 Thesis Focus

This work focusses on investigating the performance and emissions characteristics of PCI and PPCI combustion in a high CR engine. Due to several limitations in the engine test facility, fuel injection timing and quantity are the only variables utilized to control the engine operating regime during the testing process. Hence, the motivation behind this work is to understand the practicality and restrictions of operating in PCI, and/or PPCI mode on a high CR, NA engine in the absence of EGR system. Chapter 1 briefly describes the importance of restricting emissions from CI combustion, possible solutions to reduce emissions, and the practical difficulties associated with its implementation. In addition, a section on the EFIS is presented as fuel injection timing and quantity are the only variables incorporated during engine testing.

Subsequently, a detailed literature review of the various types of LTC; namely HCCI, PCI, and MPFI strategies are described in Chapter 2. This section concentrates on understanding the various techniques utilized by other researchers to operate in the LTC regime, and its advantages with respect to combustion performance and emissions. Additionally, discussions on the limitations of several proposed methods, and the difficulties linked to their implementation in the single cylinder lab at KU are also presented. It was found that HCCI operation is popular in low CR engines with port fuel injection systems. In addition, significantly high CO and HC emissions was a consistent drawback in HCCI due to unfavorable conditions in the intake port at the time of fuel injection. Conversely, scholars have proposed that advancing the fuel injection timing alone would assist to operate in the PCI combustion regime. Moreover, CO and HC emissions were comparatively low in PCI operation. However, both HCCI and PCI combustion restrict the operating regime to partial or low load conditions. Nevertheless, limited research is available on achieving LTC through HCCI, and/or PCI combustion in the absence of EGR system.

Since implementing EGR hinders the performance of a CI engine, PCI combustion by gradually advancing the injection timing was analyzed. The details of the operating conditions, data acquisition particulars, and the performance and emissions results are provided in Chapter 3. In addition, an in house built zero-dimensional heat release model was utilized to analyze the in-cylinder pressure data to provide combustion

temperature and ROHR results. Here, discussions related to the trends of in-cylinder pressure, temperature, and ROHR are included. In addition, details of the NO<sub>x</sub>, CO, THC, FSN, and aldehyde emissions results are given. Moreover, the second derivative of pressure plots are provided as they offer accurate information on the SOC timing.

Due to lower emissions with comparable combustion efficiencies observed for injections between 25° and 35° BTDC, a second set of experiments were conducted at moderately advanced injection timings, popularly known as PPCI combustion. In Chapter 4, the PPCI combustion results are given in a format similar to Chapter 3. In addition, utmost importance is provided to correlate the experimental results obtained in Chapters 3 and 4 with relevant conclusions published in the literature. Finally, a conclusion summarizing both PCI and PPCI results with potential future work is presented at the end of Chapter 4.

Since there was limited success in beating the NO<sub>x</sub>- PM tradeoff in both PCI and PPCI strategies, a brief literature review on MPFI, specifically to achieve LTC is presented at the end of Chapter 2. This section can help a future student to move beyond the efforts described here, and overcome the major shortcomings encountered in this study.

## Chapter II: Literature Review.

### 2.1 Introduction

CI engines operate in globally lean conditions. In order to quantify the air and fuel mixture in the combustion chamber, equivalence ratio ( $\Phi$ ) defined as the ratio of fuel to air by mass is typically used. For a given set of engine characteristics, such as CR, air-intake pressure, fuel injection pressure, and fuel injection timing, there is always a lower limiting value of  $\Phi$  for which stable combustion can occur. For combustion of lean mixtures, i.e. low  $\Phi$ , combustion is characterized by high temperatures around TDC. As discussed earlier, this is ideal for  $\text{NO}_x$  formation. Therefore, to reduce  $\text{NO}_x$  emissions, the availability of  $\text{O}_2$  and/or combustion temperature has to be reduced.

Exhaust Gas Recirculation (EGR) is a popular method used to reduce  $\text{NO}_x$  emissions. This technique involves mixing a part of the exhaust gas with inlet air before introducing it into the intake manifold. The exhaust gas contains significant amounts of  $\text{CO}_2$  and water that act as a thermal diluent reducing the overall combustion temperature. However, a negative impact of using EGR is an increase in PM emissions as oxidation rates decrease. Additionally, replacing  $\text{O}_2$  with EGR in the combustion chamber reduces the oxidation rate of HCs. Hence, comparatively lower combustion and thermal efficiencies are observed when employing EGR. From an emissions point of view, decreasing the combustion temperature reduces  $\text{NO}_x$  formation by lowering thermal NO kinetics rates. As a result, it is only possible to move back and forth in this so-called  $\text{NO}_x$ -PM trade-off, shown in Figure 14, by changing the magnitude of each phase of combustion. For simultaneous reduction of both  $\text{NO}_x$  and PM, LTC is one potential combustion methodology. LTC can be achieved by HCCI, PCI, MPFI techniques.

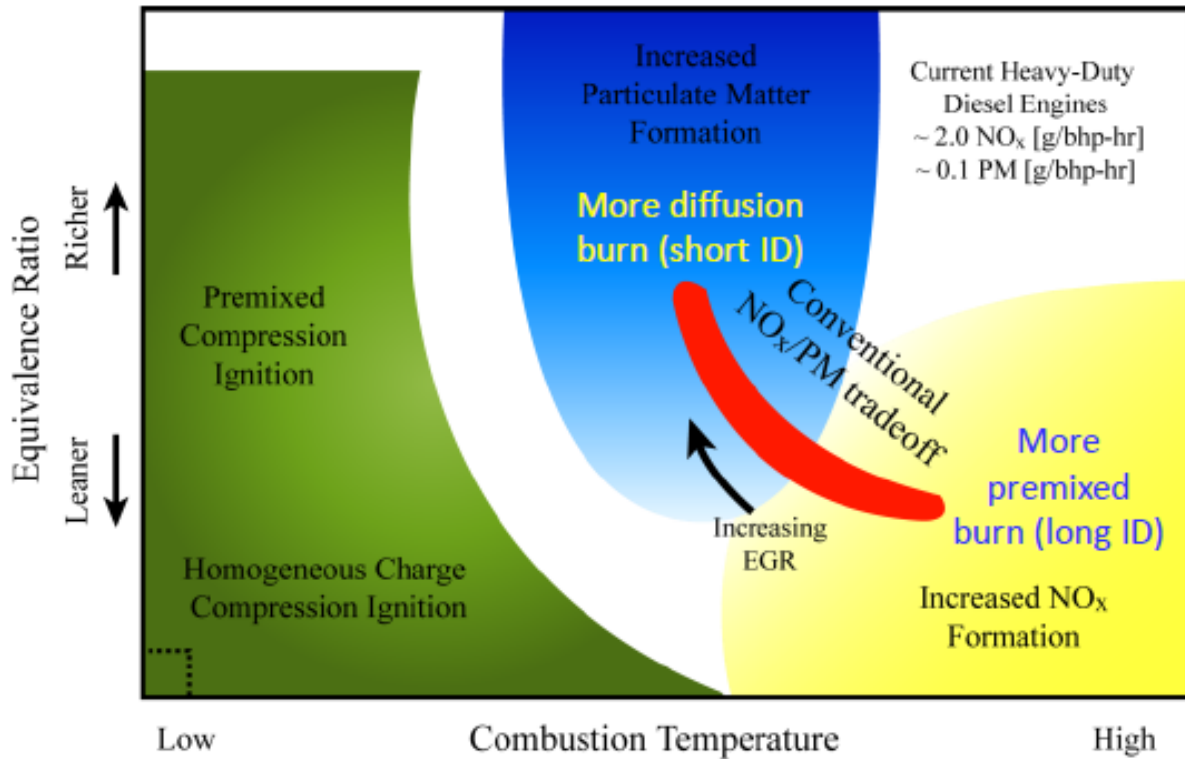


**Figure 14: Illustration of the NO<sub>x</sub> - PM tradeoff that occurs when employing EGR [17]**

In HCCI, an ultra-lean ( $\Phi \ll 1$ ) homogeneous mixture is introduced into the combustion chamber through port fuel injection. Typically, for port fuel injection of diesel fuel the intake manifold is heated to assist in fuel vaporization. This homogeneous charge is then compressed until it reaches its auto-ignition temperature and burns with negligible PM since the diffusion burn phase is comparatively low. The combustion temperature is low due to the instantaneous combustion of the ultra-lean mixture, reducing NO<sub>x</sub> formation. Additionally, HCCI can have thermal efficiency values greater than conventional CI combustion due to the nearly constant volume combustion around TDC. Hence, HCCI enables the simultaneous reduction of NO<sub>x</sub> and PM with high fuel conversion efficiencies. However, controlling HCCI combustion phasing is comparatively difficult as the high CRs used in CI engines promote knock. Furthermore, diesel fuel does not mix readily like gasoline due to its low volatility. Instead, it is possible to control HCCI combustion phasing and maintain LTC using high rates of EGR [18].



PCI is a method in which fuel is injected very early, typically close to intake valve closing. This provides sufficient time for homogeneous fuel air mixture preparation; i.e., a relatively long ignition delay. For PCI, low equivalence ratios are necessary ( $0.1 < \Phi < 0.5$ ) to prevent an excessive pressure rise during combustion. Unlike conventional CI combustion, the homogeneous mixture in the cylinder reaches its ignition temperature at the same instant and burns instantaneously. Due to the excess availability of  $O_2$ , reduced combustion temperatures are observed lowering the potential for  $NO_x$  emissions. Compared to conventional CI combustion, higher thermal and combustion efficiencies are observed in PCI combustion. Additionally, the more homogeneous charge of fuel and air assists in reducing PM emissions.

MPFI is a strategy where fuel is injected into the combustion chamber through multiple events with varying fuel quantity. The injection resulting in the main heat release is called the main injection event. Fuel injection occurring prior to the main injection event is called a pilot injection, and the injection event after the main injection is called the post injection. The number of pilot and post injections can be different and they mostly depend on the desired purpose along with the capability of the common rail system used. The fuel injected in the pilot has sufficient time to form a homogeneous mixture and combustion (ideally) starts a few degrees BTDC, typically around the time of the main injection event. The combustion of the pilot almost instantaneously burns all the fuel added during the main injection event. The post fuel injection assists in oxidizing any PM emissions created during the pilot and/or main combustion event. Additionally, the heat released from the post injection combustion can be utilized to increase the temperature of the catalytic converter. This scenario of pilot-main-post injection events in any combination provides better control over the combustion phasing while maintaining high combustion and thermal efficiencies, as compared to a conventional single injection CI combustion methodology. Using lean mixtures helps in preventing  $NO_x$  emissions while the enhanced homogeneity through the pre-mixed burn reduces PM emissions.

Prior research efforts employing the single-cylinder CI engine at KU have mostly targeted conventional CI combustion. Before attempting LTC, it is important to review the literature on the three potential options

of LTC. Principal attention has been given to understanding the theory behind the various results presented irrespective of the practicality of the experiments.

## **2.2 Homogeneous Charge Compression Ignition Combustion Brief Literature Review**

There have been many strategies reported in the literature regarding HCCI combustion control. Ryan and Callahan performed the pioneering experimental studies on HCCI for CI engines [19]. The setup they used was capable of varying the CR, intake air temperature, and EGR rate to control combustion and achieve HCCI. While operating at high load conditions with port fuel injection, knock was observed as early as 50° BTDC. Therefore, the CR was decreased from 17:1 to 8:1, as the knock limit was set at 20° BTDC. Their conclusions suggest that EGR was most effective in limiting knock and controlling the SOC. EGR also helped in extending the load range by restricting knock. PM and NO<sub>x</sub> emissions were lower than conventional CI combustion at all conditions. However, the reduction in CR led to a lower thermal efficiency than conventional operation. Furthermore, the engine was limited to steady state operation.

HCCI experiments with direct water injection were conducted by Kaneko et al. aiming to extend the operating range [20]. Light naphtha and diesel were both tested for port fuel injected HCCI combustion. Water injection strategy was used to reduce the combustion temperature. The operating range of diesel was better than naphtha fuel due to a comparatively low ignition delay and subsequent knock limitations. Additionally, water injection assisted in increasing the range of operation and ignition timing control for both fuels. Furthermore, reduced in-cylinder peak temperature and pressure helped in reducing NO<sub>x</sub> emissions. Overall, water injection resulted in increased HC emissions, decreased thermal efficiency, and increased fuel consumption.

To understand the influence of equivalence ratio and in-cylinder temperature on HCCI combustion, Suzuki et al. conducted a series of experiments. Here, they discuss the influence of in-cylinder temperature on SOC and the effect of equivalence ratio on knocking when employing a port fuel injection system for HCCI [21]. For the 100% port fuel injected case, knocking was observed when  $\Phi > 0.6$ . For knock free operation, the

engine could operate at only 60% of the total load. However, by utilizing a combination of port fuel injection and Direct Injection (DI) it was possible to operate at full load. Even though increasing the intake air pressure in DI combustion improves combustion and thermal efficiency,  $\text{NO}_x$  emissions are affected significantly. Increasing the amount of premixed fuel for a given intake air pressure reduces the  $\text{NO}_x$  emissions. However, there exists a limiting point where a further increase in the amount of premixed fuel could reduce operating range due to knock along with decreasing thermal efficiency and increasing CO and HC emissions.

Rudolf and Charles summarized the key benefits and challenges of HCCI. Reducing  $\text{NO}_x$  and PM emissions through HCCI is the obvious advantage and has been proven by many researchers [22]. The three basic strategies used to achieve HCCI combustion are port fuel injection, early or late DI, and a combination of both. Port fuel injected HCCI is not suitable for diesel fuel due to its low volatility. This results in increased fuel consumption, HC, and CO emissions. To achieve HCCI by early DI of fuel, the CR is generally reduced to avoid knocking. This implies that the fuel injected does not have an atmosphere assisting homogeneous mixture formation. Additionally, early DI results in fuel wall wetting leading to an increase in fuel consumption, CO, and HC emissions. Late DI of fuel reduces the amount of fuel wall wetting. Since the combustion temperature is low, using extremely lean mixtures for late DI combustion reduces thermal and combustion efficiencies. Additionally, utilizing close to stoichiometric equivalence ratios results in higher combustion chamber temperatures and  $\text{NO}_x$  emissions. Hence, a combination of port fuel injection and DI of fuel may be used to reduce both wall wetting and combustion temperatures. By using such a setup, fuel consumption, HC, and CO emission values comparable to conventional CI combustion may be achieved. The major drawback of this method is controlling combustion phasing. The authors suggest that varying the intake air temperature has been the most popular method followed by using different fuel blends to control combustion phasing. Additionally, they state that varying fuel injection timing is not effective in controlling combustion phasing. The common disadvantages of HCCI are reported to be: 1) limited range

of operation, 2) increased CO emissions, and 3) increased HC emissions. They conclude by saying that HCCI at high load conditions is a possibility only with a highly boosted mixture operating ultra-lean.

### **2.3 Pre-mixed Charge Compression Ignition Combustion Brief Literature Review**

There is significant research attempting successful operation of PCI in commercial vehicles. The challenge is to find a method to implement PCI in present-day ICEs without compromising on operating range and efficiency. The common disadvantages in PCI combustion, similar to HCCI is increased HC and CO emissions.

Injection strategies similar to HCCI were utilized by Odaka, et al. in order to achieve PCI combustion [23]. In their experiments, a portion of the fuel was injected into the intake manifold and the rest was injected directly into the combustion chamber. Combustion phasing was controlled by varying the percentage of premixed fuel, A/F ratio, and EGR rate. At lower A/F ratios, two distinct combustion peaks were visible in the ROHR curve indicating that the premixed fuel combustion ends before DI fuel combustion begins. However, at higher A/F ratios, there were no distinct combustion peaks. For a given percentage of fuel injected through the port, a significant reduction of NO<sub>x</sub> was observed for DI timing delayed from 10° BTDC to 7° BTDC. Further delaying the injection timing had a lowering effect on NO<sub>x</sub> emissions. For low premixed fuel ratios, the effect of DI timing had a significant effect on ROHR and emissions. However, for premixed fuel ratios higher than 75%, DI timing had a reduced effect on ROHR and emissions. PM and NO<sub>x</sub> levels at all points were lower than conventional CI combustion.

In a similar study, Kawano, et al. varied EGR and effective CRs to increase ignition delay and achieve PCI combustion close to TDC [24]. With an advanced fuel injection timing of 35°-15° BTDC, ignition delay was increased for better air fuel mixture homogeneity. It was observed that EGR had a relatively greater effect on increasing ignition delay than modulating the effective CR. Similarly, EGR had a greater impact in reducing NO<sub>x</sub>. They were successful in simultaneously reducing NO<sub>x</sub> and PM emissions at all load conditions. Indicated Specific Fuel Consumption (SFC), HC, and CO emission values were comparable to

conventional CI combustion results. By reducing the effective CR, reasonable control over the ignition time could be established. However, this reduced the power density of the engine. Like other studies, this investigation was limited to low and part load conditions to prevent an excessive pressure rise.

A thermodynamic comparison of HCCI, PCI, and conventional combustion characteristics was conducted by Tsurushima, et al. [25]. Heat balance estimates were done for this comparison using the temperature and mole fractions data of intake and exhaust mixtures. EGR supply was necessary for PCI at low loads to ensure complete combustion. Furthermore, EGR was required at high loads to control ignition timing. The authors were challenged to: 1) control the misfire resulting in increased CO and HC emissions at low load, and 2) control the pre-ignition knock at high load due to rapid combustion resulting in significant heat loss. Results of the comparison predicted that the indicated thermal efficiency of HCCI was the highest and the conventional CI combustion was the lowest. Moreover, PCI had the lowest amount of heat loss and conventional CI combustion had the highest. This was due to the short combustion periods of PCI and HCCI operation. Thermal efficiency of PCI may be improved by controlling fuel concentration through injection timing; hence, reducing the amount of unburned fuel. The major drawback of PCI was its low combustion efficiency due to cylinder wall wetting during advanced fuel injection events. The authors suggest that by delaying the injection timing this problem can be overcome, but this may result in a greater heat loss.

A series of experiments were conducted by Harada et al. to understand the importance of fuel spray pattern and its contribution in reducing emissions during PCI combustion [26]. Here, they compared the influence of spray pattern and extent of fuel penetration of a pintle type nozzle injector and a conventional multi-hole injector on PCI combustion. The extent of fuel penetration was comparatively lower for the pintle injector. The higher fuel penetration observed with multi-hole injector resulted in fuel wall wetting, subsequently increasing HC and CO emissions. For trials conducted with the pintle injector, irrespective of advancing or delaying the fuel injection timing, HC and CO emissions were comparatively low due to a lower fuel penetration. Additionally, the ROHR was higher when the fuel penetration was low as the amount of fuel

available for combustion was comparatively high. This indicated that the root cause for HC and CO emissions was fuel wall wetting and fuel accumulation in crevice volumes. They mention that designing a deeper piston bowl can assist in reducing fuel wall wetting. Furthermore, they conclude by saying that  $\text{NO}_x$  and smoke (aka PM) emissions were lower at all points in PCI as compared to conventional combustion. However, HC and CO emissions were observed to be higher. With respect to controlling combustion phasing, varying the inlet gas temperature was found to be the most influential parameter in modulating ignition timing.

In an attempt to tackle issues of PCI combustion, like cylinder wall wetting and low operating ranges, Iwabuchi et al. conducted experiments using an impinged-spray injection strategy, oxidation catalyst, and supercharger [27]. It was observed that by increasing the amount of fuel injected per stroke, PM and HC emissions increased due to excessive fuel wall wetting and subsequent poor combustion. As a result, models were developed to understand the parameters affecting fuel adherence. It was found that the magnitude of fuel wall wetting depended on the injector-hole angle, injection timing, and impingement angle. An impinged spray nozzle with impingement angle of  $60^\circ$  was the best configuration with the least penetration both horizontally (cylinder wall) and vertically (combustion chamber bottom). Additionally, by using an oxidation catalyst, for catalyst inlet temperatures of  $200^\circ\text{C}$  and above HC emissions were comparable with that of conventional CI combustion. A supercharger was simulated using an air compressor to operate at higher loads. Compared to a naturally aspirated (NA) CI engine, for a given quantity of fuel injected per stroke, both  $\text{NO}_x$  and PM emissions were significantly lower for supercharged PCI combustion.

In a similar attempt to reduce  $\text{NO}_x$  and HC emissions, Nishijima et al. conducted PCI experiments with an impinged spray fuel injection system [28]. Emissions and performance comparisons were performed for boosted and NA setups. They found that increasing the boost pressure reduced the ignition delay due to an increase in bulk gas temperature along with better atomization. This resulted in reduced HC and increased  $\text{NO}_x$  emissions as compared to NA trials. However, increasing the boost pressure past a certain limit increased the effective fuel rate due to combustion knock. Increasing the fuel injection quantity per stroke

while boosting reduced CO and HC emissions as compared to NA combustion. Furthermore, fuel consumption and NO<sub>x</sub> emission values were comparable to NA conventional CI combustion. Similar results with consistent reasons about the advantages of using an impingement type fuel injection system to reduce NO<sub>x</sub> and PM emissions were generated by Naoke et al. [29].

The effects of injection spray angle on PCI emissions were studied by Sangsuk and Rolf [30]. The results showed that simultaneous reduction of NO<sub>x</sub> and HC emissions was difficult to achieve under NA conditions. Additionally, the injection spray pattern was observed to be more influential than the SOI on emissions. PCI combustion with lower NO<sub>x</sub>, PM, and CO emissions was achieved by directing the fuel spray into the squish region (piston bowl) of the combustion chamber. A further reduction in PM emissions was observed by directing the fuel to regions of the piston bowl with the highest fuel jet travel distance. This assisted in enhanced air-fuel mixture preparation and LTC with comparatively higher ignition delay. However, the reduced combustion temperature resulted in increased CO emissions. The fuel consumption rate was comparatively more when the intake air pressure and fuel injection quantity were increased to operate at high load conditions.

The effects of using various types of injectors and EGR rates on HC, CO, NO<sub>x</sub>, and PM emissions during PCI combustion were studied by Yongjin et al. [31]. Burn duration analysis was performed for all configurations to understand the combustion characteristics and corresponding emissions. Burn duration is defined as the time taken in terms of crank angle during combustion for 10% to 90% of accumulated heat release. The burn duration for fuel injected between 25-40° BTDC was short due to the dominance of the pre-mixed burn combustion phase. This was the region where PCI combustion occurred. The burn duration was higher for fuel injections between 25-5° BTDC due to the relatively higher amount of diffusion-controlled combustion. By using an injector with a higher spray cone angle, HC and CO emissions were recorded to be higher due to increased fuel wall wetting, fuel accumulation in crevice volume, and lower combustion temperatures. However, reducing the spray cone angle and directing the fuel into the piston bowl assisted in lowering HC and CO emissions. Additionally, for a fixed spray cone angle, two injectors

(one with 8 holes and the other with 14 holes) showed different emission results. The injector with 14 holes produced lower HC, CO, and PM emissions because of enhanced atomization. However, NO<sub>x</sub> emissions were higher due to greater combustion temperatures. Furthermore, the number of injector holes did not have an effect on the rate of in-cylinder pressure rise. EGR was varied for the 14-hole injector configuration. It was observed that EGR had no significant effect on burn duration. Increasing EGR amplified the Indicated Mean Effective Pressure (IMEP) due to the extended ignition delay. The general pattern of increasing CO/HC and decreasing NO<sub>x</sub> emissions was observed with a greater EGR rate. They conclude by stating that SOC could be shifted towards TDC by increasing the EGR flow rate.

A computational study was conducted by Miyamoto et al. to analyze the influence of various parameters on NO<sub>x</sub> emissions during PCI combustion [32]. The variables considered were fuel droplet size, fuel injection quantity, and injection timing. For fixed fuel injection timing, results showed an increase in NO<sub>x</sub> and decrease in HC emissions for decreasing fuel droplet size, suggesting higher combustion temperatures due to improved atomization. Comparative results showed that the fuel injection quantity determined the global equivalence ratio of the mixture and the mass of vaporized fuel in the combustion chamber. Additionally, fuel injection timing was observed to control combustion phasing and temperature. Combustion at TDC was achieved by varying the fuel injection timing. It was concluded that fuel droplet size and injection timing are significant parameters influencing NO<sub>x</sub> emissions in PCI combustion.

Simulation efforts using practical models to quantify the extent of homogeneity in PCI combustion was conducted by Lee et al. [33]. For a given amount of fuel, the homogeneity index (HI) and Fuel Vapor Mass Fraction (FVMF) were computed by varying the injection timing from 120° BTDC to 40° BTDC. Results suggest that HI and FVMF were best for fuel injected at 120° BTDC due to the excess time available for air-fuel mixing. HI and FVMF reduced progressively towards 40° BTDC. A decrease in HI and FVMF was observed with an increase in fuel droplet size from 12 μm to 24 μm due to a reducing extent of atomization. Additionally, a decrease in HI and FVMF was observed when the fuel spray cone angle was increased from 60° to 110° due to a growth in the space utilization of the injected fuel. However, this resulted in increased



fuel penetration and subsequent fuel wall wetting. Compared to fuel injection timing, fuel droplet size, and spray cone angle; fuel injection velocity had the lowest influence on HI and FVMF. Test results with HI and FVMF were in general agreement with practical experiments conducted by other researchers of this period.

The advantages of Modulated Kinetics (MK) combustion, a slight variation of PCI combustion, were described by Kimura et al. [34]. High swirl ratios and extended delay periods in O<sub>2</sub> deficient environments are the typical characteristics of MK combustion. By increasing the swirl ratio of the inlet air, a decrease in PM and HC emissions was observed due to improved atomization resulting in higher combustion temperatures. Though the magnitude of emissions reduction was comparatively small, there was a slight improvement in performance characteristics such as ROHR, thermal efficiency, and rate of pressure raise. Similar to other PCI results, MK combustion was also restricted to low and partial loads. In subsequent research by the same authors, additional variables were included with the goal to improve fuel consumption while extending operating range [35]. Since EGR was used at high load conditions, the ignition delay reduced significantly due to comparatively higher bulk gas temperatures in the combustion chamber before SOC. This had a negative impact both on performance and emission results. To overcome this problem, the CR was reduced and cooled EGR was employed. With this combination, they were able to achieve fuel consumption values comparable to conventional CI combustion, even at high load conditions. Additionally, they recorded a 90% reduction of NO<sub>x</sub> and PM emissions when contrasted against traditional CI operation.

Walter and Gatellier attempted to beat the NO<sub>x</sub>-PM tradeoff through PCI combustion without compromising the engine operating range [36]. A fuel injection spray cone angle less than 100° was used and the piston bowl angle was reduced to match the spray profile. This assisted in improving the fuel mass burned fraction. EGR was utilized to control the ignition timing at low and partial load conditions. Since PCI combustion was knock limited, the method developed by the authors controlled the fuel injection such that the engine operation switched from PCI to conventional combustion at high load conditions. Additionally, using elevated levels of EGR at high load conditions was unfavorable to achieve the power

supply demand. Hence, the effective CR was decreased with low EGR rates to maintain similar ignition timings.  $\text{NO}_x$  emissions were 100 times less and PM emissions were 10 times lower in comparison to conventional CI combustion. Fuel consumption, CO, and HC emission values were slightly higher yet comparable to conventional combustion.

A series of experiments were conducted by Zhili and Tomaya to analyze the influence of piston geometry on HC and CO emissions [37]. They state that even though PCI combustion characteristics assist in the simultaneous reduction of  $\text{NO}_x$  and PM emissions, they result in a growth of HC and CO emissions. While combustion chamber geometry is an important factor, fuel distribution has a greater effect on HC and CO emissions. From their study, they identify top-land and ring crevice volumes, wall wetting, and misfire as the sources for HC and CO emissions. Piston geometry and fuel injection timing was varied to understand its influence on HC and CO emissions. They conclude by saying that reducing the amount of fuel squeezed into the top-land and ring crevice volumes is the best way of reducing HC and CO emissions during PCI combustion.

## **2.4 Multi-point Fuel Injection Combustion Brief Literature Review**

Experiments on the feasibility of PCI and MPFI combustion were performed by Akagawa et al. [16]. A pintle type injection nozzle was utilized to reduce fuel penetration and subsequent fuel wall wetting. Moreover, an increased spray angle was used to reduce the fuel trapped in the crevice volumes in order to lower HC emissions. Since the fuel was injected very early during initial PCI tests, injection timing had a relatively minor influence in controlling combustion phasing. Based on the experimental results, EGR rate and temperature had a greater influence on controlling ignition timing and the ROHR. In addition, by boosting the intake air this helped to generate IMEP levels comparable to conventional CI combustion. However, PCI combustion was limited to low and partial load operation. As a result, MPFI combustion was necessary to achieve performance results similar to conventional CI combustion. Overall, the MPFI combustion strategy was able successfully pass the 13-mode Japanese cycle when varying rates of EGR flow were used. In comparison with a conventional CI combustion, MPFI had lower SFC and  $\text{NO}_x$

emissions. Though PM emissions were higher, the primary constituent of PM was found to be the soluble organic fraction, which may be readily oxidized using a catalytic converter.

MK combustion trials to measure heat flux characteristics and its influence on MPFI

combustion were performed by Ogawa et al. [38]. The heat flux generated without EGR was up to 50% less than conventional CI combustion. As the amount of fuel was increased, an obvious increase in heat flux was observed. With a pilot injection, the  $\text{NO}_x$  emissions dropped as much as 50% as compared to conventional CI combustion. Additionally, the heat flux was comparatively low for MPFI combustion. For a fixed EGR rate, increasing the fuel injection quantity had a relatively small influence on the percentage increase of heat flux. A similar pattern was observed when the fuel injection pressure was increased. However, the heat flux and  $\text{NO}_x$  emissions were always higher for the MPFI strategy without EGR as compared to conventional combustion with EGR. This implied that the impact of EGR was more dominant than fuel injection timing and fuel amount on the heat flux in the combustion chamber.

Similar studies conducted by Nishijima et al. describe the advantage of water injection to suppress combustion temperature [39]. Moreover, an impinged fuel spray was utilized to reduce fuel penetration with MPFI aiding in reducing knock tendency. By injecting the water during the intake stroke at  $180^\circ$  BTDC, heat release rate curves similar to conventional CI combustion were obtained while  $\text{NO}_x$  emissions remained comparatively low. Additionally, fuel consumption, HC, CO, and PM emissions were comparable to conventional combustion.

MPFI experiments conducted by Hashizume et al. attempted to reduce  $\text{NO}_x$  emissions at high load conditions, the major disadvantage of PCI combustion [40]. Two stages of combustion were involved in the MPFI trials. In the first stage of early lean combustion, fuel was injected around  $150^\circ$  BTDC. This was followed by a second stage of diffusion-controlled combustion at elevated temperatures. For the sake of comparison, the injection timing of the second injection event was varied from  $2^\circ$  BTDC to  $30^\circ$  After Top Dead Center (ATDC). Delaying the second stage fuel injection further away from  $18^\circ$  ATDC resulted in

increased PM emissions and caused misfire due to decreasing combustion temperatures with the progress of the expansion stroke. For a given amount of fuel injected,  $\text{NO}_x$  and PM emissions were lower in MPFI combustion as compared to conventional CI combustion. However, HC emissions were higher presumably due to fuel wall wetting and/or fuel in the crevice volumes. Comparing the emissions and ROHR curves at differing fuel injection times, the authors suggest that using a lower CN fuel for the first injection and higher CN fuel for the second injection is the best way to reduce the SFC. They conclude by stating that it is possible to generate fuel consumption and HC emission values comparable to conventional combustion by boosting the intake air.

Emissions of single and dual stage injection combustion strategies were compared by Zufeng et al. [41]. They determined that extremely advanced single stage injection (i.e., PCI) combustion of lean mixtures yielded lower PM and  $\text{NO}_x$  emissions as compared to conventional combustion. However, advancing the injection timing beyond a certain limit gradually increased the  $\text{NO}_x$  emissions due to higher combustion temperatures. By employing an extremely delayed (close to TDC) single stage injection event, a simultaneous reduction of PM and  $\text{NO}_x$  emissions was observed. However, the disadvantage of this technique was the drastic increase in fuel consumption. Subsequently, two techniques were utilized when implementing MPFI combustion. One involved an initial pilot followed by the main injection event with the second option having a post-injection trailing the main injection event. In both of these techniques,  $\text{NO}_x$  emissions were lower than the single injection combustion strategy. However, CO and PM emissions were substantially higher due to comparatively lower combustion temperatures and the associated ROHR. The major advantage with the dual injection strategy was the enhanced control over combustion phasing. Furthermore, the ROHR and rate of in-cylinder pressure rise were less during the dual injection strategy as compared to the single injection; hence, the dual injection strategy had a reduced combustion noise.

The practical limitations of reducing  $\text{NO}_x$  emissions in heavy duty CI engines were discussed by Dickey et al. [42]. Charge air cooling, water injection, and EGR were the methods employed in an attempt to reduce  $\text{NO}_x$  emissions. MPFI and injection rate shaping assisted in tailoring the heat release to minimize the peak

combustion temperature to reduce  $\text{NO}_x$  emissions. Diminishing the intake air temperature assisted in reducing  $\text{NO}_x$  emissions as the combustion temperature was comparatively lower; however, the penalty on SFC was comparatively higher. Adding water emulsions into the fuel had the capability to reduce  $\text{NO}_x$  emissions, due to reduced combustion temperatures, by 1-1.3% for every 1% water content by volume in the fuel. Compared to the effects of charge air cooling and water fuel emulsions, EGR had a greater impact on reducing  $\text{NO}_x$  emissions. Introducing EGR ensured the extension diffusion burn phase of combustion. But, water emulsions in the fuel assisted in maintaining LTC. Additionally,  $\text{NO}_x$ -PM tradeoff curves were plotted for EGR sweeps at different loads and speeds. These plots assisted in selecting the flow rate of EGR for a given speed and load condition for effective control of emissions. The trials were conducted utilizing a common rail DI system including multi-hole fuel injectors. The authors describe that the fuel injection control systems used today are excellent, and for a given fuel injection strategy, further reduction in emissions by improving the quality of fuel injection is insignificant. In CI combustion, even though the bulk gas temperatures are low, the local combustion temperatures are comparatively high, which creates undesired emissions. The major drawback with conventional CI combustion is this difference between the global gas and local combustion temperatures. It was concluded that, for significant  $\text{NO}_x$  reduction, a combustion regime shift from diffusion burn phase to pre-mixed lean combustion phase is necessary. The suggested method to achieve this would be to burn all the fuel in the combustion chamber instantaneously at the global air-fuel ratio. In other words, reduce or nullify the difference between local combustion temperatures and the bulk gas temperature, which is potentially possible by HCCI combustion.

MPFI with EGR was tested on a high CR single cylinder CI engine in order to achieve simultaneous reduction of  $\text{NO}_x$  and PM by Asad et al. [43]. The duration of combustion was determined to be the primary controlling factor of emissions formed. Applying significant amounts of EGR via a single injection strategy at low loads and multiple early injections at medium loads were suggested to improve the fuel efficiency of LTC. Conventional CI combustion in high CR engines typically results in elevated noise levels and prohibitive maximum cylinder pressures at high load conditions. It was found that achieving lean LTC with

a single injection event was challenging under high load conditions; hence, MPFI combustion with an early pilot injection followed by a late post injection was utilized. The early pilot injection results in (effectively) lean HCCI combustion, and the late post injection assists in supplying the energy demand needed for high load conditions. Moreover, since post injection occurs during the expansion stroke, the combustion temperatures are still relatively low ensuring reduced  $\text{NO}_x$  emissions. The combustion phasing control was observed to be more effective with MPFI as compared to a single injection strategy. Additionally, the reduced ignition delay with MPFI strategy helped in lessening  $\text{NO}_x$  emissions due to predominantly diffusion burn (aka later) phase combustion. There was no significant increase in PM emissions observed. However, a comparatively longer ignition delay was observed for a single injection with EGR strategy. This resulted in predominantly pre-mixed burn phase combustion, and due to the excessive EGR used to maintain low combustion temperatures, comparatively higher PM emissions were observed.

Similar trials were conducted on a heavy duty CI engine by Mingfa et al. [44]. In their study,  $\text{NO}_x$  and PM emissions for single, pilot-main, pilot-pilot-main, main-post, and pilot-main-post injection strategies with and without EGR were compared. All the trials were conducted at a constant Brake Mean Effective Pressure (BMEP) of 1.55 MPa at high load and 0.38 MPa at low load. Under low load conditions, the ignition delay was higher for the single injection strategy as compared to the pilot-main injection methodology. The single injection strategy resulted in a predominantly pre-mixed burn phase, subsequently forming higher  $\text{NO}_x$  emissions due to greater combustion temperatures. The pilot-main injection option yielded better atomization and combustion had a comparatively lower heat release. Specifically, when the time difference in terms of crank angle between the pilot and main injection event were low, the heat release was comparatively reduced. Additionally, since atomization was better, there was no observable increase in SFC, PM, and CO emissions. However, irrespective of the injection strategy, fuel quantity, and injection timing, the pilot injection did not have a significant effect on emissions at high load conditions. The pilot injection improved the fuel-air mixture environment; however, due to high levels of fuel in the main injection event, combustion was predominantly diffusion controlled. Hence, the influence of a pilot

injection on  $\text{NO}_x$  and PM emissions was insignificant. Whereas, comparing the single injection and pilot-main injection strategies,  $\text{NO}_x$  and PM emissions were comparatively lower for the pilot-main injection option. Specifically, these emissions were reduced when the time interval between pilot and main event was relatively high. Moreover,  $\text{NO}_x$  emissions increased and PM emissions reduced when the pilot injected fuel quantity was increased, due to comparatively higher ROHR owing to the increased pre-mixed burn. In the initial trials with the pilot-pilot-main injection strategy, the time interval between pilot 1 and pilot 2 was set at  $8^\circ$  crank angle. It was found that, until a certain limit, the heat release and combustion temperature progressively increased for an increasing time difference between the pilot 1 and the main injection events, resulting in a corresponding increase in  $\text{NO}_x$  and decrease in PM emissions. However, further advancing the pilot 1 fuel injection timing reduced the combustion heat release and temperature. It was observed that, for an extremely advanced pilot 1 injection, the combustion of the pilot 1 concluded very early. Additionally, the exhaust gases in the combustion chamber due to the pilot combustion inhibited the main injection combustion reducing the temperature and subsequent  $\text{NO}_x$  emissions. Furthermore, PM emissions were lower presumably due to a comparatively higher ignition delay of the main injection combustion event. Compared to all strategies discussed earlier, post injection had a significant impact on emissions. Irrespective of the pilot injection quantity, timing, and EGR rate used,  $\text{NO}_x$  and PM emission trends predominantly depended on post injection at both low and high load conditions.

A two stage combustion strategy was studied by Oh et al. using a multi-dimensional computational fluid dynamics model representing a single cylinder CI engine, subsequently verified through experiments [45]. The heat release rate,  $\text{NO}_x$  and PM emissions were compared for five cases of varying pilot and main injection quantities: 2/11.46, 4/10.31, 6/9.19, 8/8.38, and 10/7.63 ( $\text{Pilot}_{(\text{mg/cycle})}/\text{Main}_{(\text{mg/cycle})}$ ). The pilot injection was fixed at  $50^\circ$  BTDC and the main injection at  $5^\circ$  ATDC. The results showed that for 2/11.46 and 4/10.31 cases, the heat release due to pilot injection combustion was comparatively low suggesting negligible or no combustion. However, heat release spikes due to pilot combustion were observed for the remaining tests. Furthermore, the  $\text{O}_2$  availability for main injection combustion was comparatively low.

Additionally, for the 10/7.63 trial, the premixed combustion phase dominated unlike all other cases where diffusion burn phase was predominant. Since the  $O_2$  availability was lower for the main combustion event, the  $NO_x$  emissions were low and PM emissions were comparatively high for 6/9.19, 8/8.38, and 10/7.63 cases. Even though the combustion was purely diffusion controlled for the 2/11.46 and 4/10.31 trials, due to the excess  $O_2$  available,  $NO_x$  emissions were comparatively higher and PM emissions were low.

A study was conducted by Park et al. using an optical single cylinder CI engine to investigate the effects of MPFI strategies on performance and emissions [46]. Initially, the effects of varying fuel injection pressure and fuel injection timing on a single injection combustion event were analyzed. It was found that increasing the injection pressure yielded a comparatively low IMEP due to the dominance of pre-mix burn combustion; hence, a comparatively low combustion duration. Alternatively, by decreasing the injection pressure, the combustion duration increased producing more power during the expansion stroke due to an extended diffusion burn phase. Since the heat release was higher for the high pressure fuel injection case,  $NO_x$  emissions were higher. Even though the  $NO_x$  emissions were reduced for the low pressure injection test, HC emissions were comparatively higher due to fuel accumulation in the injector sac volume and subsequent dribbling into the combustion chamber. The combustion of fuel injected at  $2^\circ$  BTDC resulted in a predominantly diffusion controlled combustion compared to fuel injected at  $16.4^\circ$  BTDC. The heat release rate and combustion temperature were lower for the delayed injection; hence, the  $NO_x$  emissions were comparatively lower due to reduced combustion durations and rapidly decreasing combustion temperature as the expansion process continued. For low pressure fuel injection (30 MPa), having a pilot injection at  $26^\circ$  BTDC followed by a main injection at  $6.6^\circ$  BTDC showed that most of the combustion energy released was diffusion controlled. Therefore, comparatively higher IMEP and PM emissions, and lower  $NO_x$  emissions were observed. Furthermore, varying the pilot and main injection timing had similar effect of improved IMEP as compared to single injection combustion. However, the pilot injection did not have a positive influence on HC and CO emissions as compared to single injection emission results. The ignition delay and combustion duration were observed to be comparatively lower when the pilot injection



occurred closer to TDC. However, the time interval between the pilot and main injection event did not have a significant impact on  $\text{NO}_x$  emissions. Additionally, the heat release rate and peak combustion temperature for multiple injection combustion events were lower than the single injection strategy at all conditions. Similar trials conducted with high pressure fuel injection (120 MPa) showed relatively little improvement in IMEP as the heat release rate was similar to the single injection combustion test. For cases where the time interval difference between the pilot and main injection was less than  $30^\circ$ , there was an improvement in IMEP. But, for all cases where the interval between the pilot and main injection was greater than  $30^\circ$ , the heat release rate trends were comparable due to sufficient air-fuel mixing time; hence, comparable atomization phenomena. Additionally, the fuel droplets close to the spray boundary mixed with excess air forming extreme lean mixtures, beyond the flammability limit for combustion resulting in greater HC emissions. It was found that, for a post fuel injection timing limit of  $20^\circ$  ATDC, post injection combustion assisted in decreasing PM emissions without any increase in  $\text{NO}_x$  emissions, and IMEP values comparable to the pilot-main injection case. However, including a pilot injection at or before TDC decreased the overall heat release by extending the diffusion controlled combustion phase leading to an increase in PM emissions as compared to main-post injection case. Above all, compared to pilot-main, main, post, and single injection strategies, pilot-main-post fuel injection at low pressure had the potential to decrease  $\text{NO}_x$  emissions by 30% and PM emissions by 40% with a comparatively low IMEP penalty of 3 to 4%.

Similar experiments were conducted by Hotta et al. aiming to achieve lower emissions in a high speed CI engine through the MPFI strategy [47]. At high load conditions,  $4.5 \text{ mm}^3/\text{stroke}$  of fixed pilot injection fuel quantity was varied from 0 to  $80^\circ$  BTDC with the main injection timing was fixed at  $4^\circ$  ATDC. The main injection fuel quantity was varied such that the PM emissions would not exceed a certain limit. It was found that for all pilot injection events before  $40^\circ$  BTDC, the IMEP was higher and the combustion noise was lower than single injection combustion results. In particular, for pilot injections earlier than  $55^\circ$  BTDC, the combustion chamber had an air-fuel mixture with an equivalence ratio close to one after the main injection event. However, HC emissions were comparatively higher suggesting lower  $\text{NO}_x$  emissions. For pilot

injection events after 40° BTDC, two distinct peaks in the heat release rate curve were observed resulting in increased combustion noise and lower IMEP values. At low and medium load conditions, a double pilot injection was more successful in reducing combustion noise, fuel consumption, NO<sub>x</sub>, and HC emissions as compared to the pilot-main and single injection option. When EGR was applied, it had a significantly positive impact on NO<sub>x</sub> emissions. However, HC emissions were pointedly higher for single pilot injection case. Additionally, it was found that the single pilot injection combustion event released close to 32% of the total heat before the main injection as opposed to 52% released by the double pilot injection combustion. This suggested that combustion of the double pilot was predominantly pre-mixed phase burn. However, HC emissions were higher as compared to single injection combustion due to cylinder wall wetting. This was solved by injecting the pilot relatively close to TDC (about 15-20° BTDC). The combustion results showed lower combustion noise, SFC, HC, and NO<sub>x</sub> emissions with a slight increase in PM emissions. Comparatively higher reductions of SFC, NO<sub>x</sub>, PM, and HC emissions were achieved by a combination of main and post injection of fuel close to TDC, around 5° ATDC, with high rates of EGR.

A combination of high EGR rates and MPFI strategies were used to reduce CI combustion emissions by Dronniou et al. [48]. Initially, single injection combustion tests with varying rates of EGR were studied to understand its influence on heat release and emissions. Heat capacity of the gas mixture in the cylinder was found to increase with decrease in O<sub>2</sub> concentration due to higher CO<sub>2</sub> concentration, yielding combustion with a lower adiabatic flame temperature. Additionally, reducing the heat capacity of the mixture enlarged the combustion duration due to a shorter ignition delay. These were the two primary reasons stated by the authors for reduced NO<sub>x</sub> emissions during combustion with low O<sub>2</sub> concentration. The main injection timing was fixed at 6° BTDC and the pilot injection timing was varied from 90-30° BTDC. The ROHR for the pilot and main injection combustion strategy with EGR showed three distinct peaks. The first peak occurred around 30° BTDC due to cool flame reactions, and the first heat release peak location was not influenced by the pilot injection quantity or timing. The second peak was due to pre-mixed combustion of the pilot, and its magnitude and location varied according to the pilot fuel injection timing and duration.

The third peak was due to the main injection combustion event. It was observed that increasing the pilot fuel injection quantity resulted in the advancement of the main heat release peak due to mixture stratification of pilot combustion and its subsequent reduction in ignition delay. Similar behavior was observed when the pilot injection was delayed. PM emissions decreased with increasing pilot fuel injection quantity without any penalty on NO<sub>x</sub> emissions due to extended combustion durations. However, HC and CO emissions were observed to increase with growing pilot injection quantity due to fuel entering the crevice volumes and fuel wall wetting. The simultaneous increase in CO and HC emissions suggested that the low temperatures of combustion were ineffective in burning the intermediate species produced during the pre-mixed combustion phase. Including a post injection was observed to be effective in reducing both PM and NO<sub>x</sub> emissions. Even with 50% EGR, PM emissions were nearly zero for this case. Additionally, fuel consumption and NO<sub>x</sub> emissions were lower as compared to the single injection and pilot injection combustion cases.

A six cylinder CI engine of a sports utility vehicle was optimized using the MPFI strategy with cooled EGR and a variable nozzle turbocharger in order to reduce emissions by Ishikawa et al. [49]. Using an advanced pilot fuel injection combustion event resulted in lower PM emissions with NO<sub>x</sub> emissions comparable to conventional single injection combustion. However, fuel consumption, HC, and CO emissions were all significantly higher due to cylinder wall wetting. Furthermore, increasing the pilot fuel injection quantity for early ignition did not increase the ROHR significantly suggesting that the fuel injected during the pilot was burned during the main combustion event. Under all conditions, NO<sub>x</sub> emissions were lower than single injection combustion due to the application of EGR. However, EGR usage was an added reason for increased HC and CO emissions.

The influence of MPFI strategies on NO<sub>x</sub> and PM emissions were studied using a multi-cylinder optical CI engine by Beatrice et al. [50]. The combustion noise, heat release and, hence, the NO<sub>x</sub> emissions were higher for pilot injection events around 15-20° BTDC, as compared to pilot injection close to TDC. The ignition delay for early pilot injection was comparatively higher leading to the dominance of premixed

combustion. Post injection events assisted in reducing PM emissions. However, increasing the fuel dwell time between main and post injection resulted in increased PM and decreased NO<sub>x</sub> emissions. The combustion temperature and heat release were comparatively lower as the delayed post injection fuel could not mix and burn as effectively due to the expansion process progression. Additionally, experimental visualizations, instantaneously after combustion, revealed that the flame and the combustion gases rapidly move towards the piston bowl creating significant turbulence due to swirl. This swirl created by combustion ensured better mixing of the fuel injected after the main combustion event. The amount of vapor fuel was higher for post injection as compared to pilot injection for the same reason. However, this assistance in forming better mixtures was reduced for post injection events farther away from TDC due to a reduction of turbulence in the combustion chamber. Furthermore, PM was observed to be generally in zones located at the combustion chamber center due to partial combustion of fuel rich mixtures.

Similar experiments of pilot-pilot-main and pilot-main-post injection strategies were conducted on a four cylinder CI engine by Badami et al. [51]. At low load conditions, injecting the first pilot very early was effective in reducing PM emissions as compared to injecting it close to TDC due to the predominance of pre-mixed burn phase combustion. However, varying the injection timing of pilot 1 and pilot 2 did not have a significant impact on NO<sub>x</sub> emissions. Additionally, fuel consumption values were comparatively lower for early pilot 1 injection events. However, NO<sub>x</sub> and PM values were higher than the dual injection strategy results described in [52], a research work by the same authors. The pilot-main-post injection strategy utilized at medium load conditions produced NO<sub>x</sub> and PM emissions lower than the dual injection strategy. Similar to the previous case, in the pilot-main-post strategy, the pilot injection timing did not have a significant influence on emissions as combustion was mostly diffusion controlled, and EGR assisted in reducing the combustion temperature. However, the fuel consumption was higher as compared to both pilot-pilot-main and dual injection experiments described in [52]. The performance and emission trends of pilot-main-post injection combustion at high loads were similar to medium load combustion results.

Heat release rate, PM, and NO<sub>x</sub> emissions were compared for single injection high temperature combustion, single injection LTC, and dual injection LTC experiments using two-color thermometry by Singh et al. [53]. Two types of single injection high temperature combustion experiments were conducted, one with low ignition delay, and the other with comparatively higher ignition delay. In another set of trials, two types of single injection LTC trials were conducted, one with early injection, and the other with late injection. For this case, the combustion temperatures were reduced by increasing the fuel injection pressure, decreasing the fuel injection quantity, and lowering the intake gas temperature. The short ignition delay high temperature combustion results were observed to have a majority of diffusion controlled combustion; hence, resulting in high PM emissions. Additionally, due to a high adiabatic flame temperature, NO<sub>x</sub> emissions were comparatively higher. Furthermore, approximately 1% of the total fuel energy was lost as radiative heat transfer from the hot, glowing PM. The ignition delay was doubled by varying the ignition timing for the high temperature long ignition delay case, and the heat release trends showed the dominance of pre-mixed combustion. Since the adiabatic flame temperature of combustion was high, NO<sub>x</sub> emissions were high as compared to the LTC case. However, the extended delay period ensured better air-fuel mixture preparation resulting in comparatively lower PM emissions. Similarly, lower PM emissions were observed for the LTC early single injection and dual injection trials due comparatively higher ignition delays. In contrast to the previous case, NO<sub>x</sub> emissions were significantly lower due to a lower adiabatic flame temperature. The radiative heat transfer losses for the LTC events, both single injection and dual injection, were significantly lower; approximately 0.01% because of a reduced PM formation.

The influence of injection pressure on heat release, flame luminosity, and emissions were studied by Fang et al. for an MPFI strategy using an optical CI engine [54]. Pilot fuel injection was set at 40° BTDC and main injection occurred at 5° BTDC. Two trials, one with 1000 bar fuel injection and the other with 600 bar fuel injection were compared. The fuel quantity was varied to maintain a constant BMEP. It was found that the fuel quantity had to be increased for lower injection pressures in order to maintain the BMEP value. The results showed that the higher injection pressure combustion resulted in a greater heat release and

comparatively longer ignition delay. Additionally, even though the fuel quantity was comparatively low, the in-cylinder bulk gas temperature before the start of ignition was lower for the high pressure injection case. These clearly suggested that a higher fuel injection pressure assists in atomizing and improving the spatial distribution of the fuel. The flame luminosity curve of high injection pressure combustion had comparatively higher rising and falling slopes suggesting lower PM formation along with effective oxidation of the PM formed. This was also confirmed by the flame spatial fluctuation and flame non-homogeneity trends; these terms are defined in [55]. The in-cylinder visualization images showed that the temperature for the pilot injection was not sufficient for ignition. However, the temperature was sufficient for thermal cracking while assisting in atomization and reducing PM emissions.

The effect of energy fractions of the first-stage of combustion, post fuel injection timing, EGR rate, and intake gas pressure on combustion noise, efficiency, and emissions were compared for a main-post injection strategy through experiments on a single cylinder CI engine by Ogawa et al. [56]. The IMEP was maintained at 0.7 MPa for all trials and the main fuel injection timing and quantity was adjusted such that 50% of the total heat release occurred at TDC. In the first set of trials, the ratio of energy released between the combustion of first stage due to the main injection and the second stage due to post injection was varied from 1 to 0 in stages of 0.15, 0.35, and 0.55. It was found that increasing the second stage energy fraction increased PM emissions and decreased  $\text{NO}_x$  emissions. This was due to extended combustion durations and dominance of the diffusion controlled combustion phase. However, this did not have a significant influence on CO and HC emissions along with thermal and combustion efficiencies. Additionally, combustion noise and in-cylinder pressure were comparatively lower. In the second set of trials, the energy fraction of the first stage of combustion was set at 35% and the post injection timing was varied. Delaying the post injection timing was found to reduce  $\text{NO}_x$  emissions along with thermal and combustion efficiency. However, the reducing combustion temperature due to decreasing the pre-mixed burn phase combustion increased exhaust heat loss, CO, HC, and PM emissions. In the next set of trials, for the same energy fraction as the previous case and post injection timing set at  $3.3^\circ\text{ATDC}$ , the EGR rate was varied. It was determined

that EGR rate did not have a significant impact on combustion noise and in-cylinder pressure. However, increasing the EGR rate had a significant impact on reducing NO<sub>x</sub> emissions. Moreover, HC, CO, and PM emissions were comparatively higher due to a reduced combustion temperature; hence, lower combustion and thermal efficiencies were found. Increasing the intake air pressure assisted in reducing PM, CO, and HC emissions without a significant penalty on NO<sub>x</sub> emissions. Additionally, thermal efficiency was comparatively higher.

MPFI strategies were used to implement LTC on a high CR CI engine by Asad et al. [57]. The injection timings were set at 48, 35, and 22° BTDC. Increasing the intake air temperature reduced the ignition delay resulting in a higher pre-mixed burn phase; hence a greater heat release rate and elevated combustion temperature. However, HC emissions were comparatively higher due to fuel wall wetting. To achieve LTC, high rates of EGR were applied that assisted in extending the ignition delay resulting in comparatively lower NO<sub>x</sub> emissions. Additionally, HC and CO emissions were comparable to single injection combustion tests. However, PM emissions were high due to the influence of EGR. Increasing the fuel injection pressure decreased PM emissions without significant penalty on NO<sub>x</sub>, HC, and CO emissions. Furthermore, increasing the operating engine speed at high EGR rates grew HC and CO emissions due to amplification in the quantity of fuel injected. However, this did not have an influence on NO<sub>x</sub> and PM emissions. Since the ignition delay was relatively high as compared to single injection high temperature combustion, it was found that extending the load limit was possible by using post injection close to TDC while still maintaining low combustion temperatures. Similar to others (e.g., [40, 43, 44, 46-48, 50, 51, 56]), post injection combustion was observed to be effective in reducing both PM and NO<sub>x</sub> emissions as compared to single injection combustion and multiple pilot injection combustion results.

Due to the typical characteristics of CI combustion, diffusion combustion and high temperatures, simultaneous reduction of NO<sub>x</sub> and PM emissions is challenging. PCI combustion is being studied by many researchers as it has the potential to decrease the diffusion burn phase of the combustion, while maintaining lower combustion temperatures [58]. In addition, the LTC ensures reduced heat loss characteristics.

## **Chapter III: Investigating Pre-mixed Charge Compression Ignition Combustion in a High Compression Ratio Engine.**

### **3.1 Abstract**

Utilizing a higher CR in a CI engine grants an obvious advantage of improved thermal efficiency. However, the resulting combustion temperatures promote dissociation ensuing in increased NO<sub>x</sub> emissions. Unfortunately, due to the inherent properties of CI combustion, it is difficult to achieve simultaneous reduction of NO<sub>x</sub> and PM through conventional combustion methods. Taking a different route though accomplishing HCCI in CI engines will largely eliminate NO<sub>x</sub> and PM; however, combustion can result in a significant increase in HC and CO emissions due to the low volatility of diesel fuel. Hence, this work attempts another avenue of LTC by employing PCI combustion on a comparatively higher CR (21.2) single cylinder CI engine. An injection timing sweep was conducted using a common rail injection system with a 6-hole nozzle injector. Exhaust emissions were monitored using a Fourier Transform Infrared Spectroscopy (FTIR) device and Smoke Meter to analyze the extent of the NO<sub>x</sub>-PM trade-off along with both HC and CO emissions. Finally, a fuel injection quantity sweep with the fuel injection timing fixed at 60° Before Top Dead Center (BTDC) and 100° BTDC was performed to determine the maximum amount of fuel that may be injected early in the compression stroke without a significant growth in the heat release due to combustion. As the power generated was comparatively lower at advanced fuel injection timings, thermodynamic calculations and a heat release program were utilized to comprehend the magnitude of combustion.

### **3.2 Introduction**

Kinetically controlled high temperature combustion of lean mixtures is ideal for the formation of NO<sub>x</sub> emissions. Conversely, diffusion regulated combustion of rich mixtures results in PM emissions. A reduction in NO<sub>x</sub> can be realized by extending the duration of the diffusion burn; whereas, a high percentage of kinetically controlled combustion (aka pre-mixed burn) ensures lower PM emissions. As a result, a NO<sub>x</sub>-PM emissions tradeoff becomes apparent. The core issue of restricting these emissions in CI engines



depends on the difference between the bulk gas and local combustion temperatures. Particularly, when the bulk gas temperature is low but the local combustion temperature is high,  $\text{NO}_x$  emissions are excessive. Likewise, if the  $\text{O}_2$  availability in the bulk gas is greater than the local combustion region, PM emissions will result. Hence, it is quintessential to overcome the temperature and mixture distribution differences between these two regions to promote low emissions. In other words, instantaneous ignition of a lean and homogeneous air-fuel mixture has the potential to beat this  $\text{NO}_x$ -PM tradeoff. Since there is no distinguished flame propagation, the local combustion temperatures are relatively low, subsequently reducing  $\text{NO}_x$  emissions. In addition, combustion duration is low due to the predominance of a kinetically controlled pre-mix burn phase resulting in lower PM emissions. Furthermore, compared to conventional CI combustion, higher thermal and fuel conversion efficiencies are possible with this LTC operation [19]. However, increased HC and CO emissions, restricted engine operating conditions, and combustion control challenges have restricted the large scale practical implementation of LTC engines [59].

LTC can be achieved using HCCI, PCI, and MPFI techniques. While HCCI combustion of diesel fuel through port fuel injection in a CI engine is possible [19-22, 58, 60, 61], one significant disadvantage is the increase of HC/CO emissions and fuel consumption due to the low volatile nature of diesel fuel [19, 20, 27, 59, 61, 62]. Heating the intake manifold and utilizing dedicated fuel vaporizers have assisted in reducing the amount of fuel wall wetting in the intake port [19, 60, 61]. However, these setups are currently unavailable at the authors' university and the idea itself is likely impractical from a commercial application point of view. Moreover, another major drawback of HCCI, even when employing high rates of Exhaust Gas Recirculation (EGR), is the restriction in operating conditions to lower loads [19-22, 58, 60, 63]. Furthermore, controlling combustion phasing even in stationary operation is challenging due to knock (and noise) limitations [58].

PCI combustion is a more applicable approach to achieve LTC by employing extremely advanced direct in-cylinder fuel injection to provide sufficient time for the fuel to atomize with the air in the combustion chamber, forming a nearly homogeneous mixture. For a fixed amount of fuel injection quantity and

pressure, advancing the fuel injection timing earlier than  $80^\circ$  BTDC resulted in a gradual increase of the HI and FVMF [33]. The resulting short duration LTC event had a negligible diffusion controlled phase, forming relatively low  $\text{NO}_x$  and PM emissions [16, 26-28, 32-34]. However, delaying the fuel injection timing to around  $50^\circ$  BTDC comparatively increased the combustion temperature and the duration of combustion resulting in greater  $\text{NO}_x$  emissions, but without a notable increase in PM emissions. Furthermore, delaying the fuel injection timing close to TDC deteriorates the homogeneity of the air-fuel mixture. Hence, PM emissions are comparatively greater due to an extension of the diffusion burn phase. Typically, for advanced fuel injection, since the combustion chamber and the cylinder walls are at a low temperature, fuel consumption, HC, and CO emissions are significantly high due to fuel wall wetting, fuel entering the crevice volumes, and incomplete combustion of over-lean mixtures below the flammability limit [16, 20-24, 26-29, 32-36, 38, 39]. Utilizing pintle-nozzle injectors, and/or impinged fuel injection strategy is a common method used to reduce fuel penetration and subsequent HC emissions [16, 26-28, 33, 34, 39]. Employing a narrow fuel spray angle, reducing the crevice volume, and increasing the piston bowl depth are alternate approaches attempted to reduce HC emissions [16, 26, 28, 30, 31, 36, 37]. While reduced fuel penetration assisted in enhancing the fuel conversion rate at low load conditions, significantly higher SFC was observed while operating at high load conditions [16, 20, 22-24, 26-29, 32-35, 38, 39].

Unfortunately, similar to HCCI, PCI combustion is limited to low load conditions when EGR is not employed [20, 26, 28, 32, 33, 39]. Increasing the fuel injection quantity to operate at high load conditions and moving from lean to nearly stoichiometric equivalence ratios has been found to degrade the combustion stability [36]. In addition, a rapid increase in heat release is observed leading to CI combustion knock [36, 58]. As a result, reducing the geometric, or effective CR of the engine, has been shown to facilitate an extension in the engine operating range while also providing for better combustion timing control [24, 27, 34-36]. Lowering the CR increases the ignition delay period allowing for a comparatively lower diffusion burn phase by promoting pre-mixed combustion. As a result, a successful reduction of  $\text{NO}_x$ , without any substantial increase in HC and CO emissions can be achieved with lower pressure fuel injection (about 30-

50 MPa) [24, 33-35]. The extent of fuel penetration was stated to be minimal due to a reduced fuel jet velocity and comparatively larger fuel droplets. However, low pressure fuel injection strategies may fail to form a homogeneous mixture. Hence, the reduction in  $\text{NO}_x$  emissions may be potentially due to incomplete combustion, and not because of LTC operation. Comparatively higher PM emissions that were found are added evidence of a heterogeneous mixture formation during these experiments.

For a given amount of fuel, the thermal efficiency of a thermodynamic cycle can be increased by employing a high CR engine [5]. Furthermore, LTC operation has the potential to further increase this efficiency while simultaneously reducing both  $\text{NO}_x$  and PM emissions. However, knock limitations due to an excessive pressure rise during LTC often require researchers to lower the CR. In order to determine what limitations are evident using the authors' high CR (21.2) engine and NA test cell, it is necessary to attempt PCI combustion, and analyze its advantages and restrictions in improving the combustion performance and subsequent emissions. An available cooled EGR system was not employed in the first set of experiments; hence, combustion phasing was controlled by varying the fuel injection timing, pressure, and amount. An initial characterization of PCI combustion was first accomplished followed by a series of trials to analyze the emissions and performance characteristics as a function of varying fuel injection timing and quantity. Furthermore, thermodynamic evaluations are performed to comprehend the extent of combustion.

### **3.3 Experimental Setup**

Combustion performance and emissions testing was performed on a single cylinder, NA, air cooled, DI, CI Yanmar L100V engine with specifications as shown in Table 1. A 12 hp Dyne Systems alternating current dynamometer is connected to the engine through a driveshaft and monitored by an Inter-Loc V controller that regulates the engine speed. A Futek torque transducer (model #TRS-705) is used to measure the real time torque. The dynamometer is calibrated through the controller prior to each test. In-cylinder pressure and crank angle position data is provided by a Kistler pressure transducer (model #6052c) and a Kistler crank angle encoder (model #2614B), respectively, at a resolution of 0.2 degrees crank angle. The final in-

cylinder pressure data are an average measurement of 60 thermodynamic cycles measured at every 0.2 degrees of crank angle in every cycle.

A Merriam laminar flow element (model #50MW20-2) is employed to measure the intake air flow rate. A large-volume plenum is placed in line with the air flow measurement and the intake manifold to reduce the fluctuations in measurement due to the rapid opening and closing events of the intake valves. A Micro-Motion Coriolis flow meter (model # CMF010M) is utilized to measure the fuel flow rate. An Omega differential pressure transducer (model #PX277-30D5V) is used to measure the ambient, intake manifold, and exhaust manifold pressure data. The air flow, fuel flow, temperature and pressure data are various points are recorded at a frequency of 10 Hz.

**Table 1. Yanmar single cylinder engine specifications**

Manufacturer and model	Yanmar L100V
Type	Vertical Direct-Injection Compression Ignition
Engine Intake	Naturally Aspirated
Cooling	Air-Cooled
Cycle	4-Stroke
Number of Cylinders	1
Number of Valves	1 Intake, 1 Exhaust
Bore [mm]	86
Stroke [mm]	75
Displacement [L]	0.435
CR	21.2
Continuous Rated Output [hp]	8.3
Rated Speed [rpm]	3600
Clearance Volume [m <sup>3</sup> ]	$2.161 \times 10^{-5}$
Connecting Rod Length [m]	0.188
Crank Radius [m]	0.038
Piston Face Area [m <sup>2</sup> ]	$5.808 \times 10^{-3}$
Inlet Valve Closing [° ATDC]	122
Exhaust Valve Opening [° BTDC]	144
Number of Injectors	1
Injector Holes	6
Injector Hole Diameter [mm]	0.17
Engine Oil	Shell 15W-40

The exhaust gas passes through a heated sampling line into an AVL Smoke Meter (model #415-s) which measures the Filter Smoke Number (FSN). Subsequently, the exhaust gas flows through an AVL SESAM FTIR analyzer which has an integrated flame ionization detector to measure total hydrocarbons (THC) and chemiluminescence detector to measure NO<sub>x</sub>, and paramagnetic detector to measure O<sub>2</sub>. The FTIR system is capable of measuring regulated emissions, such as CO<sub>2</sub>, CO, nitrogen oxide, and NO<sub>2</sub>. Additionally, the FTIR system is capable of measuring non-regulated exhaust components, including ammonia, nitrous oxide, isocyanic acid, hydrogen cyanide, alcohols, and aldehydes. A total of 300 readings are taken over a duration of five minutes at a rate of one measurement per second. These 300 measurements are logged through a separate computer using a LabVIEW program for logging the output. The emission analyzer is calibrated once after every emissions test is completed.

**Table 2. Default ECU fuel parameters [64].**

Fuel parameter	Magnitude
Fuel injection pressure [MPa]	48±0.1
Fuel injection timing [°BTDC]	12.5

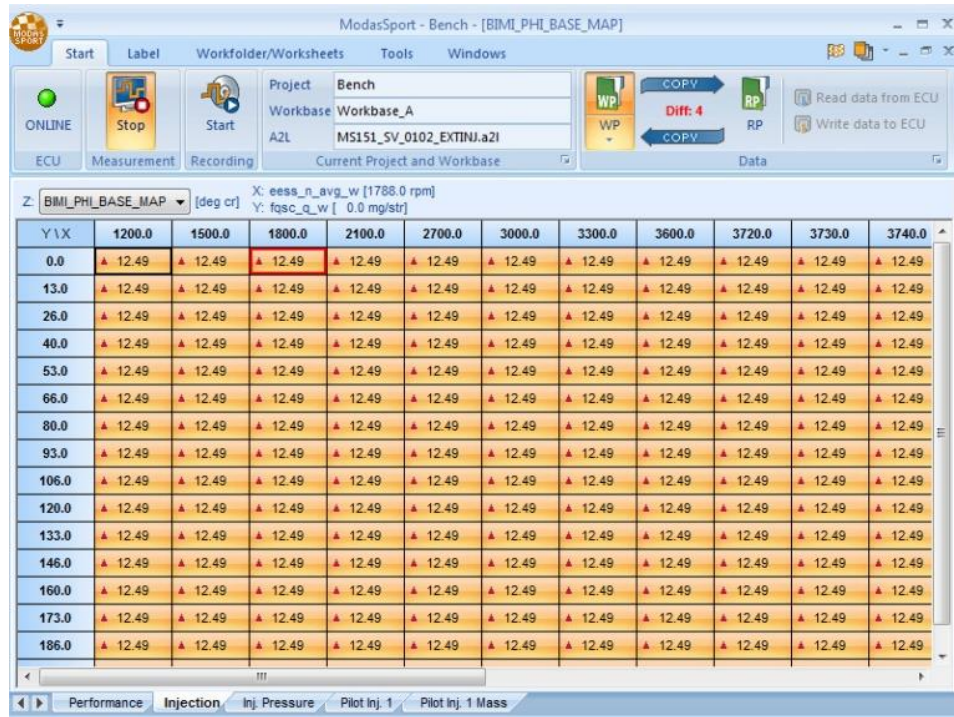


**Figure 15: Screenshot of fuel injection timing ECU map.**

Previous efforts of Mangus [64] successfully replaced the original manufacturer inline pump mechanical fuel injection system with a common rail fuel injection system including a Fiat Punto multi-hole injector (Grande MJD 1.3) with six injector holes. A Bosch MS15.1 Diesel ECU running Bosch Modasport is utilized to control the common rail EFIS. An automation system on a dedicated computer communicates with the ECU and controls the common rail fuel injection system variables, such as fuel rail pressure, fuel injection pressure, and fuel injection timing. Additionally, the crank angle encoder and the torque transducer provide real-time information that is used to generate a corresponding fuel parameters signal. Adjustable maps of fuel rail pressure, fuel injection timing, and fuel injection pressure are integrated with default fuel parameters settings provided in Table 2. Fuel injection quantity can be varied by adjusting the fuel input percentage as illustrated in Figure 15; analogous to a gas throttle pedal. For this percentage, 0% to 100% is calibrated based on the torque limit of the engine [64].

**Table 3. Properties of tested fuel.**

Property	ULSD
Density [kg/m <sup>3</sup> ]	837.58
Kinematic Viscosity [cSt]	2.58
Dynamic Viscosity [cP]	2.16
Cetane Number	40
Energy Content [kJ/kg]	41530
Volumetric Energy Content [MJ/m <sup>3</sup> ]	34785

Ultra-Low Sulphur Diesel (ULSD) with properties given in Table 3 was used as the standard test fuel during the testing process [65-67]. Prior to testing, the engine is warmed up by running at 1800 rpm until exhaust and oil temperatures deviate by less than 1% over the course of a minute, signifying that the engine has warmed up and reach a reasonable steady-state. Further information about the test bed apparatus and common engine testing procedures using this setup are provided in [64, 65]. PCI combustion was attempted by early fuel injection to accommodate a higher air and fuel mixing duration. In order to accomplish this, the fuel injection timing was changed to 60° BTDC and 100° BTDC for the respective tests as described in the following sections. A heat release model was additionally utilized to analyze the in-cylinder pressure data [68].

### **3.4 Fuel Injection Timing Sweep**

In the first set of experiments, performance data was collected at 1800 rpm with a desired constant fuel injection quantity of 21.0 mg/stroke. Since extremely advanced fuel injection combustion was never tested on this setup before, a comparatively low fuel quantity was injected to observe the in-cylinder pressure data while ensuring safety of the equipment. For this, the fuel injection timing was advanced from 15° BTDC to 80° BTDC starting from the default fuel injection timing (12.5° BTDC) in relatively small increments.



Initially at  $12.5^\circ$ , combustion appears to start slightly after TDC with both the pressure trace (Figure 16a) and the sudden increase in the ROHR (Figure 17a) suggesting that the combustion process is predominantly pre-mixed. This is not unexpected given the relatively low amount of fuel injected and low load of the engine (full load is 18.0 N-m and the engine operates largely pre-mixed up until 9.0 N-m) [69]. For fuel injection events earlier than  $12.5^\circ$  BTDC but prior to  $30^\circ$  BTDC in Figure 16a, the fuel and air appear to be well-mixed with a growing in-cylinder pressure. Comparing the motoring curve with these tests illustrates that the SOC occurs significantly earlier than desired; i.e., into the compression stroke. This is likely due to the high CR of the engine promoting compression temperatures beyond the auto-ignition temperature of ULSD (about 530 K [70]). As presented in Figure 18, the calculated global in-cylinder temperature exceeds the auto-ignition temperature approximately at  $40^\circ$  BTDC and the maximum temperature grows with advanced injection timing (related to pressure via the ideal gas law). Similarly, the ROHR shown in Figure 17a indicates premixed combustion for all events. Furthermore, up to  $30^\circ$  BTDC the high-frequency oscillation in the combustion traces illustrate the presence of CI engine knock.

Interestingly, starting at  $30^\circ$  BTDC the in-cylinder pressures begin to fall while smoothing out and CI knock is no longer seen. In addition, measured torque becomes negative at  $40^\circ$  BTDC as the majority of combustion now happens during the compression stroke. As fuel injection is advanced, the ignition delay time also grows promoting more time for mixing. However, as indicated in Figure 17, combustion was already largely premixed; hence, an increase in ignition delay will not significantly impact the level of premixed versus diffusion burn. Given the relatively high CR of the engine and the fact that the auto-ignition temperature of ULSD is achieved well into the compression stroke, the combustion process appears to becoming more gradual. This is also evident in the heat release plot in Figure 17b as the pre-mixed spike goes away at  $50^\circ$  BTDC. This observation is consistent with the results of Lee et al. and Miyamoto et al., where the homogeneity of the fuel was found to increase at advanced injection timings due to the surplus time available for mixing [32, 33]. By this analogy, the homogeneity of the fuel air mixture for injection earlier than  $25^\circ$  BTDC is comparatively high. Ideally, in such a situation, the in-cylinder pressure and

temperature must have a significant spike as a vast majority of the fuel burns instantaneously. However, the ROHR and cylinder pressure begin to reduce gradually for earlier injection events suggesting poor combustion efficiencies, and an overall lowering in the fraction of fuel mass that is consumed by combustion. Similar results of decreasing ROHR at advanced injection timings was observed by Nishijima et al. [28]. This is evident from the increasing total hydrocarbon and CO emissions (described later).

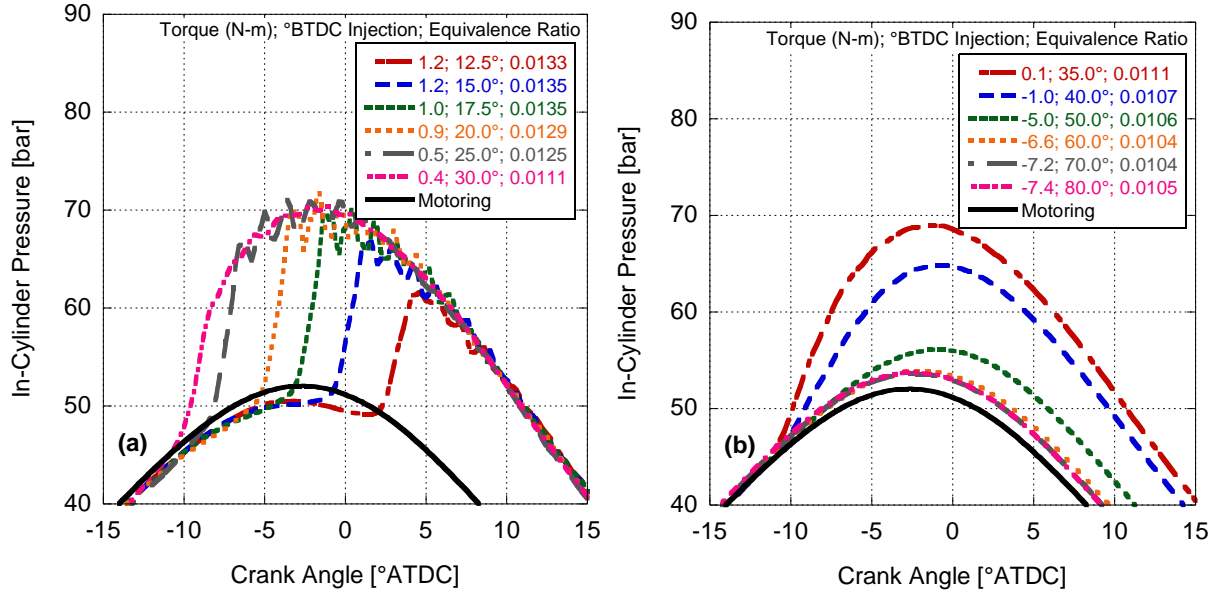


**Figure 16: In-cylinder pressure vs. crank angle for 21.0 mg/stroke fuel injection quantity for fuel injection timing (a) 12.5 to 30° BTDC, and (b) 35 to 80° BTDC.**

During these experiments, a decrease in actual equivalence ratio was found as seen in Figure 19. Based on the ECU set point and the fact that the air flow rate into the engine was relatively constant (maximum deviation of 1.5% between any two points considered), the equivalence ratio should have remained around 0.0135 (open squares in Figure 19). However, the fuel flow rate reduced for injection events earlier than 20° BTDC, and the decrease in fuel quantity is gradual after a significant dip observed at 30° BTDC. Overall, there was an approximately 23% reduction in the fuel injection quantity (16.5 mg/stroke) at 50° BTDC and earlier as compared to the fuel injected at 12.5° BTDC (21.0 mg/stroke). The change in the fuel injection quantity is assumed the “corrections” made by the ECU while generating the fuel control signals.

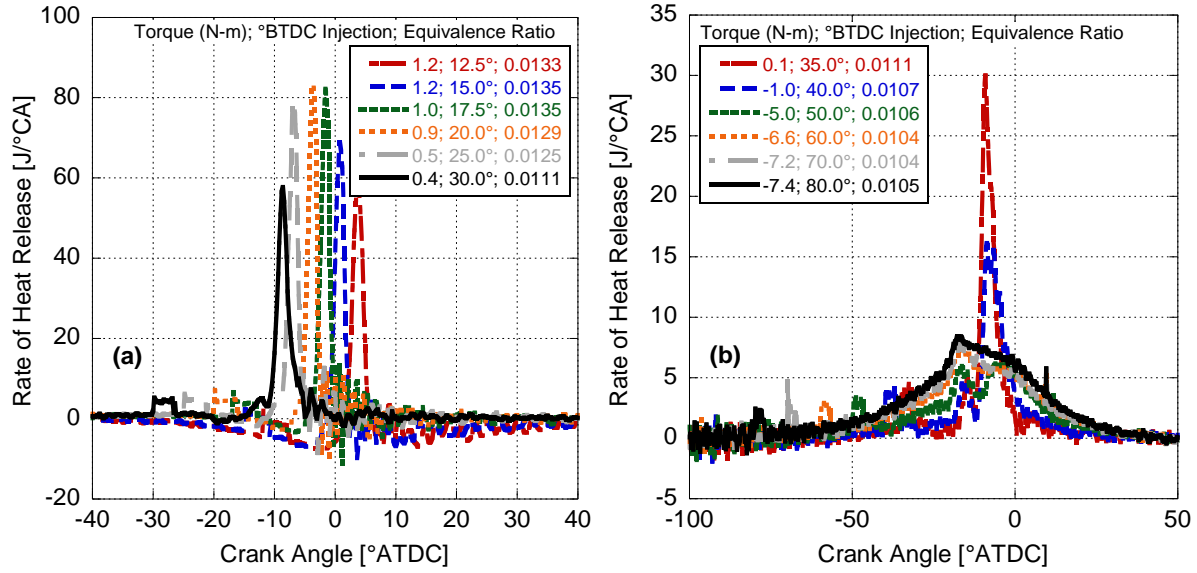


**Figure 17: Rate of heat release vs. crank angle for 21.0 mg/stroke fuel injection quantity for fuel injection timing (a) 12.5 to 30° BTDC, and (b) 35 to 80° BTDC.**

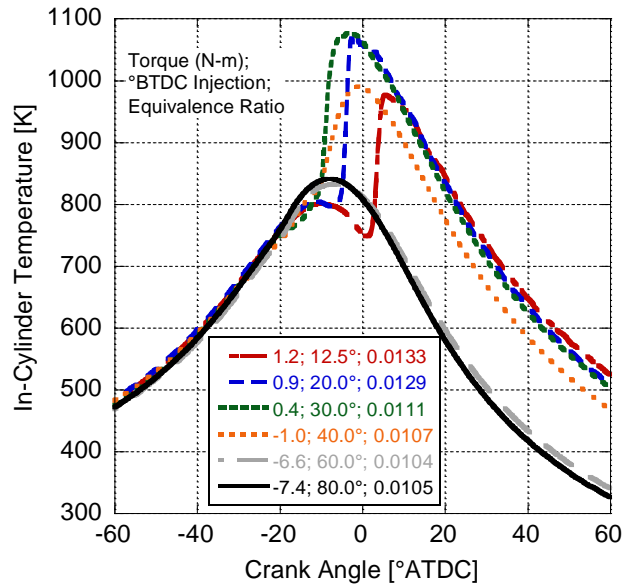


**Figure 18: In-cylinder temperature vs. crank angle for selected injection events from injection timing sweep trial.**

The ECU generates the fuel input signal based on the demand fuel throttle input command and the fuel injection pressure. Additionally, it is also influenced by the engine speed and engine torque values. During these trials, the fuel throttle percentage and the fuel injection pressure were set to a constant value.

Moreover, the dynamometer ensured that the engine speed was maintained at 1800 rpm. In addition, the torque maps fed to the ECU have only positive values. As a result, negative engine torque at injection events earlier than 30° BTDC may be forcing the ECU to manipulate the fuel input signal resulting in a reduced fuel quantity injected. Furthermore, the soft limit setting in the ECU for early fuel injection by default is set at 20° BTDC. For earlier fuel injection, the ECU warns the user about overpassing the soft limit, which could also factor into the reduced fuel injection quantity.

In regards to NO<sub>x</sub> emissions (Figure 20), they were found to increase between 12.5° BTDC and 25° BTDC reflecting the growth in temperature and ROHR for the respective trials. Of note, NO<sub>x</sub> and other emissions are presented on a part per million basis instead of a more normalized g/kWh basis due to the fact that negative torque (and negative power) is generated at few of the injection timings. This may skew the results slightly due to the change in fuel quantity added (i.e., Figure 19), but trends are still apparent. A significant drop in NO<sub>x</sub> emissions was observed for injections earlier than 25° BTDC due to reduced combustion temperatures and corresponding ROHR profiles. Particularly, for injections earlier than 30° BTDC, NO<sub>x</sub> emissions are comparatively low as the in-cylinder temperature is significantly reduced as indicated in Figure 18; hence, reflecting the impact of temperature upon thermal NO kinetics. Of interest, injecting at 30° BTDC finds that NO<sub>x</sub> emissions are relatively low even though global temperatures appear high.

While the in-cylinder combustion temperature was relatively constant for injections 20° through 30° BTDC, a significant drop in NO<sub>x</sub> emissions was observed for the injection at 30° BTDC. Looking at the in-cylinder pressure trace of Figure 16a finds that this is the transition point between a dramatic premixed combustion event and a more gradual burn. In addition, the decrease in ringing combustion (as evidenced by the loss of high-frequency oscillations in the pressure trace across this same range of injection timings) also points to a more gentle and gradual combustion event. As elucidated by Dickey, et al., decreasing the difference between the global and local combustion temperatures could result in lower NO<sub>x</sub> emissions, the potential for which is comparatively high at 30° BTDC due to increasing homogeneity of the mixture [28, 42].

Another possible explanation for the lower  $\text{NO}_x$  emissions is Negative Temperature Coefficient (NTC) behavior during the dual stage combustion of diesel fuel in this temperature range. During the compression stroke, the alkyl radicals  $R$  in the fuel reacting with  $\text{O}_2$  molecule could form: 1. alkyl-peroxide radical, 2. alkenes with hydroperoxyl ( $\text{HO}_2$ ), or 3. cyclic ether with hydroxide ( $\text{OH}$ ) [71, 72]. The alkyl-peroxide radicals go through isomerization and subsequent decomposition leading to auto ignition. However, auto ignition is stalled if the amount of heat gained by a fuel droplet is less than the amount of heat lost through conduction, convection, and radiation. This gain and loss of heat, called net heat, is found to determine the overall reaction rate of the combustion and the flame propagation [73]. In other words, the energy transferred to the fuel droplet is insufficient to successfully go through the isomerization and subsequent auto-ignitions; a higher likelihood the earlier the fuel is injected due to a relatively lower rate of temperature change from the compression event. It is observed that the reaction rate constant is reduced due to the relatively less reactive  $\text{HO}_2$  formed [71, 72, 74]. While operating in this temperature regime, increasing the temperature could lead to the appearance of cool flames (first stage of combustion); but, does not alter the reaction rate until the temperature is high enough for the instigation of the second stage of combustion. This results in incomplete combustion of the mixture, leading to lower  $\text{NO}_x$  emissions. Of note, NTC behavior is comparatively low for equivalence ratios less than 1 and, unfortunately, experimental and/or numerical data of NTC trends for equivalence ratios less than 0.5 is limited in the literature [75].

For injections earlier than  $30^\circ$  BTDC,  $\text{NO}_x$  emissions are comparatively low as the in-cylinder temperature is significantly reduced as indicated in Figure 18; hence, reflecting the impact of temperature upon thermal  $\text{NO}$  kinetics. The witnessed trend could also be due to the NTC phenomenon which is comparatively dominant at temperatures between 750 and 950 K [75]. This observation of decreased combustion temperatures and  $\text{NO}_x$  emissions at advanced fuel injection events is consistent with the results found by other researchers [24, 33-35].

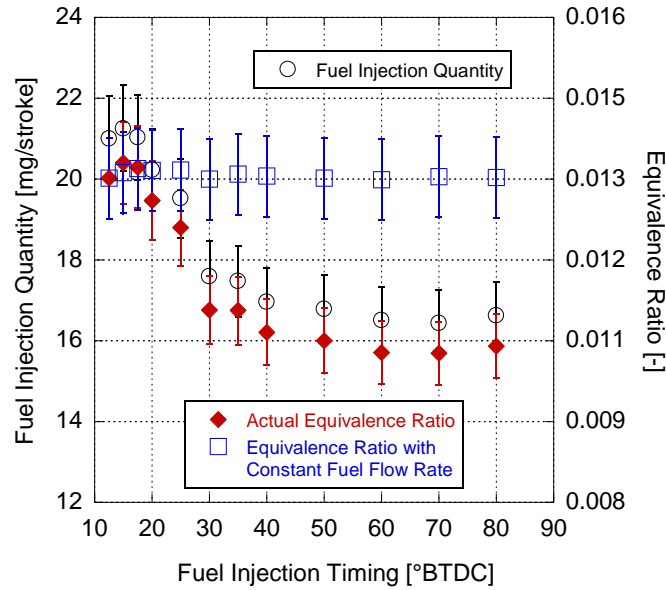


**Figure 19: Fuel injection quantity and equivalence ratio vs. fuel injection timing for fuel injection timing sweep trial.**

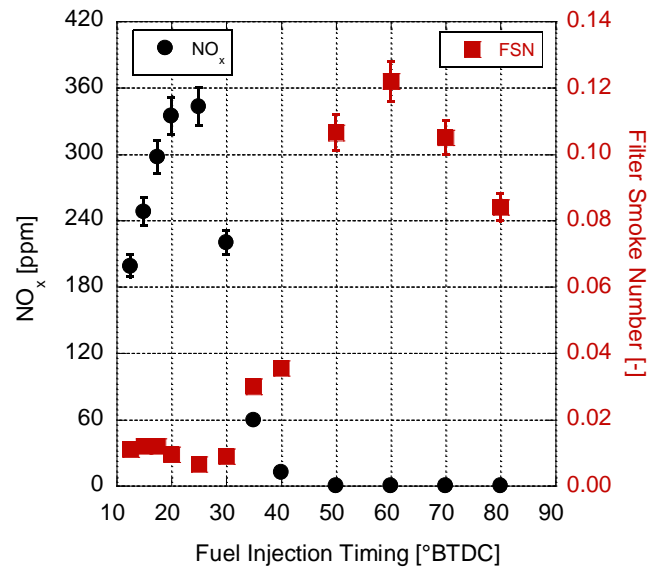


**Figure 20: Nitrogen oxides and FSN emissions results at various fuel injection timings.**

Smoke emissions in Figure 20 appear initially to be largely in agreement with the NO<sub>x</sub> emissions following the so-called NO<sub>x</sub>-PM tradeoff. When NO<sub>x</sub> is high, PM is low; however, now, this tradeoff does not follow the common shifting between the pre-mixed and diffusion burn regimes for conventional CI combustion. As the injection event is advanced into the compression stroke, there is an increased likelihood of wall

wetting and fuel entering the crevice volumes along with reduced combustion efficiencies because the cylinder temperature is comparatively cooler at the time of injection. Investigating further, Figure 21 presents cutouts of the filter paper from the AVL Smoke Meter during the earlier injection events with the circles representing the area of exhaust sampling on the filter paper. Smoke meter results of 12.5° to 30° BTDC were not added as there was no significant difference noticeable by the naked eye. As one can see from the image, the filter paper shade gradually gets darker for advanced injection events. Additionally, the brown color of the paper strongly suggests a growth in the amount of HCs finding their way into the exhaust stream. Since the measuring principle of the Smoke Meter does not distinguish between the deposits due to carbon particle and HCs, it is postulated here that the growth in FSN is due not to PM but to an increase in the amount of unburned fuel until wall wetting and crevice flows become significant enough to reduce the amount of fuel burned; thus, lowering FSN at extremely advanced timings. Again, injection at 30° BTDC appears to be a deviation from the trends; relatively low PM at a reduced NO<sub>x</sub> level with a filter paper image largely clear.

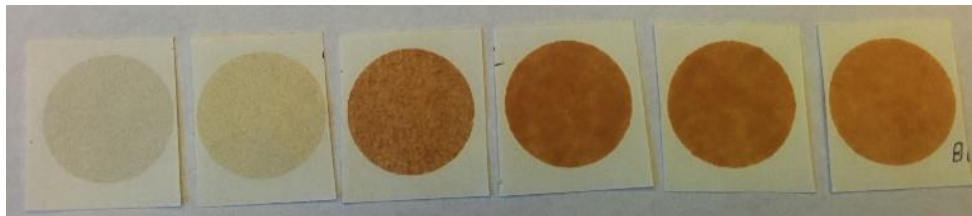


**Figure 21: Image of the filter papers from the AVL Smoke Meter during emissions measurement for 35° to 80° BTDC injection events (left to right).**

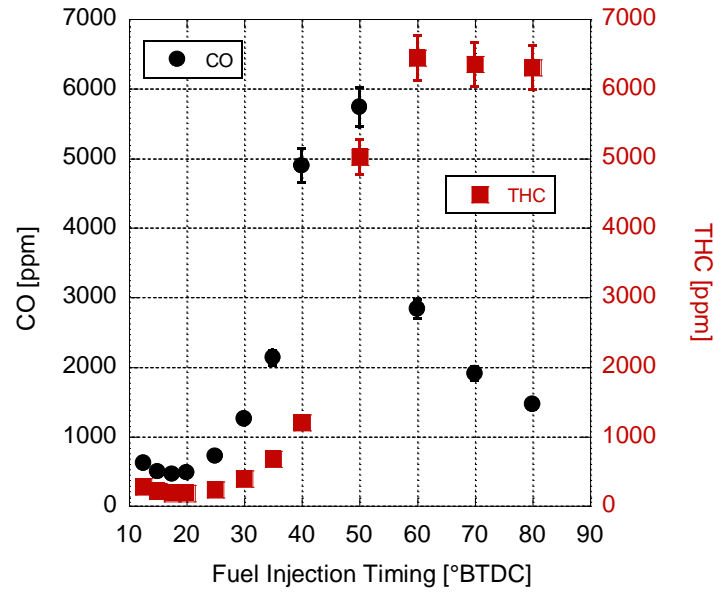
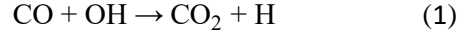


**Figure 22: THC and CO emissions results at various fuel injection timings.**

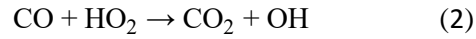
With respect to the THC and CO emissions in Figure 22, they follow a trend similar to the smoke emissions. When the FSN is low, THC and CO emissions are low; whereas, when FSN increases so does both THC and CO. It appears that at advanced injection events (before 30° BTDC) when the mixture at this stage is relatively homogeneous, there is a decrease in the combustion efficiency. Furthermore, during the late stages of combustion and the exhaust blowdown process, any additional fuel that found its way to the crevices may re-enter the cylinder and find its way into the exhaust subsequently increasing THC emissions. However, CO emissions start decreasing at extremely advanced injection timing even though THC emissions level off.

It has been well established that CO is the major byproduct of HC oxidation, which is subsequently converted into CO<sub>2</sub> [76]. Since HC oxidation inhibits this conversion, CO oxidation occurs later in the combustion cycle after the disappearance of all the HC species [77]. Therefore, CO emissions follow THC emissions for injection between 12.5° and 20° BTDC when combustion efficiencies and temperatures are relatively high. For injections earlier than 20° BTDC, there is a gradual increase in THC emissions due to incomplete combustion. With respect to CO conversion, it occurs according to the following at relatively high temperatures (around 1100 K) due to the excessive availability of OH radicals:





Hence, looking at Figure 18, it appears that between 25° and 50° BTDC combustion temperatures are near this regime. As a result, CO emissions increase due to inhibition by HC oxidation. Interestingly, at comparatively steady temperatures (gradual variation), CO conversion follows a different kinetic route given by the presence of high concentrations of HO<sub>2</sub> species:



The temperature variations for injection events earlier than 50° BTDC are more gradual; consequently, favoring CO conversion through HO<sub>2</sub> radicals. This results an observed reduction in CO emissions from 60° to 80° BTDC. It is important to note that while OH radicals are available at low temperature regimes, reaction kinetics do not prefer CO conversion by OH radicals. Hence, CO conversion by Equation (1) is negligible for early injection events.

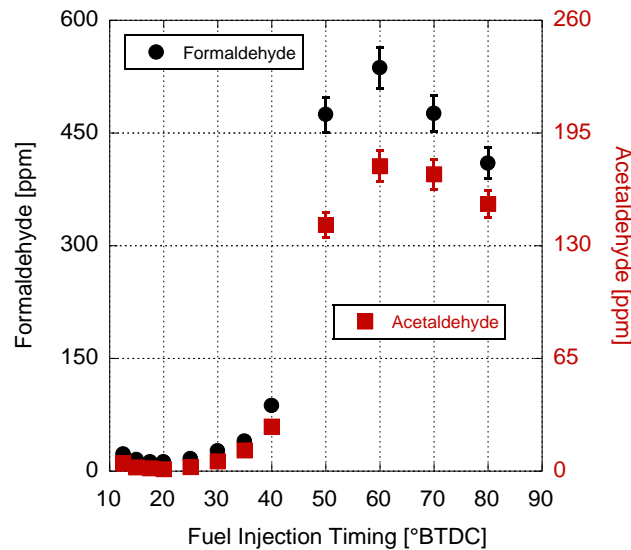
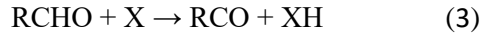


**Figure 23: Formaldehyde and acetaldehyde emissions results at various fuel injection timings.**

In addition to regulated emissions, unregulated aldehyde emissions were also measured. Compared to conventional combustion, aldehydes are higher during HCCI and PCI combustion [78]. Particularly, aldehyde emissions in HCCI combustion are significantly higher as compared to PCI combustion [79].

Formaldehydes constitute more than half of the total aldehyde emissions in CI engines, and the remaining half is composed of other heavy aldehydes [80]. Formaldehydes are intermediate species formed during the oxidation of HCs that are nearing the explosion limit at low temperatures. This phenomena has been utilized to visually indicate the SOC in both SI and CI engines by other researchers [81-83].

Formaldehyde and acetaldehyde were both observed to be comparatively low for injection events later than 35° BTDC. For injections earlier than 40° BTDC, both acetaldehyde and formaldehyde emissions generally increase. Similar observations of increasing formaldehyde and acetaldehyde emissions with decreasing torque produced by the engine was observed by Storey, et al. [79]. However, for injections earlier than 60° BTDC, both formaldehyde and acetaldehyde are observed to reduce gradually. It has been discerned that during LTC of lean mixtures, aldehydes react with radicals (e.g., X) according to [77]:



where the generalized radical X provides a representation of OH, O<sub>2</sub>, hydrogen, and methyl groups. Additionally, the conversion effectiveness of these radicals is in this same order as represented by Equation (3). Hence, the availability of OH for injections earlier than 50° BTDC is greater since they are the byproducts of CO converting to CO<sub>2</sub> via Equation (2) as explained before. As a result, aldehyde emissions are comparatively lower for early injection events because of conversion by OH.

Overall, it appears that there is a local optimum of combustion when a particular amount of fuel is injected at 30° BTDC. Combustion efficiencies remain relatively high; whereas, NO<sub>x</sub> emissions decrease even though global temperatures are still significant. To provide further insight into the impact of high CRs on extremely lean combustion, fuel sweeps were accomplished at earlier injection timings (60° and 100° BTDC based on previous PCI efforts in the literature [16, 27, 32]) to understand the influence of the amount of fuel.

### 3.5 60° and 100° BTDC Injection Timing Fuel Sweep

A second set of trials was conducted at a constant 60° BTDC fuel injection timing. During this test, the fuel quantity was reduced gradually from 37 mg/stroke to 13.4 mg/stroke. Unfortunately, the FTIR malfunctioned during the tests; however, in-cylinder pressure data were recorded. As illustrated in Figure 24, no matter the amount of fuel injected, only gradual combustion is seen and no noticeable pressure rise was found. These smooth pressure traces suggest that SOC occurs relatively early in the compression stroke, restricting any dynamic pressure increases. The calculated in-cylinder temperature plot of Figure 25 corroborates this finding. Moreover, negative torque is found for all scenarios and as the quantity of fuel injected decreases, the peak cylinder pressure gradually diminishes. While motoring the engine, the torque transducer measures a negative torque of 8.5 N-m. Hence, for fuel injection quantities less than 10.4 mg/stroke, the extent of combustion is negligible as depicted by Figure 24b.

In order to attempt to establish the SOC and obtain a better understanding of the delay between fuel injection and the initial phase of combustion, a heat release program was used to analyze the in-cylinder pressure data [68]. Various methods have been employed in the literature to accurately quantify ignition delay and SOC timing. Computational methods using detailed chemical kinetics have proven to be only partially accurate due to the complex in-cylinder physical and chemical processes [84-89]. Instead, the second derivative of the measured in-cylinder pressure trace has been verified to provide dependable evidence regarding SOC timing [5, 9, 90, 91]. In specific, the SOC is defined as the first minimum of the first derivative of pressure after the SOI. Additionally, the second derivative of pressure is observed to be zero at this point.

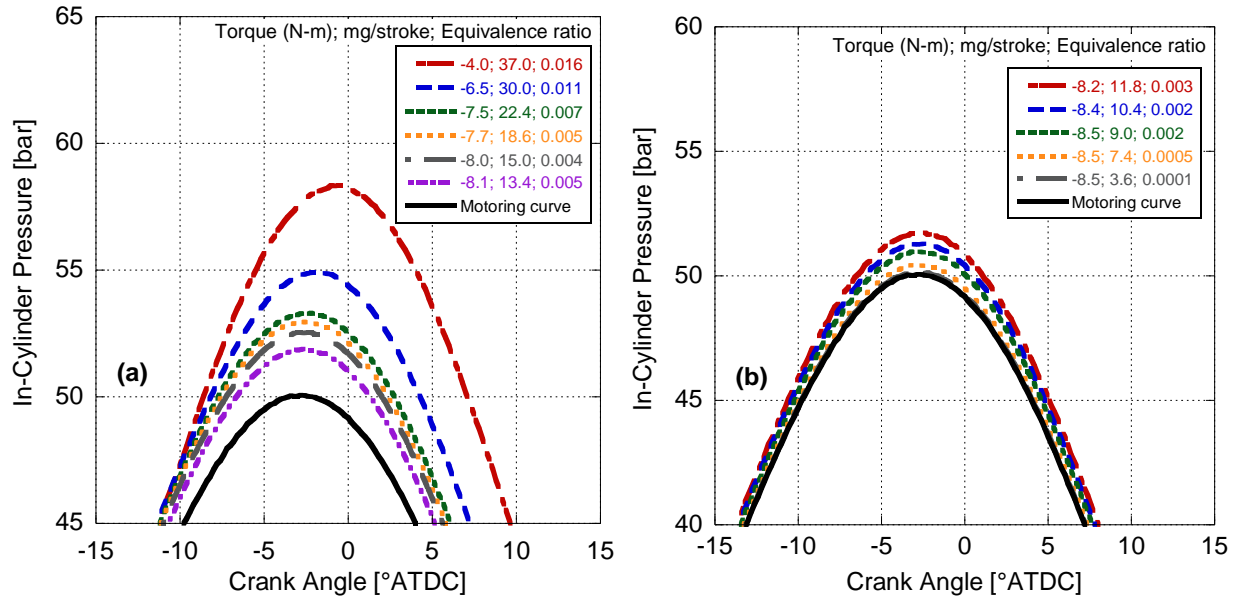


**Figure 24: In-cylinder pressure vs. crank angle for 60° BTDC fuel injection timing for fuel injection quantity**

**(a) 37.0 to 13.4 mg/stroke, and (b) 11.8 to 3.6 mg/stroke.**

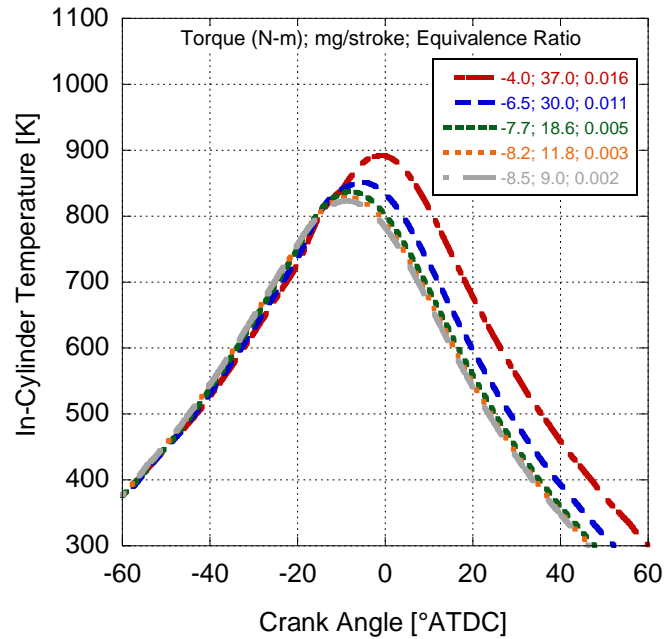


**Figure 25: In-cylinder temperature vs. crank angle for selected injection events at 60 BTDC from injection quantity sweep trial.**

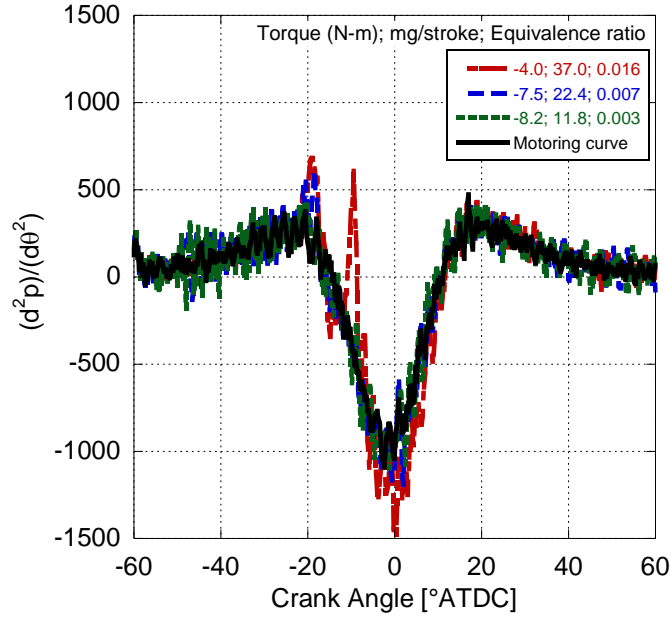


**Figure 26: Second derivative of pressure vs. crank angle for 60° BTDC fuel injection timing for fuel injection quantities 37, 22.4, and 11.8 mg/stroke.**

In Figure 26, for the 37 mg/stroke fuel injection event, the second derivative of pressure becomes zero and crosses over to the positive quadrant at approximately 12° BTDC indicating the SOC. Additionally, the second derivative of pressure suggests that the vaporized fuel starts burning a few degrees before TDC. Hence, it appears that even though the pressure trace shows no indication of combustion, there is a small premixed combustion event. However, for fuel quantities less than 37 mg/stroke there is no clear distinction for SOC, and the second derivative of pressure plot follows the motoring curve very closely. Therefore, characterization of when combustion begins cannot be established easily during early injection events at extremely low equivalence ratios.

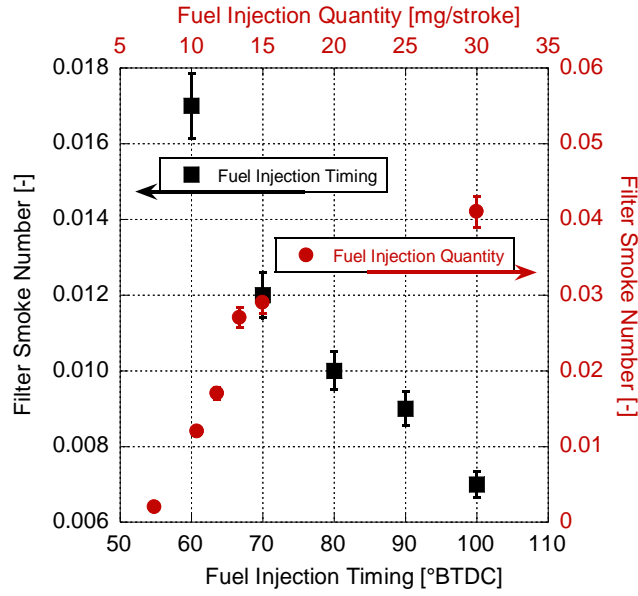


**Figure 27: Fuel injection timing for 11.8 mg/stroke injection quantity vs. FSN and fuel injection quantity for 60° BTDC injection timing vs FSN.**

With respect to emissions, two sets of smoke meter measurements were recorded. In the first set, the fuel injection timing was fixed at 60° BTDC and the fuel injection quantity was varied from 30.0 to 7.5 mg/stroke, represented by the red dots, and red axes in Figure 27. Perceptibly, the FSN value decreased for lower fuel quantities; here, this is assumed to be due to the gradual reduction in fuel quantity rather than suggesting an apparent improvement in combustion efficiency. In the second set, the fuel injection quantity was fixed at 11.8 mg/stroke and the fuel injection timing was advanced from 60° to 100° BTDC, represented by the black squares and black axes in Figure 27. Similar to the previous trend of Figure 20, the FSN values obtained here may be misleading due to the limitations of the smoke meter's measuring principle (i.e., distinguishing between HC and soot). Overall, the trends suggest that extremely advanced fuel injection timing for a given fuel quantity may result in lower smoke emissions [16, 27, 32]; however, care must be taken to ensure that significant wall wetting and crevice flow does not result. Hence, FSN may decrease the

earlier fuel is injected because more fuel finds its way into the crankcase becoming unavailable for combustion.

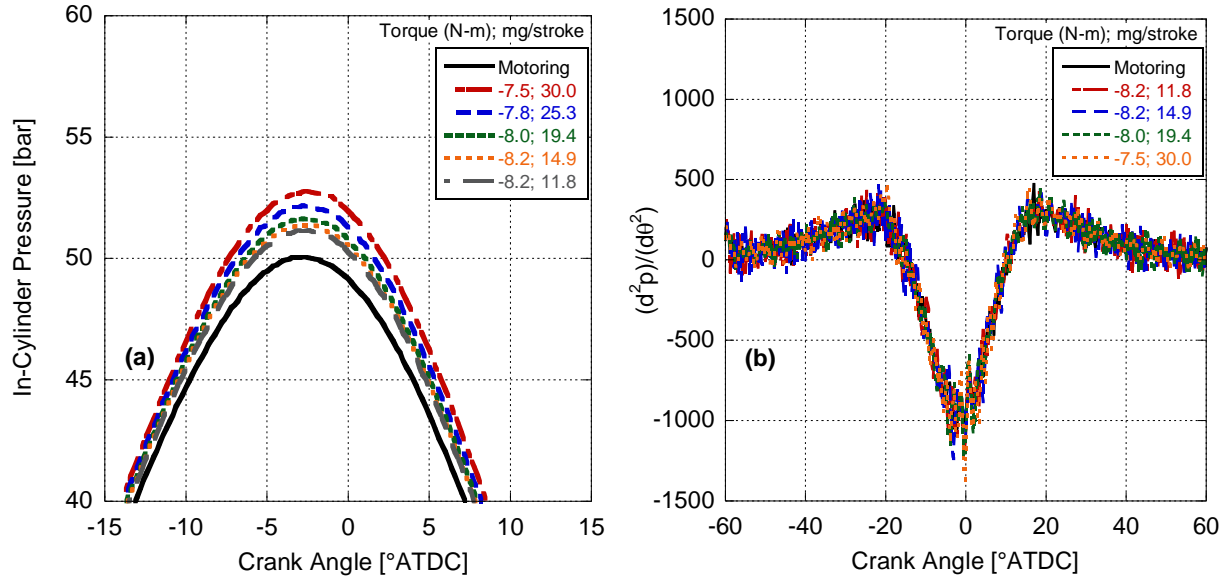


**Figure 28: (a) In-cylinder pressure vs. crank angle and (b) second derivative of pressure vs. crank angle for 100° BTDC fuel injection timing for fuel injection quantity 30.0 to 11.8 mg/stroke.**

Finally, similar results to 60° BTDC were observed in the last set of trials where the injection timing was advanced to 100° BTDC. The initial fuel injection quantity was set to 30 mg/stroke and reduced gradually to 11.8 mg/stroke. The pressure versus crank angle plots of these trials are given in Figure 28a. For the 30 mg/stroke event at 100° BTDC, the in-cylinder pressure and torque generated are significantly low as compared to the same fuel quantity injected at 60° BTDC. The cylinder temperature and pressure are comparatively cooler at 100° BTDC which hinders the fuel vaporization and subsequent atomization. Additionally, the fuel that is able to vaporize burns before the end of compression stroke resulting in heat transfer to the walls due to the excessive time available. The second derivative of pressure trials, shown in Figure 28b, were similar to the previous case, where all the points tested at 100° BTDC followed the motoring curve very closely. Yet again, the available data is not sufficient to conclusively state that the injected fuel is flowing past the exhaust without burning; however, based on the THC and CO emission

results from Figure 23b for advanced fuel injection events, it is possible that the amount of fuel combusting is comparatively low.

### **3.5 Conclusions**

PCI combustion through DI of fuel early in the compression stroke was attempted at low loads for a high CR engine. Following conventional trends, advancing the fuel injection timing slightly grew  $\text{NO}_x$  emissions with smoke emissions remaining relatively constant as the pre-mixed combustion phase grew. Once combustion became more gradual and CI knock was eliminated,  $\text{NO}_x$  emissions largely fell as smoke, THC, CO, and aldehyde emissions grew validating literature trends with advanced injection timings. However, there appears to be an optimum injection timing that reduces  $\text{NO}_x$  emissions without the corresponding growth in partial combustion products while still generating positive torque. Unlike prior PCI efforts, this ideal injection timing setting ( $30^\circ$  BTDC) occurs later in the compression stroke (vs.  $60^\circ$  BTDC and  $100^\circ$  BTDC) owing to the high CR of the engine. In other words, since the mixture is hotter with high CR engines, it is not possible to inject at extremely advanced timing without significant combustion occurring resulting in negative torque. Furthermore, it is assumed that at extremely advanced injection timings, significant wall wetting and crevice flow occurs requiring modification of the fuel injection pressure, injector type, and/or fuel injection angle. In follow up experiments, fuel injection quantity sweeps were conducted at  $60^\circ$  and  $100^\circ$  BTDC. Here, for fuel quantities lesser than 30 mg/stroke, the pressure trace and the second derivative of pressure followed the motoring curve very closely, suggesting a significant decrease in the quantity of fuel participating in combustion as compared to conventional injection timings.

As a result, it may be possible to achieve limited PCI operation with high CR engines; however, further experimentation is needed to explore this potential range and how EGR might impact the outcomes. Moreover, the results presented here may help better understand fuel-air mixture behavior before attempting LTC through a MPFI strategy on a high CR engine.



## **Chapter 4: Performance and Emissions Analysis of Partially Pre-Mixed Charge Compression Ignition Combustion**

### **4.1 Abstract**

With an objective to investigate the performance and emissions behavior of a high CR CI engine operating in PPCI mode, a series of experiments were conducted using a single cylinder NA engine with a high pressure rail fuel injection system. Moderately advanced DI strategy was implemented in order to attempt to achieve PPCI combustion under low load conditions. During experimentation, the fuel injection pressure, engine speed, and engine torque were kept constant, while the fuel injection timing was varied between 25° to 35° BTDC in steps of 2.5°. At each injection timing, fuel quantity was varied to maintain the required load level. In-cylinder pressure, performance parameters, and emissions were measured in the process and analyzed using a zero-dimensional heat release model. The experimental results suggest that the fuel injection timing at which PPCI is observed varies with the operating engine load condition. In specific, it was necessary to advance the fuel injection timing when operating at higher load conditions in order to exploit the advantages of PPCI combustion. In general, NO<sub>x</sub> emissions, IMEP, peak cylinder pressure, and ROHR decreased with advanced injection timings. Conversely, an opposite effect on CO, PM, and total hydrocarbons (THC) emissions were observed at advanced injection timings. Unfortunately, similar to most results recorded in the literature, the engine operation was limited to low load conditions restricted by the significantly high peak in-cylinder pressure.

### **4.2 Introduction**

The levels of air pollution primarily associated with the transportation sector pose a genuine health concern around the world today [92]. Additionally, the number of on-road vehicles has been increasing consistently over the last two decades due to growing population [93]. These reasons have stimulated the United States EPA to impose stringent emission regulations [94]. In particular, NO<sub>x</sub>, CO, PM, and volatile organic compounds have been recognized as a cause for deteriorating air quality [95]. Even though there have been

significant improvements in reducing emissions from CI engines through design modifications and effective calibration, there is a need to address the critical glitch in  $\text{NO}_x$  and PM emissions to successfully meet future emission regulations [96]. In particular, the tradeoff between  $\text{NO}_x$  and PM emissions through conventional CI combustion in conjunction with complex aftertreatment systems intended to reduce emissions from lean burn engines results in a significant expense, both for the consumer and the manufacturer. Defeating this tradeoff using LTC of ultra-lean mixtures (equivalence ratios less than 0.3) can be a positive solution for the simultaneous reduction of  $\text{NO}_x$  and PM with only minor performance losses [97]. In this area, HCCI, PCI, and MPFI are the common approaches to achieve LTC.

For a CI engine, varying the injection timing alone to move towards the LTC regime is possible; hence, it is considered a relatively inexpensive, practical, and an effective method to control emissions. In specific, LTC can be realized through DI of a single fuel pulse via the PCI methodology. For this option, the fuel is injected relatively early in the compression stroke (approx.  $60^\circ$  to  $100^\circ$  BTDC) in order to provide sufficient time for the fuel to mix and form a (nearly) homogeneous mixture before the SOC. Moreover, the primary drawback of inaccurate ignition timing control as observed for HCCI achieved through port fuel injection mechanism can be diminished by the DI of fuel. During the combustion of this nearly homogeneous mixture, due to the excessive air available and the lower temperatures of combustion, both PM and  $\text{NO}_x$  emissions can be decreased significantly [98]. In addition, thermal and combustion efficiencies are expected to be comparatively high due to the pre-dominant premixed burn. However, since the in-cylinder temperature and pressure at the time of fuel injection is comparatively low, THC and CO emissions may be comparatively higher due to incomplete vaporization and spray impingement on the cylinder walls (i.e., wall wetting) [20-22, 27, 99, 100]. In addition, increasing the amount of fuel injected drastically surges the peak cylinder pressure and noise; subsequently, restricting PCI operation to low load conditions [26, 28, 32, 33, 39].

Substantial research efforts towards resolving the major disadvantages of PCI combustion have been attempted in the literature. Employing narrow spray cone angle, pintle injectors, and impinged injection

systems are typical solutions suggested to reduce cylinder wall wetting [16, 26, 28, 30, 31, 36, 37, 101-103]. Additionally, using Exhaust Gas Recirculation (EGR) can assist in vaporizing the injected fuel due to the surplus heat carried by the exhaust gas [104] while also mitigating CI knock [19, 24]. Moreover, reducing the geometric CR has been a popular approach to promote more mixing time while avoiding an excessive pressure rise [24, 27, 34-36]. Uncommon approaches like injecting water into the combustion chamber have also assisted in expanding the operating regime by extending the ignition delay [20, 39]. Unfortunately, all these methods employed to expand the PCI operating regime have a significant negative impact on combustion performance. Moreover, based on the results of an earlier test conducted at KU, it was evident that achieving PCI combustion in the absence of EGR was challenging due to the comparatively high CR (21.2) of the engine. The in-cylinder temperature was observed to be higher than the required auto-ignition temperature for diesel fuel at 40° BTDC. Therefore, SOC occurred early in the compression stroke; hence, homogeneous mixture formation was not possible for fuel injected before 60° BTDC.

To tackle the disadvantages of PCI, an alternative approach is to inject moderately early (25° to 35° BTDC) to attempt to work the boundary between conventional and PCI combustion; aka PPCI. In PPCI, THC and CO emissions are expected to be lower than PCI owing to the in-cylinder conditions favoring vaporization. Furthermore, the potential for operating at higher load conditions is comparatively enhanced due to improved control over ignition timing. However, due to comparatively less time available for mixture preparation, the cylinder is relatively less homogeneous. This could potentially lead to higher NO<sub>x</sub> emissions due to greater combustion temperatures, typical as found in combustion of non-homogeneous mixtures.

Generally, it has been observed that advancing the injection timing away from conventional set points (5° to 14° BTDC) results in a gradual increase in the ignition delay [33, 98]. As a result, the ROHR, peak cylinder pressure, and NO<sub>x</sub> emissions are observed to increase. Additionally, SFC, CO, THC, and PM emissions decrease [24, 26, 28, 98, 105-107]. However, in a certain range of advanced injection timings (approx. 25° to 35° BTDC), THC and CO emissions are found to be comparable to conventional combustion

emissions with combustion efficiency remaining relatively high. Furthermore, PM emissions are reduced and NO<sub>x</sub> emissions begin to decrease because of a more homogenous combustion process. As a result, the NO<sub>x</sub> and PM trade-off is defeated slightly without a significant growth in partial combustion products. Unfortunately, the amount of fuel consumed at a fixed engine load is higher in this PPCI mode. Moreover, for a fixed fuel quantity, the IMEP goes down at these advanced injection timings [24, 26, 28, 98, 105, 106]. Continued advancement in injection timing (earlier than 40° BTDC), as discussed earlier, leads to an increase in SFC, CO, PM and THC emissions; whereas, ROHR, in-cylinder peak pressure, and NO<sub>x</sub> emissions all decrease.

In order to explore the potential of PCI and PPCI combustion using a high CR engine, a series of experiments were previously conducted by varying the fuel injection timing and fuel amount at various load conditions for a single cylinder CI engine. An AVL SESAM FTIR analyzer and AVL Smoke Meter (model #415-s) were utilized to measure emissions at the various test points. A zero dimensional heat release model developed by a fellow graduate student was utilized to analyze the in-cylinder pressure data to generate vital information, such as ROHR and in-cylinder temperature. A brief description of the experimental setup and the zero-dimensional model utilized for testing can be found in Chapter III. For the interest of the reader, comprehensive depiction of the experimental setup can be found in the works of Langness et al. and Mangus et al. [18, 64]. Similarly, the zero-dimensional model is thoroughly explained by Mattson et al. [68]. The previous findings suggested that it is infeasible for a high CR engine to operate in true PCI mode because of the temperatures reached during the compression process. However, it appeared that PPCI was possible in a limited range due to the findings of lower NO<sub>x</sub> emissions with CO, THC, and PM emissions remaining relatively constant. Hence, this chapter seeks to build on these findings and explore the potential regime of PPCI in a high CR engine.

### **4.3 Experimental Results**

In the first set of experiments, the engine torque was maintained at 0.5, and successively at 1.0, and 1.5 N-m while fuel injection timing was varied from 25° to 35° BTDC in steps of 2.5°. At each injection timing,

the fuel flow rate was adjusted to maintain the required engine torque values. In-cylinder performance and emissions data were recorded in the process. Additionally, experiments were conducted at 0.5 and 1.5 N-m with 12.5° BTDC injection to compare conventional operation with PPCI combustion. Prior to testing, the engine was made to run for about 15 minutes to warm the engine oil and heat the cylinder walls. Throughout all tests, the engine speed was maintained at 1800 rpm. A high-pressure rail fuel injection system added fuel at a pressure of  $47 \pm 0.2$  MPa. Emissions and performance data were collected only after the engine stabilized and the engine exhaust temperature fluctuations were at a minimum (i.e.,  $\pm 1^\circ \text{C}$ ). The in-cylinder pressure data captured is an average of 60 thermodynamic cycles recorded at a resolution of 0.2° crank angle per measurement. Air flow and fuel flow measurements along with temperature and pressure data at various points were measured at a frequency of 10 Hz for 120 seconds. Finally, the emissions from the FTIR were measured for just over 240 seconds and the Smoke Meter values were the average of two measurements each sampled for 120 seconds. ULSD with properties shown in Table 3 was used as the test fuel.

Initially, the fuel injection timing was set to 12.5° BTDC, and the targeted engine load was 0.5 N-m. To maintain the engine load at 0.5 N-m (or any given load), the engine fuel quantity is varied until the engine torque reading displayed on the dynamometer controller reads 0.5 N-m. Of note, it is a relatively difficult task to maintain the engine torque at 0.5 N-m (or at any low load set point) for the entire data collection period as small changes in engine temperature and cycle-to-cycle random variations can lead to some fluctuations in the engine torque measured by the Futek torque transducer (model # TRS-705). Hence, it is possible for the actual engine load to be slightly more or less than the ideally required value. Successively, the fuel injection timing was advanced from 25° to 35° BTDC in steps of 2.5°. At each step, the fuel injection quantity was adjusted to maintain the engine load at (preferably) 0.5 N-m.

The in-cylinder pressure data and the corresponding ROHR data for the 0.5 N-m engine load trial are shown in Figure 29. For the 12.5° BTDC injection, i.e., the conventional combustion event, the peak in-cylinder

pressure occurs slightly after TDC and demonstrates ringing combustion (aka CI knock). As the injection timing is advanced to 25° BTDC and earlier, the pressure trace begins to smooth suggesting a more gradual increase in pressure. This is because the extended ignition delay period allows the injected fuel to mix and form more homogeneous mixtures. Combustion is all pre-mixed and coupled with a double compression event (i.e., increasing pressure due to piston compression) this leads to a higher peak cylinder pressure and ROHR. Furthermore, unlike conventional combustion, the peak cylinder pressure occurs slightly before TDC. However, a significant amount of knock may still be observed in the pressure curve around the peak pressure timing suggesting incomplete air-fuel mixture distribution in the combustion chamber.

Interestingly, for advanced injection events (between 25.0° to 35.0° BTDC), the ROHR (Figure 29b) peak reduces gradually while peak pressures remain relatively constant. The gradual reduction in the knock intensity and smoothening of the in-cylinder pressure could potentially cause the decrease in ROHR observed at advanced injection timings. Furthermore, as the injection timing is advanced, the timing where the in-cylinder pressure separates from the motoring curve is also advanced comparatively. This is also observed in the second derivative of pressure curve (Figure 30a). In specific, the point at which the second derivative of pressure crosses over from the negative quadrant to the positive (indicating SOC) progressed for earlier injection events.

Moving forward, the in-cylinder temperature (Figure 30b) is observed to increase gradually while advancing the injection from 25° to 32.5° BTDC due to an added energy release (greater equivalence ratios) coupled to the double compression event. This can be seen in the average temperature slope plot shown in Figure 31a. Here, the average of the temperature slope ( $dT/d\theta$ ) was computed for measurements between -5° and 15° ATDC at each injection event for the 0.5 N-m load condition. Clearly, as the injection timing is advanced, the average temperature slope increases for injection between 12.5° and 32.5° BTDC. Hence, while peak pressures remain constant due to a slower ROHR (smoother combustion) as injection timing is advanced, global peak temperatures increase because more fuel is being added. Moreover, the combustion

chamber and the cylinder is relatively hotter towards the end of data collection time (approximately five minutes) since combustion happens earlier and there is more time for heat transfer to the walls. Hence, it is assumed that more heat is initially transferred from the walls to the gas during compression and the early stages of combustion adding to the temperature rise. Of note, there is a drop in the average temperature slope and global temperature (Figure 30b) value for injection at 35.0° as compared to 32.5° BTDC. Here, the equivalence ratio dropped slightly when attempting to maintain 0.5 N-m. Hence, this is assumed to simply be a (mostly) random deviation in the trend (note the variance in torque of Figure 31b) of increasing temperatures with advanced injections.

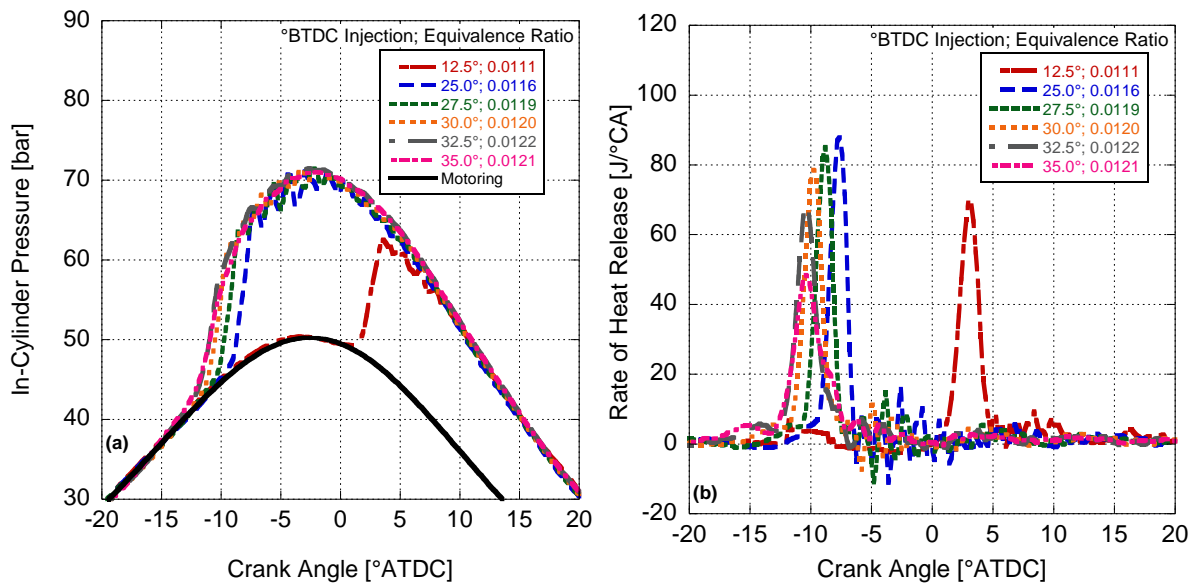


**Figure 29: (a) In-cylinder pressure and (b) rate of heat release vs. crank angle at 0.5 N-m engine torque for fuel injection timing from 12.5° to 35.0° BTDC.**

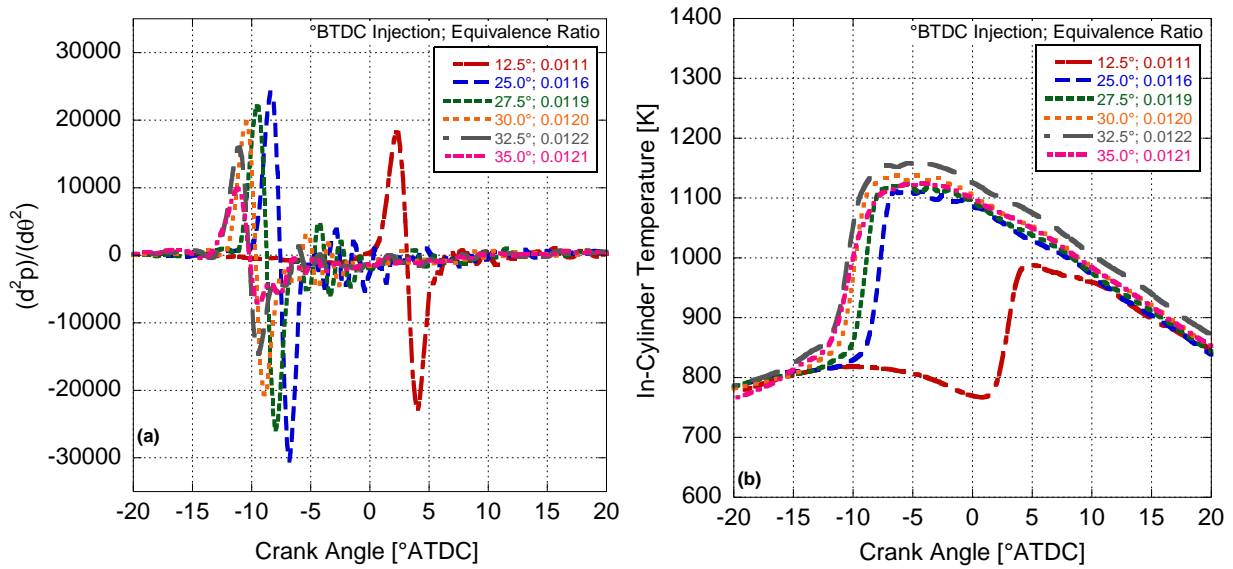


**Figure 30: (a) Second derivative of pressure and (b) in-cylinder temperature vs. crank angle at 0.5 N-m engine torque for fuel injection timing from 12.5° to 35.0° BTDC.**

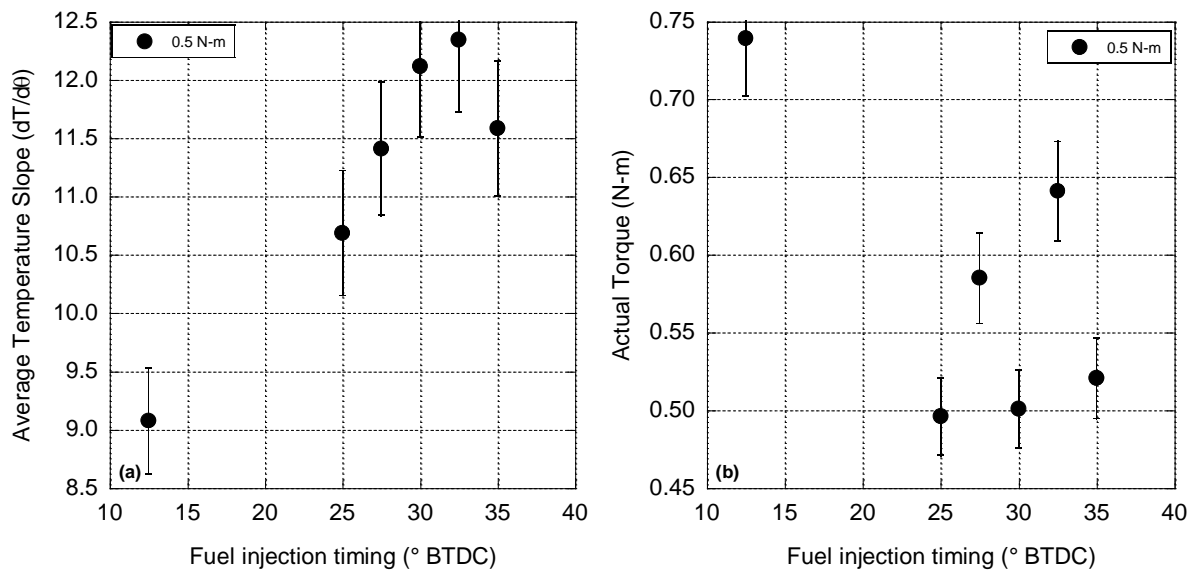


**Figure 31: (a) Average temperature slope and (b) actual torque vs. fuel injection timing for 0.5 N-m engine load conditions.**

In a following test, the added fuel amount was adjusted so that a constant engine load of 1.0 N-m was achieved while the fuel injection timing was varied from 25.0° to 35.0° BTDC in steps of 2.5°. The peak in-cylinder pressure (Figure 32a) increased gradually for injections between 25.0° to 30.0° BTDC and then



remained relatively constant. Additionally, the knock effect was observed to fade for advanced injection timings. Again, homogeneity increases at advanced injection timings due to the excess time available to mix causing the pressure trace to smooth out and reduce the knock intensity. Moreover, while the ROHR (Figure 32b) increased slightly for 25.0° and 27.5° BTDC, it was seen to decline for injections between 27.5° to 35.0° BTDC. Furthermore, from the second derivative of pressure plot (Figure 33a) it is clear that SOC occurred earlier for advanced injection events. This largely followed the previous trends at 0.5 N-m.

Meanwhile, the peak in-cylinder temperature (Figure 33b) followed the peak pressure trend with its average slope value (Figure 34a) initially increasing and then decreasing at advanced injections. In addition, similar to the previous results, the actual engine load demonstrated some variability due to combustion instabilities (Figure 34b). However, for fuel injection at 35.0° BTDC, while the fuel added increased (equivalence ratio grew consistently), the in-cylinder temperature, ROHR, and the average of the temperature slope decreased. In addition to the influence of combustion instabilities, this may be a function of a reduction in combustion efficiency and growing amount of wall wetting. In other words, more fuel might be finding its way to the crevices resulting in a reduced amount of early combustion resulting in lower temperatures and ROHR. Then, some of this fuel might find its way back from the crevices after combustion begins (at a more optimum combustion timing) adding to the energy released and allowing the load setting to be reached.

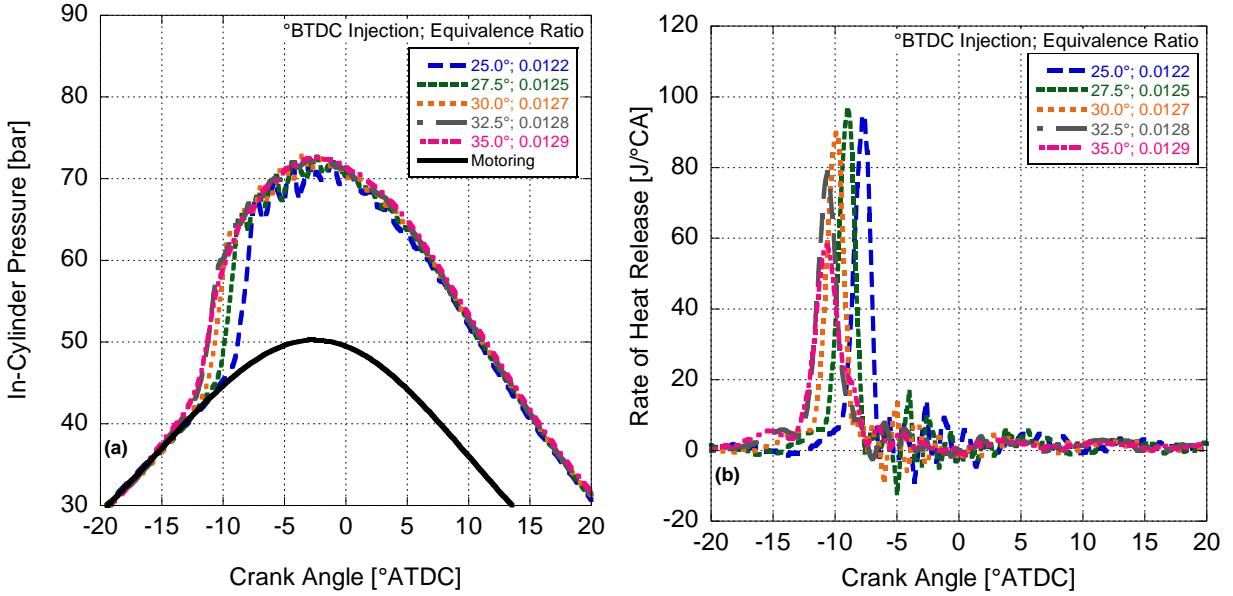


Figure 32: (a) In-cylinder pressure and (b) rate of heat release vs. crank angle at 1.0 N-m engine torque for fuel injection timing from 12.5° to 35.0° BTDC.

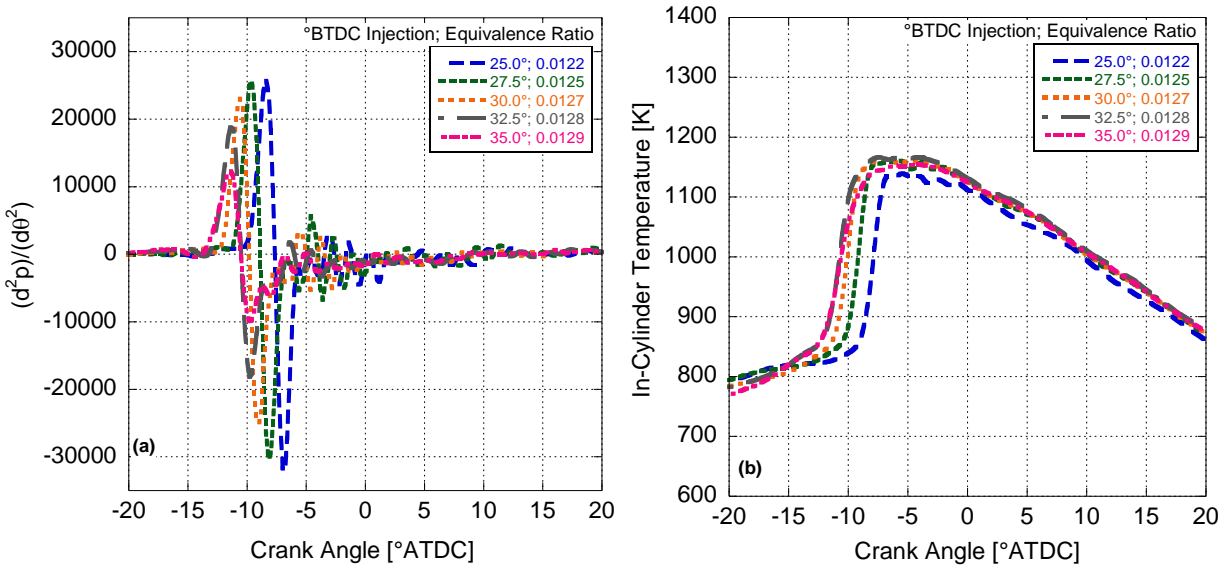
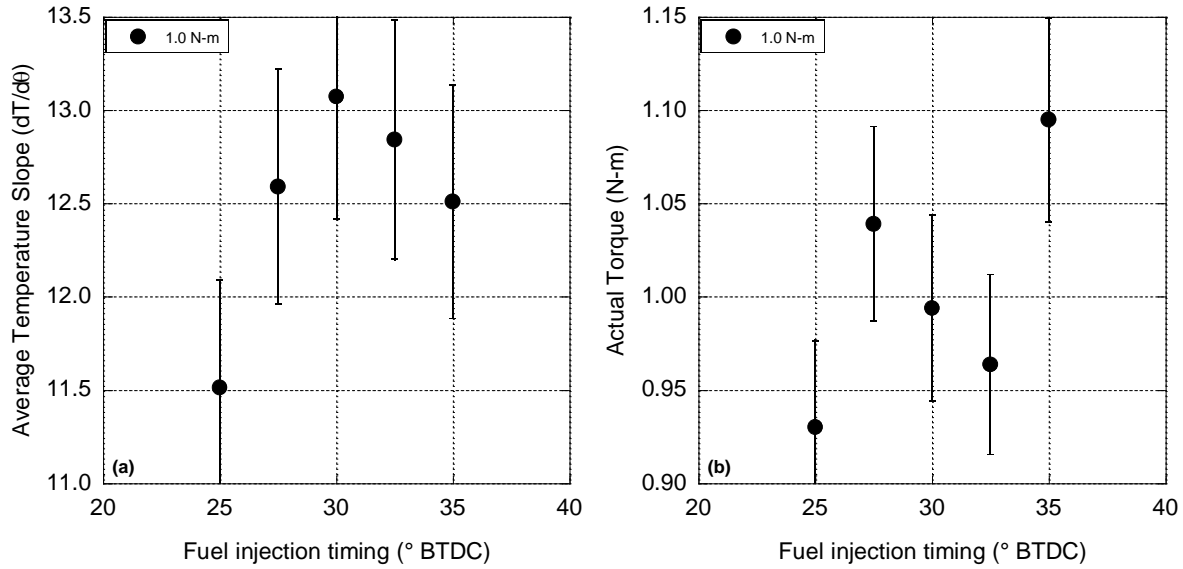
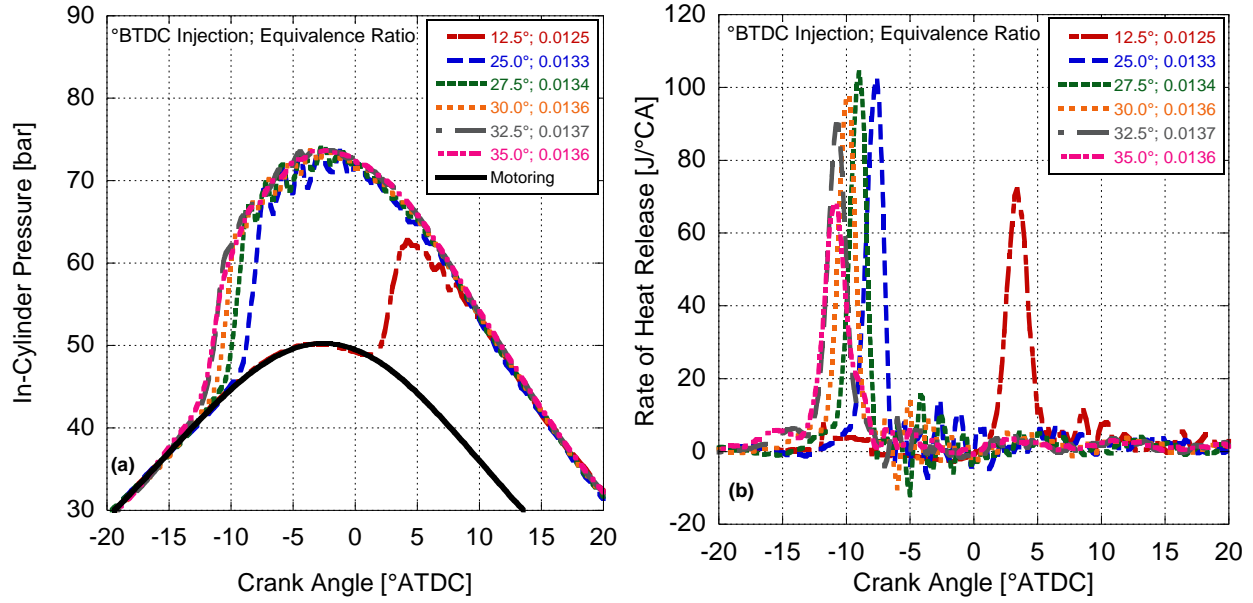


Figure 33: (a) Second derivative of pressure and (b) in-cylinder temperature vs. crank angle at 1.0 N-m engine torque for fuel injection timing from 12.5° to 35.0° BTDC.



**Figure 34: (a) Average temperature slope and (b) actual torque vs. fuel injection timing for 1.0 N-m engine load conditions.**

In the final set of tests, the fuel injection quantity was further boosted and adjusted to maintain an engine load of 1.5 N-m while the fuel injection timing was varied from 12.5° to 35.0° BTDC in steps similar to the previous trials. The in-cylinder pressure results (Figure 35a) are comparable to the previous outcomes where the peak pressure is seen to increase and then remain relatively constant. The ROHR (Figure 35b) was nearly constant for fuel injected at 25.0° and 27.5° BTDC, but then gradually decreased between 27.5° and 35.0° BTDC. Additionally, the second derivative of pressure plot (Figure 36a) suggested that SOC timing is advanced for earlier injection events. Similar to earlier cases, the peak in-cylinder temperature (Figure 36b) increased between 25.0° and 32.5° BTDC; but, there was a small drop in temperature at 35.0° BTDC. This is bolstered by the average temperature slope trends given in Figure 37a that follow the in-cylinder temperature trends. As a result, it is assumed that combustion instabilities, as evidenced by the engine torque plot (Figure 37b), coupled with changes in the amount of heat transfer along with combustion efficiency and wall wetting all play a role in reducing temperatures at this extremely advanced injection timing.



**Figure 35: (a) Rate of heat release and (b) in-cylinder pressure vs. crank angle at 1.5 N-m engine torque for fuel injection timing from 12.5° to 35.0° BTDC.**

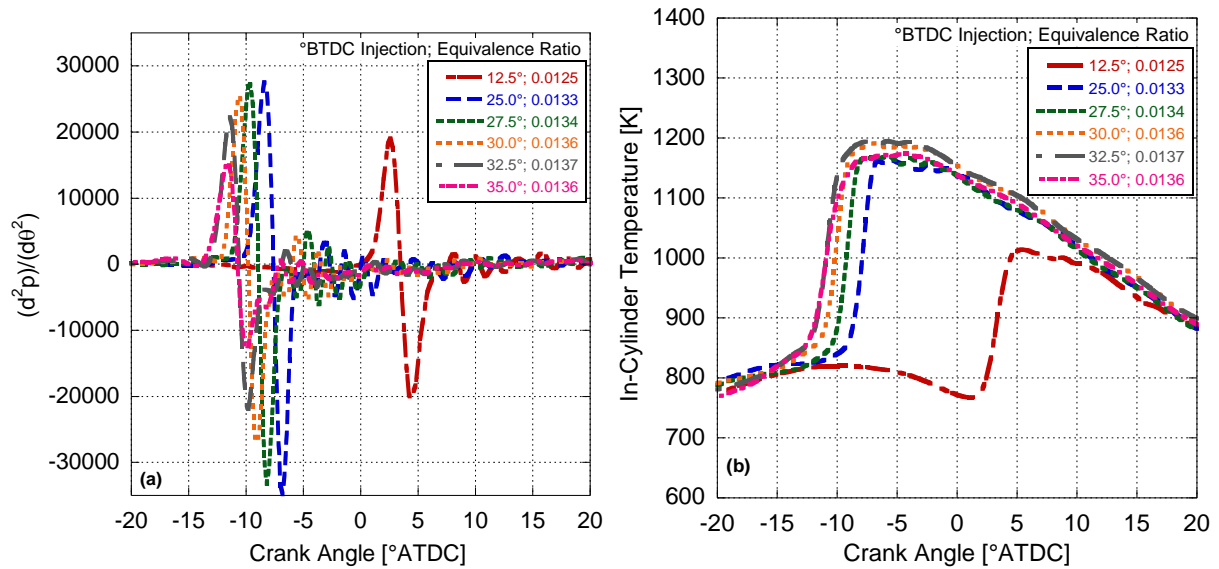


**Figure 36: (a) Second derivative of pressure and (b) In-cylinder temperature vs. crank angle at 1.5 N-m engine torque for fuel injection timing from 12.5° to 35.0° BTDC.**

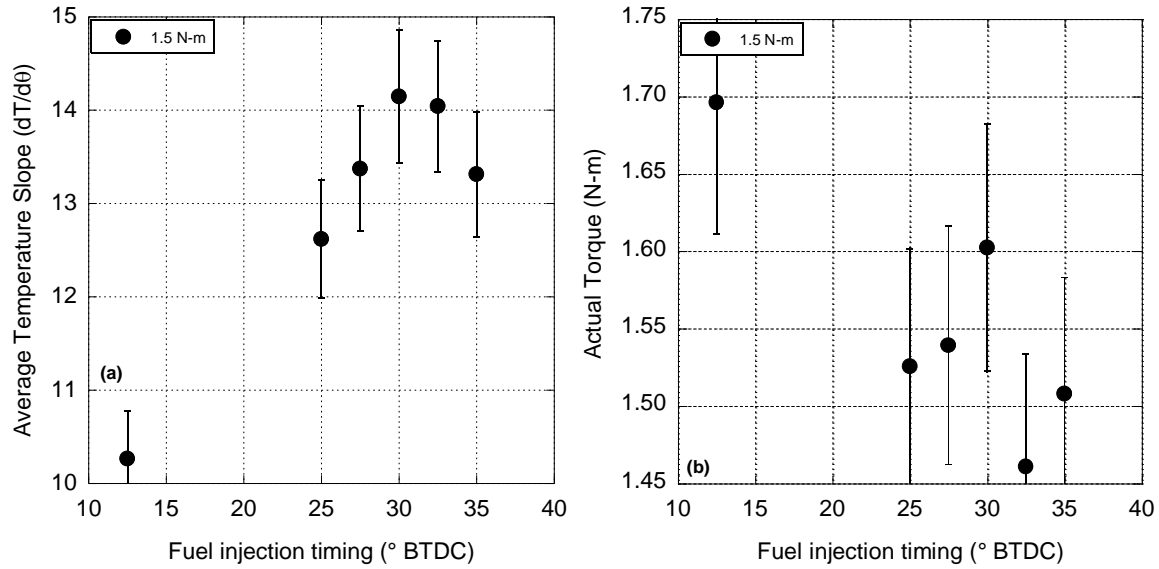


**Figure 37: (a) Average temperature slope and (b) actual torque vs. fuel injection timing for 1.5 N-m engine load conditions.**

Interestingly, the intensity (and wavelengths) of knock was observed to be fairly consistent at the corresponding operating engine load across all fuel injection timings (Figure 38). In other words, fuel injection quantity seemed to have no significant impact on the intensity of knock at a given injection timing. This may be the result of running the engine at relatively similar low loading events; i.e., the equivalence ratio only changes by 0.0016.

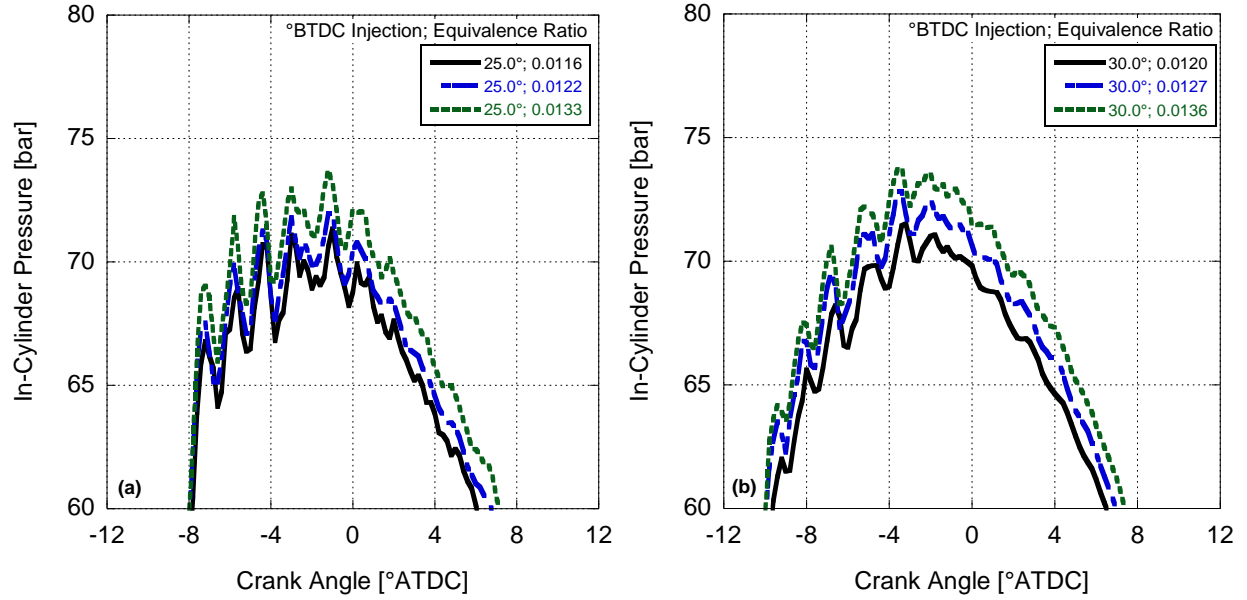


**Figure 38: In-cylinder pressure vs. crank angle at 0.5, 1.0, and 1.5 N-m load conditions for (a) 25.0° BTDC and (b) 30.0° BTDC fuel injection timing.**

The growth in the in-cylinder pressure observed when the injection timing is advanced is consistent with experimental results obtained by Lewander, et al. [108] when they attempted to achieve PPCI operation starting from conventional CI combustion. Reviewing the fuel injection quantity utilized and equivalence ratios during the various engine load sweeps in Figure 39 finds that it (largely) grows with advanced timings. This is because the generated energy in the combustion chamber is not consumed as effectively since the power produced acts against the piston moving towards the TDC in the compression stroke. Hence, at advanced fuel injection timings, the amount of fuel injected is increased to meet the set demand engine load while the equivalence ratio of the mixture also grows (Figure 39). Therefore, combustion results in a double compression event with higher peak in-cylinder pressures and temperatures for advanced fuel injections until combustion efficiencies and wall wetting begins to play a more dominant role. Additionally, the rate of increase for fuel injected appears comparable for all the three load sweeps.

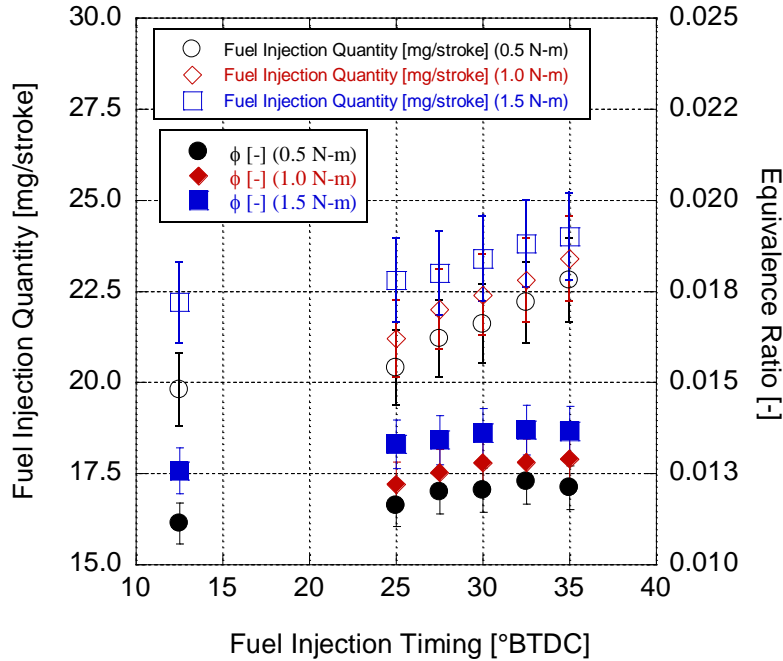


**Figure 39: Fuel injection quantity and equivalence ratio vs. fuel injection timing for fuel injection timing sweep.**

In regards to  $\text{NO}_x$  emissions (Figure 40a) for the 0.5 N-m load setting, a drastic increase was observed during the initial injection timing advancement from  $12.5^\circ$  to  $25.0^\circ$  BTDC due to the rapid surge in the combustion temperature (Figure 30a). Subsequently,  $\text{NO}_x$  emissions remained largely unchanged until  $30^\circ$  BTDC. Similar results of increasing  $\text{NO}_x$  emissions for comparatively higher ignition delay events was obtained by Hildingsson, et al., and Lewander, et al. [108, 109]. Further advancing the injection timing resulted in decreasing  $\text{NO}_x$  emissions. Referring to the in-cylinder pressure trace (Figure 29a),  $30^\circ$  BTDC is the point of transition where the knocking effect disappears and combustion becomes more gradual; however, there is no significant decrease in the peak combustion temperatures. One of the possible explanations for the decrease in  $\text{NO}_x$  emissions, as described by Dickey, et al., could be the reduction in the temperature difference between local combustion and bulk gas temperatures as combustion becomes more homogeneous [42]. Another potential justification for reducing  $\text{NO}_x$  emissions could be the NTC behavior of diesel fuel during CI combustion (refer to Chapter III for a detailed explanation).

PM emissions increased initially during the injection advancement from 12.5° to 25.0° BTDC (Figure 40a). This may be due to the growth in the amount of fuel injected as illustrated in Figure 39. Since combustion is already primarily pre-mixed at 12.5° BTDC and the combustion trace shows knocking combustion at 25.0° BTDC (Figure 29a), one can assume that the mixture is still fairly heterogeneous. As the injection event is advanced, homogeneity grows and PM emissions begin to fall even though more fuel is being added. Both the FSN and PM eventually increase for the 35.0° BTDC injection event suggesting (again) that 35.0° BTDC is the point where combustion efficiency begins to degrade. This falls in line with the previous discussion surrounding the decrease in global temperature at this injection timing.

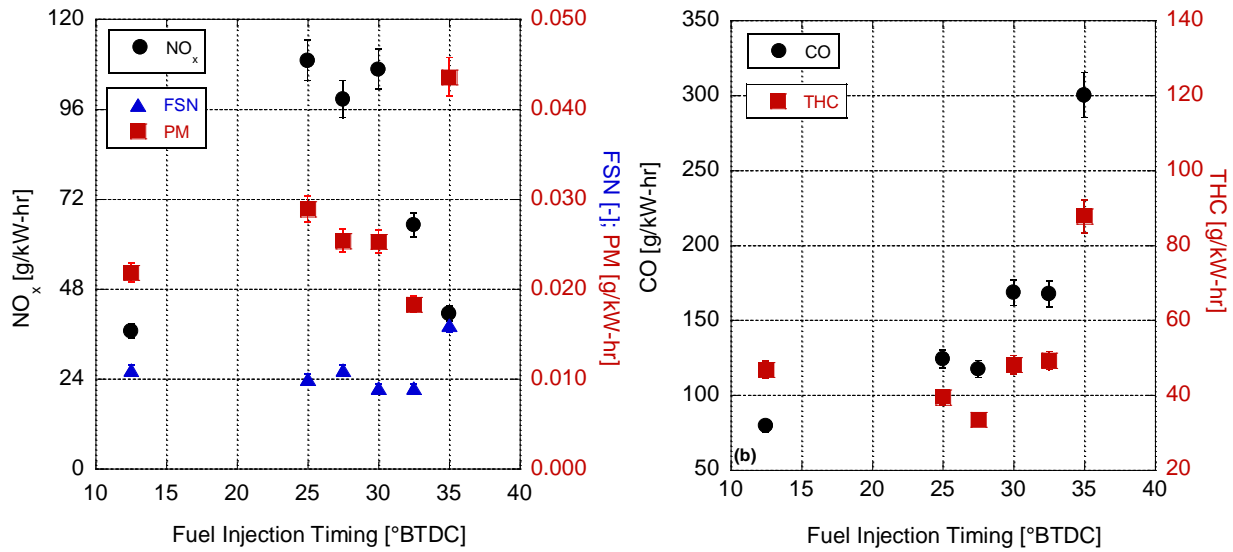


**Figure 40: (a) Nitrogen oxides, FSN, and particulate matter, and (b) carbon monoxide and hydrocarbon emissions at 0.5 N-m load for various fuel injection timings.**

With respect to CO emissions at 0.5 N-m in Figure 40b, advancing the injection timing resulted in growing emissions with the 35.0° BTDC injection event demonstrating a relatively large jump. While combustion temperatures do increase (Figure 30b) and there is plenty of O<sub>2</sub> available for complete combustion, the growth in fuel injected that subsequently provides more carbon appears to be a factor. Moreover, Opat, et al. [110] determined that the amount of fuel that evaporates before SOC grows gradually due to an advancing ignition delay period. Hence, the mixture may be overleaned and pockets of fuel and air may



exist that are too lean to promote effective combustion as this extremely low equivalence ratio. Eventually, the growth in wall wetting and combustion inefficiencies at 35° BTDC begin to dominate. However, unlike conventional trends, THC<sub>s</sub> decrease while CO emissions increase with the initial advancement of injection timing. Because THC oxidation inhibits CO conversion and CO conversion initiates only after all THC species disappears (detailed explanation provided in Chapter III), it is assumed here that the growth in mixture homogeneity with advanced injection promotes THC oxidation, but temperatures do not grow enough to facilitate the completion of CO oxidation.

As added evidence, as explained earlier in Chapter III, the conversion of CO to CO<sub>2</sub> follows this pathway:



The OH radical produced through Equation (1) is highly effective in converting the aldehydes formed during the oxidation of THC. As seen in Figure 41, unlike THC emissions, the formaldehyde emissions for 12.5° and 25.0° BTDC injection events are more comparable. This could be attributed to the reduction in the amount of OH radicals available due to the poor conversion rate of CO into CO<sub>2</sub>. Note, it has been shown that more than 50% of the aldehyde emissions consist of formaldehydes; hence, formaldehydes are selected to represent aldehydes in this scenario [80, 111]. In addition, due to the dependence of aldehyde conversion on the availability of OH radicals, formaldehyde trends follow CO emissions trends closely. In addition, formaldehydes react and convert in the presence of other radicals like O<sub>2</sub>, hydrogen, and methyl groups; nevertheless, they are not as effective as OH radical [77]. Therefore, the minor decrease in formaldehyde emissions observed initially could be due to formaldehyde conversion through radicals other than OH.

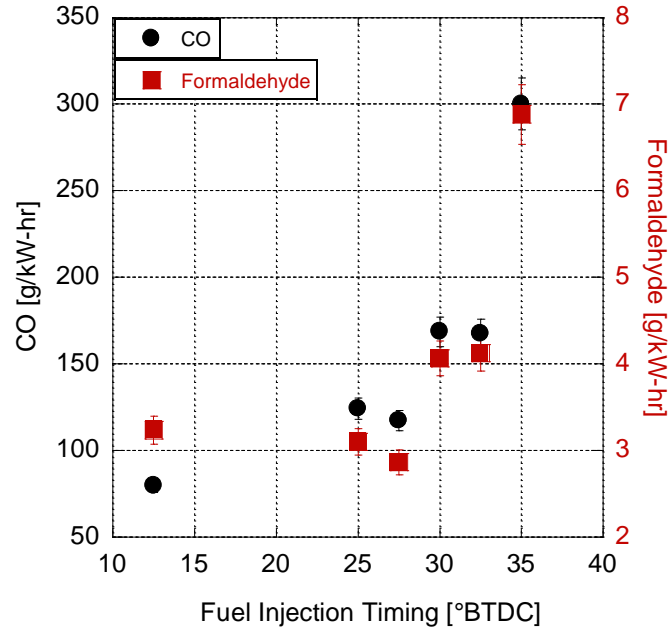


**Figure 41: Carbon monoxide and formaldehyde emissions at 0.5 N-m load for various fuel injection timings.**

Eventually, for injections earlier than 27.5°, THC, formaldehyde, and CO emissions grow and a noticeable jump is seen for the 35.0° BTDC injection event. This is because the combustion chamber pressure and temperature are comparatively low at 35.0° BTDC leading to poor fuel atomization and vaporization. Hence, fuel wall wetting and growth of crevice volume flow could be the potential reasons for the increase in THC emissions. Furthermore, the lower combustion temperatures results in worse combustion efficiencies. Both the CO and THC trends obtained are in agreement with the experimental results presented by Li, et al. where both CO and THC were stated to increase for higher premix times [112]. In their work, premix timing was defined as the difference between the duration of fuel injection and the ignition timing. Conversely, the work of Lewander, et al. concluded that injection timing had no significant impact on CO emissions [108].

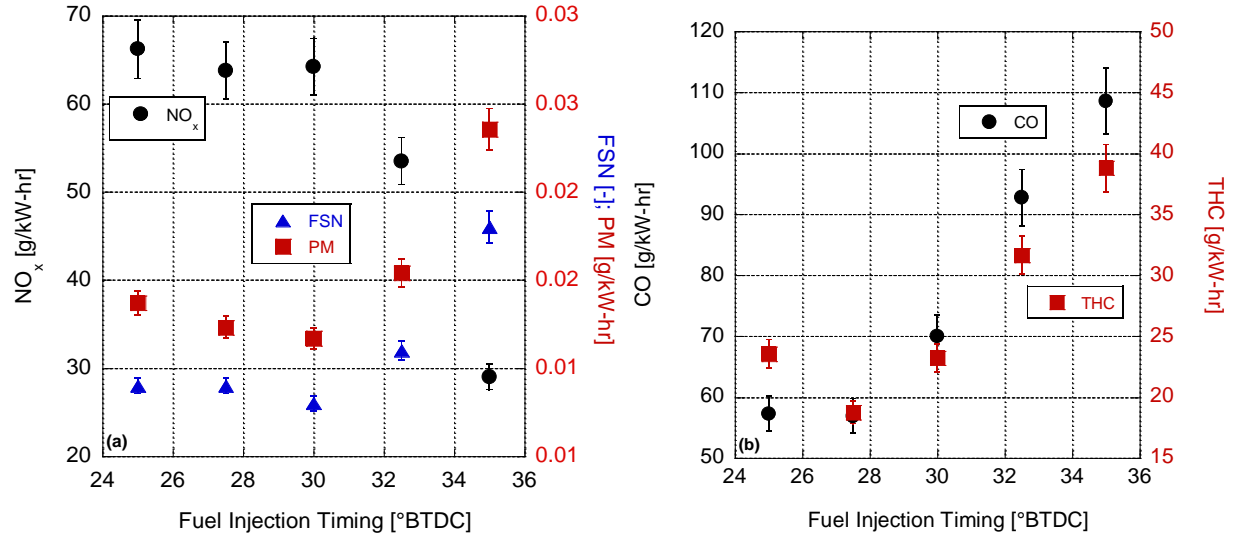


**Figure 42: (a) Nitrogen oxides and particulate matter, and (b) carbon monoxide and hydrocarbon emissions at 1.0 N-m load for various fuel injection timings.**

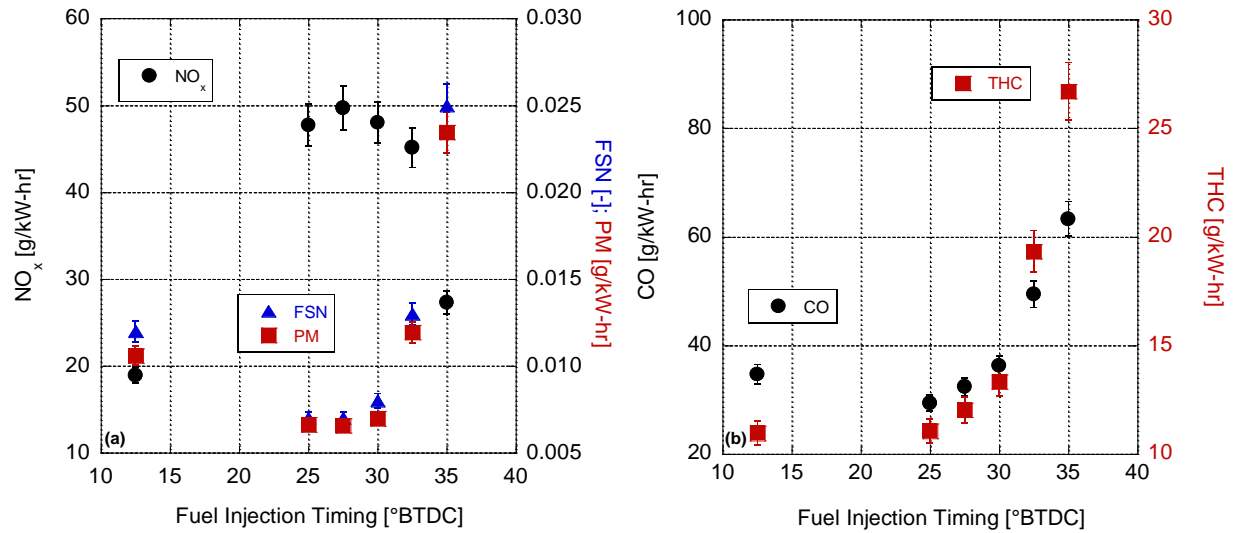


**Figure 43: (a) Nitrogen oxides and particulate matter, and (b) carbon monoxide and hydrocarbon emissions at 1.5 N-m load for various fuel injection timings.**

$\text{NO}_x$ , PM, CO, and THC emission trends for the 1.0 N-m and 1.5 N-m load sweeps are shown in Figure 42 and Figure 43, respectively.  $\text{NO}_x$  trends are comparable for all load conditions considered. However, unlike the 0.5 N-m load case, PM and CO emissions decreased during the initial injection advancement from conventional combustion for the 1.5 N-m load condition. In both cases, the actual torque measured (Figure

31b and Figure 37b) dropped while the equivalence ratio increased (0.0005 vs. 0.0008). However, at 1.5 N-m the equivalence ratio is around 15% higher that will lead to a greater in-cylinder temperature (Figure 30b vs. Figure 36b). Therefore, it is assumed here that the respective increase in temperature (which acts exponentially upon chemical kinetics) enhances oxidation sufficiently to reverse the earlier found trends at 0.5 N-m. The trends after this point are largely equivalent as homogeneity increases while combustion efficiency decreases with a greater potential of wall wetting. It is important note that while the emission trends for 1.0 and 1.5 N-m load condition were comparable, the magnitudes of all the emissions were comparatively less for the 1.5 N-m load condition because of the increased rate of power produced per unit time.

Overall, for both 0.5 and 1.5 N-m load conditions, there were no points in the injection sweep where both  $\text{NO}_x$  and PM emissions were lower than conventional combustion emissions (12.5° BTDC). Hence, there was no success in beating the  $\text{NO}_x$ -PM trade-off during the injection timing sweep. However, CO and THC emissions are comparable to the conventional combustion results for the 1.5 N-m load case. In general, PM, CO, and THC emissions were observed to be lower than the conventional emission results at advanced injection timings in all three load conditions. However, the injection timing at which these emissions are low depend on the operating load condition. The major drawback is the significantly high  $\text{NO}_x$  emissions in these regions. Moreover, the high CR of the engine limits the region in which this behavior may be observed due to a comparatively lower ignition delay period. Furthermore, the compromise in the combustion performance characteristics is negligible until the fuel injection is advanced beyond 30° BTDC.

Comparing the PCI trial results (discussed in Chapter III) with the results here on a ppm basis finds that  $\text{NO}_x$ , FSN, CO, and THC emissions all have similar trends as presented in Figure 44.  $\text{NO}_x$  emissions for the 1.5 N-m load condition trial appear to be comparatively more due to the relatively higher in-cylinder temperature because of greater equivalence ratios. For the same reason,  $\text{NO}_x$  emission values for the previous trial are lower than these findings as the amount of fuel injected and the subsequent in-cylinder combustion temperature were lower. Similarly, for both CO and THC emissions, the 1.5 N-m load condition

results recorded the (generally) least magnitude of emissions at all points suggesting improved combustion efficiency due to higher combustion temperatures. Conversely, while the FSN plot shows similar trends for both chapters, the variation in the magnitude of the FSN value is not obvious like the rest of the emissions discussed earlier. For all the conditions considered, the FSN value decreases at advanced injection timings until a certain point, after which there is a gradual increase in the FSN value. While FSN trends are in agreement with the NO<sub>x</sub>-PM tradeoff scenario, unfortunately, the magnitude of the FSN values are not as apparent when comparing the findings of the two chapters.

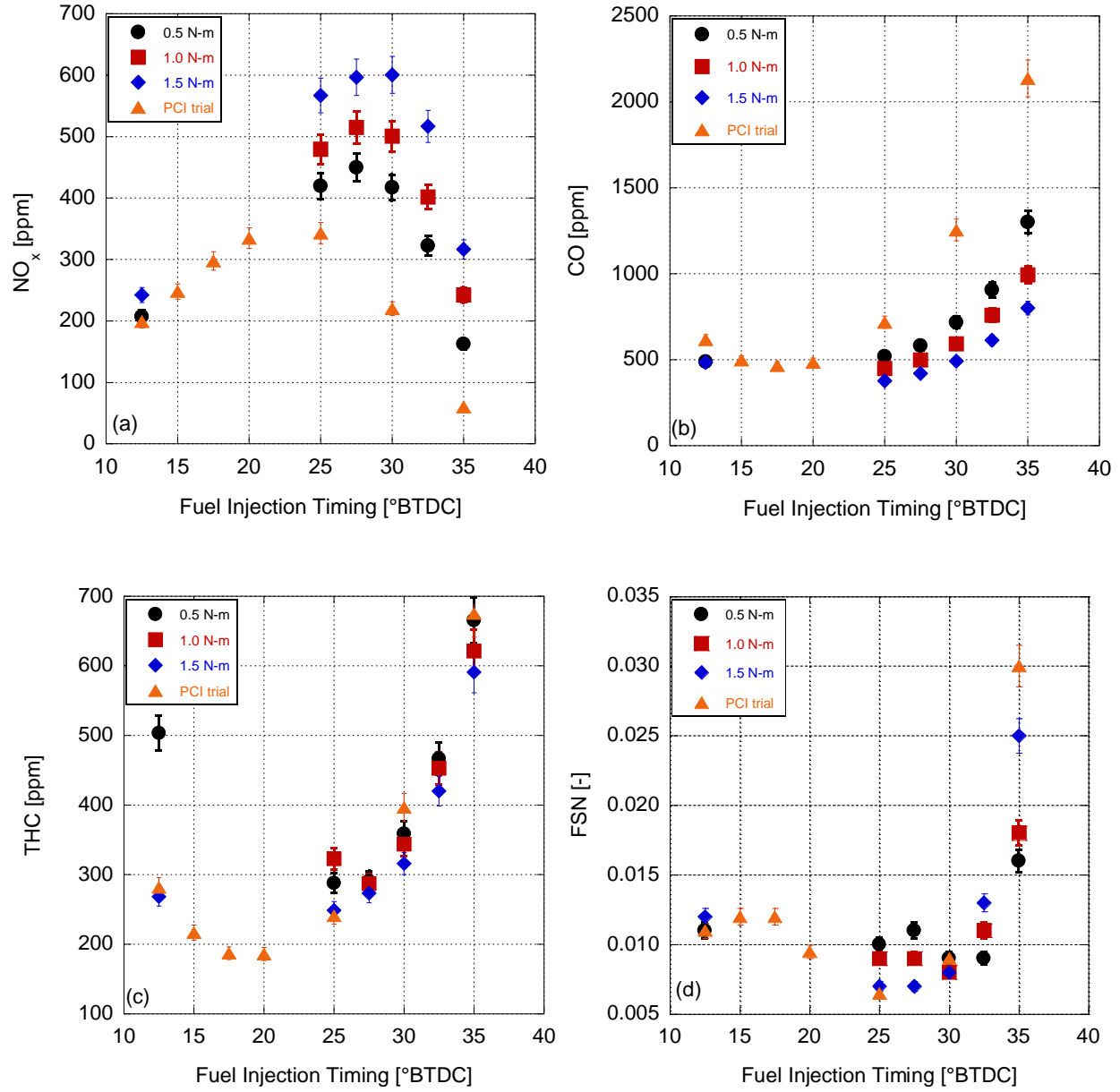


**Figure 44: (a) Nitrogen oxides, (b) carbon monoxide, (c) hydrocarbon emissions, and (d) FSN for PCI and PPCI trials at various fuel injection timings.**

#### 4.4 Conclusion

Due to the demand for reducing  $\text{NO}_x$  and PM emissions determined by the stringent regulations set by EPA, it is imperative to focus on transforming CI engines from conventional combustion to LTC mode. LTC offers the advantage of lowering the emissions while maintaining high combustion performance

efficiencies. Chapter 3 of this thesis discussed the experimental results obtained when PCI combustion was attempted on a single cylinder CI engine. During the injection timing sweep, initially,  $\text{NO}_x$  emissions increased while smoke emissions remained largely low and unchanged. After a certain point, advancing the injection timing further reduced CI knock resulting in gradual in-cylinder pressure rise. Additionally,  $\text{NO}_x$  emissions decreased, and CO, THC, and aldehydes grew correspondingly. Unlike the general conclusion presented in the literature on PCI ( $60^\circ$  to  $100^\circ$  BTDC), the ideal injection timing setting where both  $\text{NO}_x$  and smoke emissions were comparable to conventional combustion emissions occurred at injections around  $30^\circ$  BTDC. In a follow up experiment, fuel injection quantity sweeps were conducted at  $60^\circ$  and  $100^\circ$  BTDC as a possible precursor to LTC trials through MPFI combustion. Here, it was found that for fuel quantities lesser than 30 mg/stroke, the amount of fuel participating in combustion was significantly low compared to conventional injection timings.

Due to lower emissions with comparable combustion efficiencies observed for injections between  $25^\circ$  and  $35^\circ$  BTDC, a second set of experiments were conducted at moderately advanced injection timings, popularly known as PPCI combustion. Hence, in Chapter 4, PPCI combustion through DI of fuel was attempted at 0.5, 1.0, and 1.5 N-m engine load conditions. Injection timing sweeps were carried out at all three engine loads to analyze the combustion characteristics at various operating conditions. Similar to Chapter 3, an in house built heat release model was utilized to compute thermodynamic characteristics of the measured combustion data, and predict SOC. The goal of beating the  $\text{NO}_x$ -PM tradeoff was not achieved as the trends partially followed conventional combustion emission trends. Advancing the injection away from the conventional combustion timing, initially, resulted in a higher peak combustion pressure and temperature due to which, PM, CO, and THC emissions decreased comparatively. However,  $\text{NO}_x$  emissions were significantly high at these points. Conversely, advancing the injection timing beyond a certain point resulted in comparatively lower combustion temperatures and pressures due to combustion chamber conditions not favoring air-fuel atomization. This drives the need to increase the fuel injection quantity to meet the desired engine load level resulting in higher PM, CO, and THC emissions. Though the advantage

of such a scenario is lower  $\text{NO}_x$  emissions, the decline in the combustion performance cannot be neglected. Therefore, for the operating conditions discussed in Chapter 4, from an emissions stand point, there is no real benefit in operating in PPCI mode and it would be beneficial to stick to the conventional combustion regime.

The major disadvantage encountered in the current Yanmar setup, particularly important for LTC, is the restricted ignition delay period due to the high CR. Additionally, it is a challenging task to maintain the safety of the equipment while investigating PPCI, and/or PCI by advancing the injection timing as the peak combustion pressure increases rapidly. To overcome the peak combustion pressure issue, EGR could surface to be a suitable solution. Utilizing EGR would significantly benefit in increasing the ignition delay. In addition, using hot EGR gasses would assist in evaporating and atomizing the injected fuel effectively. Through EGR, a substantial success in beating the  $\text{NO}_x$ -PM tradeoff could be realized without significant performance drop. Moreover, EGR could enable to operate in PCI, and/or PPCI mode on a high CR engine at comparatively higher load conditions.



## References

1. Majewski, W.A. and M.K. Khair, *Diesel emissions and their control*. 2006: Society of Automotive Engineers.
2. *Hydrocarbon emissions characteristics with changing engine load data available at:* [www.dieselnet.com](http://www.dieselnet.com).
3. Chen, J.H., et al., *Terascale direct numerical simulations of turbulent combustion using S3D*. Computational Science & Discovery, 2009. **2**(1): p. 015001.
4. Depcik, D.C., *ME 636 Course Notes, Chapter 7: CI Engine Combustion, Pg: 48*.
5. Heywood, J.B., *ICE fundamentals*. Vol. 930. 1988: Mcgraw-hill New York.
6. Pulkrabek, W.W., *Engineering fundamentals of the ICE*. Vol. 249. 2004: Pearson Prentice Hall New Jersey.
7. Davis, S.C., S.W. Diegel, and R.G. Boundy, *Transportation Energy Data Book: Edition 31*. 2012, Oak Ridge National Laboratory (ORNL).
8. Patterson, D.J. and N.A. Henein, *Emissions from combustion engines and their control*. 1981.
9. Stone, R., *Introduction to ICEs*. 1999.
10. Newhall, H.K. and S. Shahed. *Kinetics of nitric oxide formation in high-pressure flames*. in *Symposium (International) on Combustion*. 1971. Elsevier.
11. Weidenbaum, M.L., *The high cost of government regulation*. Business Horizons, 1975. **18**(4): p. 43-51.
12. Forbes, A., *Bosch Fuel Injection Systems*. 2001.
13. *Single hole injector nozzle available at:* <http://www.tpub.com/engine3/en32-75.htm>.
14. *Multi hole injector nozzle information available at:* <http://vegburner.co.uk/suitability.htm>.
15. *Pintle fuel injector nozzle information available at:* <http://www.dieselmotors.info/fuel-systems/diesel-engine-fuel-injectors.html>.

16. Akagawa, H., et al., *Approaches to solve problems of the premixed lean diesel combustion*. 1999, SAE Technical Paper.
17. Depcik, D.C., *ME 636 Course Notes, Chapter 7: CI Engine Combustion*, Pg:69.
18. Langness, C., *Effects of Natural Gas Constituents on Engine Performance, Emissions, and Combustion in Compressed Natural Gas-Assisted Diesel Combustion*. KU ScholarWorks, 2014.
19. Ryan, T.W. and T.J. Callahan, *Homogeneous charge compression ignition of diesel fuel*. 1996, SAE Technical Paper.
20. Kaneko, N., et al., *Expansion of the operating range with in-cylinder water injection in a premixed charge compression ignition engine*. 2002, SAE Technical Paper.
21. Suzuki, H., N. Koike, and M. Odaka, *Combustion control method of homogeneous charge diesel engines*. 1998, SAE Technical Paper.
22. Stanglmaier, R.H. and C.E. Roberts, *Homogeneous charge compression ignition (HCCI): benefits, compromises, and future engine applications*. 1999, SAE Technical Paper.
23. Odaka, M., et al., *Search for optimizing control method of homogeneous charge diesel combustion*. 1999, SAE Technical Paper.
24. Kawano, D., et al. *Ignition and combustion control of diesel HCCI*. in *2005 SAE Brasil Fuels and Lubricants Meeting, SFL 2005*. 2005.
25. Tsurushima, T., et al., *Thermodynamic characteristics of premixed compression ignition combustions*. 2001, SAE Technical Paper.
26. Harada, A., et al., *The effects of mixture formation on premixed lean diesel combustion engine*. 1998, SAE Technical Paper.
27. Iwabuchi, Y., et al., *Trial of new concept diesel combustion system-premixed compression-ignited combustion*. 1999, SAE Technical Paper.
28. Nishijima, Y., Y. Asaumi, and Y. Aoyagi, *Premixed lean diesel combustion (PREDIC) using impingement spray system*. 2001, SAE Technical Paper.

29. Shimazaki, N., H. Akagawa, and K. Tsujimura, *An experimental study of premixed lean diesel combustion*. 1999, SAE Technical Paper.
30. Lee, S. and R.D. Reitz, *Spray targeting to minimize soot and CO formation in premixed charge compression ignition (PCCI) combustion with a HSDI diesel engine*. SAE paper, 2006(2006-01): p. 0918.
31. Jung, Y., et al., *Improvement of premixed compression ignition combustion using various injector configurations*. 2011, SAE Technical Paper.
32. Miyamoto, T., et al., *A Computational Investigation of Premixed Lean Diesel Combustion-Characteristics of fuel-air mixture formation, combustion and emissions*. 1999, SAE Technical Paper.
33. Lee, J.-H., et al., *Effects of injection conditions on mixture formation process in a premixed compression ignition engine*. 2000, SAE Technical Paper.
34. Kimura, S., et al., *New combustion concept for ultra-clean and high-efficiency small DI diesel engines*. 1999, SAE Technical Paper.
35. Kimura, S., et al., *Ultra-clean combustion technology combining a low-temperature and premixed combustion concept for meeting future emission standards*. 2001, SAE Technical Paper.
36. Walter, B. and B. Gatellier, *Development of the high power NADI™ concept using dual mode diesel combustion to achieve zero NOx and particulate emissions*. 2002, SAE Technical Paper.
37. Chen, Z. and T. Iwashina, *HC and CO Formation Factors in a PCI Engine*. 2009, SAE Technical Paper.
38. Ogawa, H., et al., *A study of heat rejection and combustion characteristics of a low-temperature and pre-mixed combustion concept based on measurement of instantaneous heat flux in a direct-injection diesel engine*. 2000, SAE Technical Paper.
39. Nishijima, Y., Y. Asaumi, and Y. Aoyagi, *Impingement spray system with direct water injection for premixed lean diesel combustion control*. 2002, SAE Technical Paper.

40. Hashizume, T., et al., *Combustion and emission characteristics of multiple stage diesel combustion*. 1998, SAE Technical Paper.
41. Bao, Z., et al., *Investigation Into Partially Premixed Combustion in a Light-Duty Diesel Engine Based on Different Injection Strategies*. 2014, SAE Technical Paper.
42. Dickey, D.W., T.W. Ryan, and A.C. Matheaus, *NOx control in heavy-duty diesel engines-what is the limit?* 1998, SAE Technical Paper.
43. Asad, U., et al., *Fuel injection strategies to improve emissions and efficiency of high CR diesel engines*. SAE International Journal of Engines, 2009. 1(1): p. 1220-1233.
44. Mingfa, Y., et al., *Experimental study of multiple injections and coupling effects of multi-injection and EGR in a HD diesel engine*. 2009, SAE Technical Paper.
45. Oh, Y., et al., *Two-stage Combustion Strategy for Reducing NOx Emissions in a Compression Ignition Engine*. 2011, SAE Technical Paper.
46. Park, C., S. Kook, and C. Bae, *Effects of multiple injections in a HSDI diesel engine equipped with common rail injection system*. 2004, SAE Technical Paper.
47. Yoshihiro, H., I. Minaji, and N. Kiyomi, *Achieving lower exhaust emissions and better performance in an HSDI diesel engine with multiple injection 2005-01-0928 [C/CD]*. SAE Technical Paper. Detroit: Society of Automotive Engineers Inc, 2005.
48. Dronniou, N., et al., *Combination of high EGR rates and multiple injection strategies to reduce pollutant emissions*. 2005, SAE Technical Paper.
49. Ishikawa, N., et al., *DI diesel emission control by optimized fuel injection*. 2004, SAE Technical Paper.
50. Beatrice, C., et al., *Downsizing of common rail DI engines: influence of different injection strategies on combustion evolution*. 2003, SAE Technical Paper.
51. Badami, M., et al., *Influence of multiple injection strategies on emissions, combustion noise and BSFC of a DI common rail diesel engine*. 2002, SAE Technical Paper.

52. Badami, M., F. Millo, and D. D'amato, *Experimental investigation on soot and NO<sub>x</sub> formation in a DI common rail diesel engine with pilot injection*. 2001, SAE Technical Paper.
53. Singh, S., R.D. Reitz, and M.P. Musculus, *2-color thermometry experiments and high-speed imaging of multi-mode diesel engine combustion*. 2005, SAE Technical Paper.
54. Fang, T., et al., *Combustion and soot visualization of low temperature combustion within an HSDI diesel engine using multiple injection strategy*. 2006, SAE Technical Paper.
55. Fang, T., et al., *Low temperature combustion within a small bore high speed direct injection (HSDI) diesel engine*. 2005, SAE Technical Paper.
56. Ogawa, H., et al., *Semi-Premixed Diesel Combustion with Twin Peak Shaped Heat Release Using Two-Stage Fuel Injection*. 2016, SAE Technical Paper.
57. Asad, U., et al., *Low temperature combustion strategies for compression ignition engines: operability limits and challenges*. 2013, SAE Technical Paper.
58. Tsurushima, T., et al., *The effect of knock on heat loss in homogeneous charge compression ignition engines*. 2002, SAE Technical Paper.
59. Gan, S., H.K. Ng, and K.M. Pang, *Homogeneous charge compression ignition (HCCI) combustion: implementation and effects on pollutants in direct injection diesel engines*. Applied Energy, 2011. **88**(3): p. 559-567.
60. Ganesh, D. and G. Nagarajan, *Homogeneous Charge Compression Ignition (HCCI) Combustion of Diesel Fuel with External Mixture Formation*. 2009, SAE International.
61. Singh, A.P. and A.K. Agarwal, *An Experimental Investigation of Combustion, Emissions and Performance of a Diesel Fuelled HCCI Engine*. 2012, SAE Technical Paper.
62. Christensen, M., A. Hultqvist, and B. Johansson, *Demonstrating the multi fuel capability of a homogeneous charge compression ignition engine with variable CR*. 1999, SAE Technical Paper.
63. Han, X., M. Wang, and M. Zheng, *An Enabling Study of Neat n-Butanol HCCI Combustion on a High Compression-ratio Diesel Engine*. 2015, SAE Technical Paper.

64. Mangus, M.D., *Implementation of Engine Control and Measurement Strategies for Biofuel Research in Compression-Ignition Engines*. 2014.
65. Langness, C., M. Mangus, and C. Depcik, *Construction, Instrumentation, and Implementation of a Low Cost, Single-Cylinder Compression Ignition Engine Test Cell*. 2014, SAE Technical Paper.
66. Mangus, M., et al., *Investigating the compression ignition combustion of multiple biodiesel/ULSD (ultra-low sulfur diesel) blends via common-rail injection*. Energy, 2015. **89**: p. 932-945.
67. Mattson, J.M. and C. Depcik, *First and Second Law Heat Release Analysis in a Single Cylinder Engine*. SAE International Journal of Engines, 2016. **9**(2016-01-0559): p. 536-545.
68. Mattson, J.M.S., *Power, Efficiency, and Emissions Optimization of a Single Cylinder Direct-Injected Diesel Engine for Testing of Alternative Fuels through Heat Release Modeling*. 2013, University of Kansas.
69. Mattson, J.M., M. Mangus, and C. Depcik, *Efficiency and Emissions Mapping for a Single-Cylinder, Direct Injected Compression Ignition Engine*. 2014, SAE Technical Paper.
70. Phillips, C., *Material Safety Data Sheet for no.2 Diesel Fuel*. . 2007.
71. Zádor, J., C.A. Taatjes, and R.X. Fernandes, *Kinetics of elementary reactions in low-temperature autoignition chemistry*. Progress in energy and combustion science, 2011. **37**(4): p. 371-421.
72. Griffiths, J., *Why cool flames are a hot prospect*. New Scientist, 2004. **182**(2450): p. 28-29.
73. Xu, G., et al., *Inverse influence of initial diameter on droplet burning rate in cold and hot ambiances: a thermal action of flame in balance with heat loss*. International Journal of Heat and Mass Transfer, 2003. **46**(7): p. 1155-1169.
74. Battin-Leclerc, F., *Detailed chemical kinetic models for the low-temperature combustion of hydrocarbons with application to gasoline and diesel fuel surrogates*. Progress in Energy and Combustion Science, 2008. **34**(4): p. 440-498.
75. Titova, N., S. Torokhov, and A. Starik, *On kinetic mechanisms of n-decane oxidation*. Combustion, Explosion, and Shock Waves, 2011. **47**(2): p. 129-146.

76. Westbrook, C.K. and F.L. Dryer, *Chemical kinetic modeling of hydrocarbon combustion*. Progress in Energy and Combustion Science, 1984. **10**(1): p. 1-57.
77. Glassman, I., R.A. Yetter, and N.G. Glumac, *Combustion*. 2014: Academic press.
78. Prikhodko, V.Y., et al., *Emission characteristics of a diesel engine operating with in-cylinder gasoline and diesel fuel blending*. SAE International Journal of Fuels and Lubricants, 2010. **3**(2010-01-2266): p. 946-955.
79. Storey, J.M., et al., *Mobile source air toxics (MSATs) from high efficiency clean combustion: catalytic exhaust treatment effects*. SAE International Journal of Engines, 2008. **1**(2008-01-2431): p. 1157-1166.
80. Sharp, C.A., S.A. Howell, and J. Jobe, *The effect of biodiesel fuels on transient emissions from modern diesel engines, part II unregulated emissions and chemical characterization*. 2000, SAE Technical Paper.
81. Kosaka, H., et al., *Two-Dimensional Imaging of Formaldehyde Formed During the Ignition Process of a Diesel Fuel Spray*. 2000, SAE Technical Paper.
82. Schießl, R., et al., *Double-pulse PLIF imaging of self-ignition centers in an SI engine*. 2001, SAE Technical paper.
83. Graf, N., et al., *In-cylinder combustion visualization in an auto-igniting gasoline engine using fuel tracer-and formaldehyde-LIF imaging*. 2001, SAE Technical paper.
84. Chiang, C. and A. Stefanopoulou. *Sensitivity analysis of combustion timing and duration of homogeneous charge compression ignition (HCCI) engines*. in *2006 American Control Conference*. 2006. IEEE.
85. Choi, Y. and J.-Y. Chen, *Fast prediction of start-of-combustion in HCCI with combined artificial neural networks and ignition delay model*. Proceedings of the Combustion Institute, 2005. **30**(2): p. 2711-2718.
86. Inhelder, J., C. Frouzakis, and K. Boulouchos, *A discussion of approaches for predicting end-gas autoignition in homogeneous charge engines*. 1993, LVV Internal Report 93/20, ETHZ.

87. Livengood, J. and P. Wu. *Correlation of autoignition phenomena in ICEs and rapid compression machines*. in *Symposium (International) on Combustion*. 1955. Elsevier.
88. Tanner, F., *Liquid jet atomization and droplet breakup modeling of non-evaporating diesel fuel sprays*. 1997, SAE Technical Paper.
89. Weisser, G., F.X. Tanner, and K. Boulouchos, *Modeling of ignition and early flame development with respect to large diesel engine simulation*. 1998, SAE Technical Paper.
90. Assanis, D.N., et al., *A predictive ignition delay correlation under steady-state and transient operation of a direct injection diesel engine*. *Journal of Engineering for Gas Turbines and Power*, 2003. **125**(2): p. 450-457.
91. Hariyanto, A., et al., *Application of wavelet analysis to determine the start of combustion of diesel engines*. 2007, SAE Technical Paper.
92. Gulia, S., et al., *Urban air quality management-A review*. *Atmospheric Pollution Research*, 2015. **6**(2): p. 286-304.
93. Schrank, D.L. and T.J. Lomax, *The 2007 urban mobility report*. 2007: Texas Transportation Institute, Texas A & M University.
94. Olivier, J.G., J.A. Peters, and G. Janssens-Maenhout, *Trends in global CO2 emissions 2012 report*. 2012, PBL Netherlands Environmental Assessment Agency The Hague, The Netherlands.
95. Zhang, K. and S. Batterman, *Air pollution and health risks due to vehicle traffic*. *Science of the total Environment*, 2013. **450**: p. 307-316.
96. Helmantel, A. and I. Denbratt, *HCCI operation of a passenger car common rail DI diesel engine with early injection of conventional diesel fuel*. 2004, SAE Technical Paper.
97. Lechner, G.A., et al., *Evaluation of a narrow spray cone angle, advanced injection timing strategy to achieve partially premixed compression ignition combustion in a diesel engine*. 2005, SAE Technical Paper.



98. Kiplimo, R., et al., *Effects of spray impingement, injection parameters, and EGR on the combustion and emission characteristics of a PCCI diesel engine*. Applied Thermal Engineering, 2012. **37**: p. 165-175.
99. Boot, M., et al., *Spray impingement in the early direct injection premixed charge compression ignition regime*. 2010, SAE Technical Paper.
100. Han, M., D.N. Assanis, and S.V. Bohac, *Sources of hydrocarbon emissions from low-temperature premixed compression ignition combustion from a common rail direct injection diesel engine*. Combustion Science and Technology, 2009. **181**(3): p. 496-517.
101. Fang, T., et al., *Effects of injection angles on combustion processes using multiple injection strategies in an HSDI diesel engine*. Fuel, 2008. **87**(15): p. 3232-3239.
102. Genzale, C.L., R.D. Reitz, and M.P. Musculus, *Effects of spray targeting on mixture development and emissions formation in late-injection low-temperature heavy-duty diesel combustion*. Proceedings of the combustion institute, 2009. **32**(2): p. 2767-2774.
103. Kim, M.Y. and C.S. Lee, *Effect of a narrow fuel spray angle and a dual injection configuration on the improvement of exhaust emissions in a HCCI diesel engine*. Fuel, 2007. **86**(17): p. 2871-2880.
104. Boot, M., et al., *Uncooled EGR as a means of limiting wall-wetting under early direct injection conditions*. 2009, SAE Technical Paper.
105. Mallamo, F., M. Badami, and F. Millo, *Effect of CR and injection pressure on emissions and fuel consumption of a small displacement common rail diesel engine*. 2005, SAE Technical Paper.
106. Kanda, T., et al., *PCCI operation with early injection of conventional diesel fuel*. 2005, SAE Technical Paper.
107. Martin, G.C., et al., *Early direct-injection, low-temperature combustion of diesel fuel in an optical engine utilizing a 15-hole, dual-row, narrow-included-angle nozzle*. SAE International Journal of Engines, 2008. **1**(2008-01-2400): p. 1057-1082.

108. Lewander, M., et al., *Investigation of the combustion characteristics with focus on partially premixed combustion in a heavy duty engine*. SAE International Journal of Fuels and Lubricants, 2008. 1(2008-01-1658): p. 1063-1074.
109. Hildingsson, L., et al., *Fuel octane effects in the partially premixed combustion regime in compression ignition engines*. 2009, SAE Technical Paper.
110. Opat, R., et al., *Investigation of mixing and temperature effects on HC/CO emissions for highly dilute low temperature combustion in a light duty diesel engine*. 2007, SAE Technical Paper.
111. McGill, R., et al., *Emission performance of selected biodiesel fuels*. 2003, SAE Technical Paper.
112. Li, T., M. Suzuki, and H. Ogawa, *Characteristics of smokeless low temperature diesel combustion in various fuel-air mixing and expansion of operating load range*. 2009, SAE Technical Paper.